ANALYSIS OF ICE AND METOCEAN MEASUREMENTS, CHUKCHI SEA, 2010-2011

Prepared for:

ConocoPhillips Alaska Inc.
Anchorage, Alaska
Attn: John Cologgi

Via:

Olgoonik Fairweather LLC
Attn: Jeff Hastings and Sheyna Wisdom

By:
T.D. Mudge, D.B. Fissel, N. Kulan, E. Ross, D. Sadowy, D. Billenness, K. Borg, S. Hunt, A. Slonimer, A. Kanwar, and A. Bard

ASL Environmental Sciences Inc.
#1 - 6703 Rajpur Place, Victoria, B.C., Canada, V8M 1Z5

ASL File: PR-739
December 2011
Draft Version

The correct citation for this report is:

T.D. Mudge, D.B. Fissel, N. Kulan, E. Ross, D. Sadowy, D. Billenness, K. Borg, S. Hunt, A. Slonimer, A. Kanwar, and A. Bard, 2011. Analysis of Ice and Metocean Measurements, Chukchi Sea, 2010-2011. Report for ConocoPhillips Alaska Inc., Anchorage, Alaska by ASL Environmental Sciences Inc., Victoria, B.C. Canada. x + 120 p.

EXECUTIVE SUMMARY

A program of ice keel depth and ice velocity measurements was carried out off northwestern Alaska in support of oil and gas exploration by ConocoPhillips Alaska Inc. (CPAI) in the Chukchi Sea from July 2010 to July 2011. The data collection program involved the deployment and operation of two underwater, internally recording instruments at two sites (Site 1 and Site 2) in 37-46 m depth for nearly a year. The 2010 to 2011 data sets represent the third year of a multiyear measurement program planned for the two offshore sites in the Chukchi Sea, offshore of Wainwright, Alaska.

Key results of the 2009 to 2010 measurement program included:

Ocean Wave measurements

In late September to early November 2010, there were four storms during which the significant wave heights exceeded 4 m. The largest wave event (October 31, 2010) at Site 1 reached a maximum significant wave height value of 4.3 m (8.3 m maximum individual wave height) with a corresponding peak period of 9 s. At Site 2, during this same event, the largest significant wave height was 3.5 m. During this event, coastal wind speeds at Point Lay and Wainwright ranged from 15-30 knots. The largest measured wave event at Site 2 occurred on September 25, 2010 with a significant wave height of 4.1 m (maximum wave height of 8.6 m). For all non-ice measurement times, the average significant wave heights in 2010-2011 were 1.3 m at Site 1 and 1.1 m at Site 2. The largest measured wave events in 2010-2011 were lower than the largest events of 2009-2010, when the largest measured significant wave heights were 5.4 m (site 1), but were larger than the peak wave events in 2008-2009.

Large Ice Keels

Very deep ice keels were observed at both Sites 1 and 2 with 4 keels at Site 1 and 12 keels at Site 2 measuring over 20 m ice draft. The deepest keels at Sites 1 and 2 were 22.2 m and 28.7 m respectively.

Keels exceeding 11 m ice draft were measured in all months from December 2011 to June 2011 at both sites. The total number of ice keels having ice drafts exceeding 5, 8 and 11 m were 8948, 2163 and 414 respectively for Site 1 and 10,998, 2971 and 785 for Site 2. The average widths for the individual ice draft thresholds of 5, 8 and 11 m were 28.0, 35.6 and 43.4 m for Site 1 and 29.4, 37.0 and 46.2 m for Site 2, respectively.

By comparison to the first year of measurements, 2008-2009 there was a notable reduction at Site 1 for the total number of keels and the total distance of ice measured (in 2008-2009, the number of keels > 5 m ice draft were 14,484 and in 2009-2010: 6,723). The site 1 maximum keel ice draft was reduced in 2010-2011 by comparison to the 2008-2009 maximum keel ice draft at Site 1 of 26.4 m, which was very similar to the maximum ice draft of 26.7 m at this site in 2009-2010. At site 2, the largest measured ice draft over this two

year period of measurements (no data was obtained in 2008-2009) was 30.0 m in 2009-2010 vs. 28.7 m in 2010-2011.

There were occurrences of ice keels with very large horizontal dimensions of up to a few hundred meters. The widest keels, using a threshold of 5 m, were 223 m for Site 1 and 294 m for Site 2.

Ice Velocities

The region had a very dynamic ice regime with ice movement occurring 97.4% to 96.4% of the time at Sites 1 and 2 respectively from July 2010 to July 2011. The greatest percentage of no-motion events for a month in this measurement period was 10.4% at Site 2 in January 2011.

Over 20 occurrences of large ice velocities were measured throughout the year with peak ice velocities of 91 cm/s at Site 1 and over 30 occurrences with peak ice velocities of 142 cm/s at Site 2. The episodes of large ice velocities were associated with strong wind events having peak speeds up to 21 m/s (40 knots). At site 2, the median ice drift was generally highest in June (40 cm/s) and lowest (6-11 cm/s) from February to March. The peak ice velocities for 2010-2011 are considerably greater than in 2009-2010 (76 and 115 cm/s at sites 1 and 2, respectively) and more comparable to 2008-2009 (112 and 124 cm/s at sites 1 and 2, respectively).

Ocean Currents

The ocean currents at Site 1 were weaker than those observed at Site 2 with median speeds that are 25 to 45% lower. The maximum measured current speeds were 99 cm/s at site 2 and 67 cm/s at site 1. From September to late December, current speeds were typically large and associated with strong wind events. From January to May, the currents are typically weak with a few episodes of larger currents speeds when the Wainwright winds exceeded 8 m/s (15 knots). The surface currents at Site 1 were variable but predominantly directed to the ENE, whereas the surface current direction at Site 2 aligned along an E-W axis which is very consistent with the previous years of measurements.

ACKNOWLEDGEMENTS

Many persons and organizations contribute to making a project of this scope possible, including:

ConocoPhillips Alaska Inc.	
John Collogi and Jim Darnall	Project Managers
Olgoonik-Fairweather	
Jeff Hastings	Project Manager
Sheyna Wisdom	Project Manager
Christa Koos	Logistical Support
Tom Ainsworth	Logistical Support
MV Tukpuk	
Bob Shears and crew	Logistical Support at Wainwright
MV Westward Wind	
Captain Steve Fogg and crew	Exceptional skill and facilities.
Aldrich Marine	
Dave Aldrich and marine techs	Logistics, mooring handling and project management on the *Westward Wind*
ASL Environmental Sciences Inc.	
Dave English Rick Birch Jeremy Lawrence Wally Horniak Ben Garrett Thomas Martinez	Equipment Preparation and Technical Assistance
Carol Stewart Des Buermans Bernadette Fissel	Administrative Assistance

TABLE OF CONTENTS

LIST OF FIGURES

LIST OF TABLES

1 INTRODUCTION

1.1 STUDY OBJECTIVES

The ConocoPhillips Alaska Inc. (CPAI) team is examining geotechnical and environmental forcing issues related to offshore production systems for the Chukchi Sea exploration lease areas off northwestern Alaska. As part of the study, ASL Environmental Sciences (ASL) was contracted to collect and analyze data on ice drafts and ice velocities in the lease areas. Additionally, ocean current profiles, non-directional waves, salinity and temperature of seawater at deployment depth were also measured and analyzed.

Measurements of ice drafts and velocities were obtained with upward looking sonar instrumentation in taut-line moorings at two sites in the Chukchi Sea (Figure 1-1). The 2010-2011 measurement program began in late July 2010. It is part of an ongoing program conducted by ASL for CPAI that started in September 2008 in the Chukchi Sea. This report presents the results of the measurements obtained in the third year of the Chukchi Sea measurement program from July 2010 to July 2011.

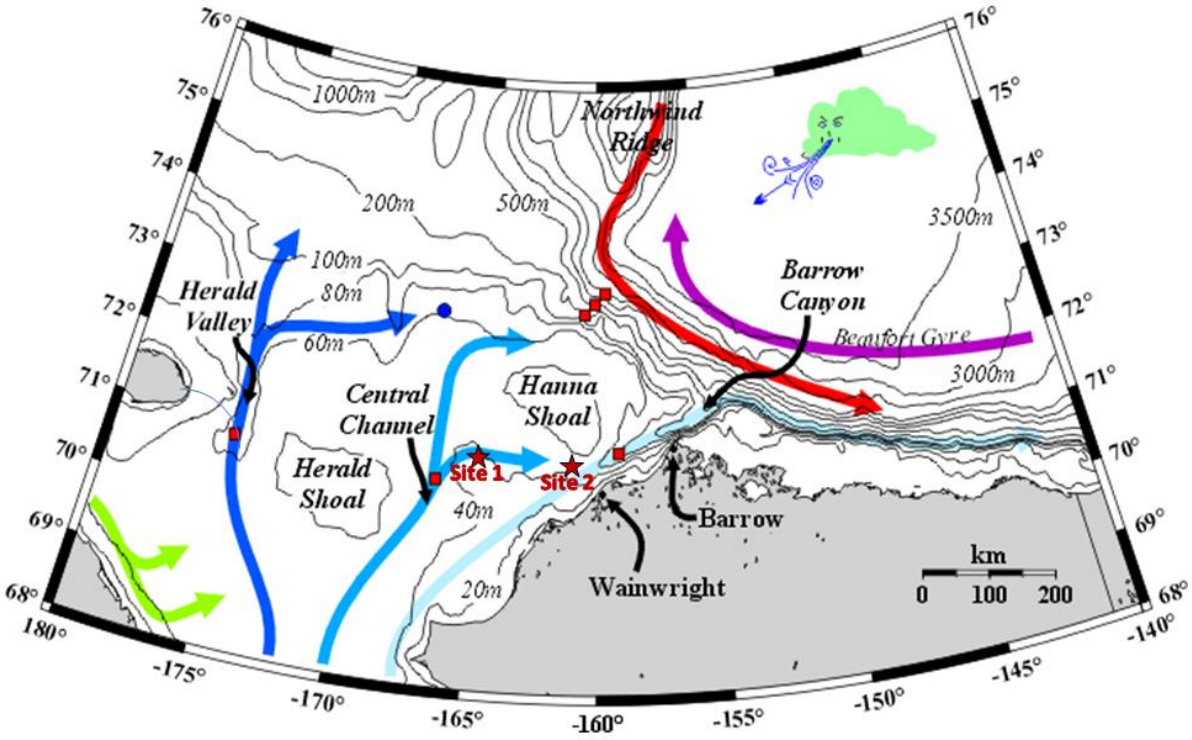

Figure 1-1. The location of the two measurement sites (dark red stars), Site 1 and Site 2, are plotted on a map by University of Alaska Institute of Marine Science (Weingartner et al., 2009) of the Chukchi and Beaufort Seas. Also plotted are the main currents and the depth contours from 20 to 3500 m. Pacific waters (3 shades of blue), Siberian Coastal Current (green), Atlantic Water on the continental

slope (red) and the anticyclonic circulation of the Beaufort Gyre surface waters (purple). The red squares represent the locations of previous oceanographic moorings operated by the U. of Alaska.

The field portion of the project was conducted for CPAI via Olgoonik Fairweather LLC (Fairweather) of Anchorage, Alaska. Fairweather provided logistical support to the ASL field personnel in the recovery and redeployment of Site 1 and Site 2 equipment in July 2010 and July 2011. ASL provided assistance in deployment and recovery of the equipment, in addition to processing and analyzing the collected data sets.

1.2 OVERVIEW OF THE STUDY AREA AND SEASONAL ICE CONDITIONS

The Chukchi Sea is a shelf sea with water depths of less than 200 m and it is part of the western Arctic Ocean. However, it is closely linked to the Pacific Ocean both atmospherically (through the Aleutian Low) and oceanographically (through Bering Strait). The water masses in the study area are dominated by the inflow of Pacific waters that enter the Arctic Ocean through Bering Strait (Figure 1-1). The three branches of Pacific waters are color-coded with dark blue being the most nutrient-rich waters and light blue being the least nutrient-rich (Weingartner et al., 2009).

The Site 1 measurement site lies in a 37 m deep region southwest of Hanna Shoal where the central channel flow has split into a predominately easterly flow. Site 2 is located to the south of Hanna Shoal in the same branch of the bifurcated central channel flow at about 46 m depth. On average, the flow direction in the vicinity of both Sites 1 and 2 is eastward. While the average current speed of the central channel flow is approximately 8 cm/s (Weingartner et al., 2009), short-term wind forced currents can dominate with larger observed currents of up to 50 cm/s.

The sea ice in the region is characterized by three major categories: the offshore, mobile polar pack ice of the Arctic Ocean, a narrow region of landfast ice adjacent to the coast, and a poorly studied area of highly mobile coastal zone ice (Norton and Gaylord 2004, Figure 1-2), also known as transition zone. Landfast ice zone is typically on the order of 10 km wide, however, the ice is frozen to the seafloor only over the shallowest part (< 2m) part of the inner shelf and floats in the outer part. Between the landfast ice zone nearshore and the offshore polar pack ice zone, there is a transitional zone, also known as the *stamukhi* zone, where the most intense ridging occurs, roughly between 15 to 40 m isobaths. The large ridge fragments, either as mobile or grounded ice features, are referred to as *stamukhi* ice. Under offshore movements of the mobile ice, large areas of open water can occur as polynyas or large-scale flaw leads in the transition zone adjacent to the landfast ice. Movement of ice in the landfast zone, called ice shove or *ivu* by the Inupiaq, may occur any time but is more common during freeze-up and break-up. In the landfast ice zone, ice movements ranging from 5 to 395 m near Point Barrow have been reported by Huntington et al. (2001) and Mahoney et al. (2004).

Sea-ice is for the most part consolidated in the region over winter. By early May, the on-average, anti-cyclonic (clockwise) pattern of movement known as Beaufort Gyre, which moves the polar pack ice with it, produces a semi-permanent polynya (Chukchi flaw zone) within about 100 km of the coast. The presence of a semi-permanent flaw zone in the northern Chukchi Sea is due to an abrupt change in landmass distribution resisting the westward movement of polar pack ice past Point Barrow and defines the coastal ice regime in the Chukchi Sea. The dominant direction of motion for ice floes in the northern Chukchi Sea flaw zone is East-Northeast, while polar pack ice moves westward on-average. The maximum speed attained by individual ice floes in the flaw zone can be much larger than the polar pack ice according to a study by Norton and Gaylord (2004) based on analysis of satellite imagery. Their findings also indicate that fastest ice floes move to the West-

Southwest, opposite to the dominant ice floe motion. Medium to large size floes can reach speeds as large as 140 cm/s (Norton and Gaylord, 2004). Site 2, about 50 km northwest of Wainwright, lies within the flaw zone while Site 1, about 190 km west-northwest of Wainwright, is most likely dominated by coherent pack ice.

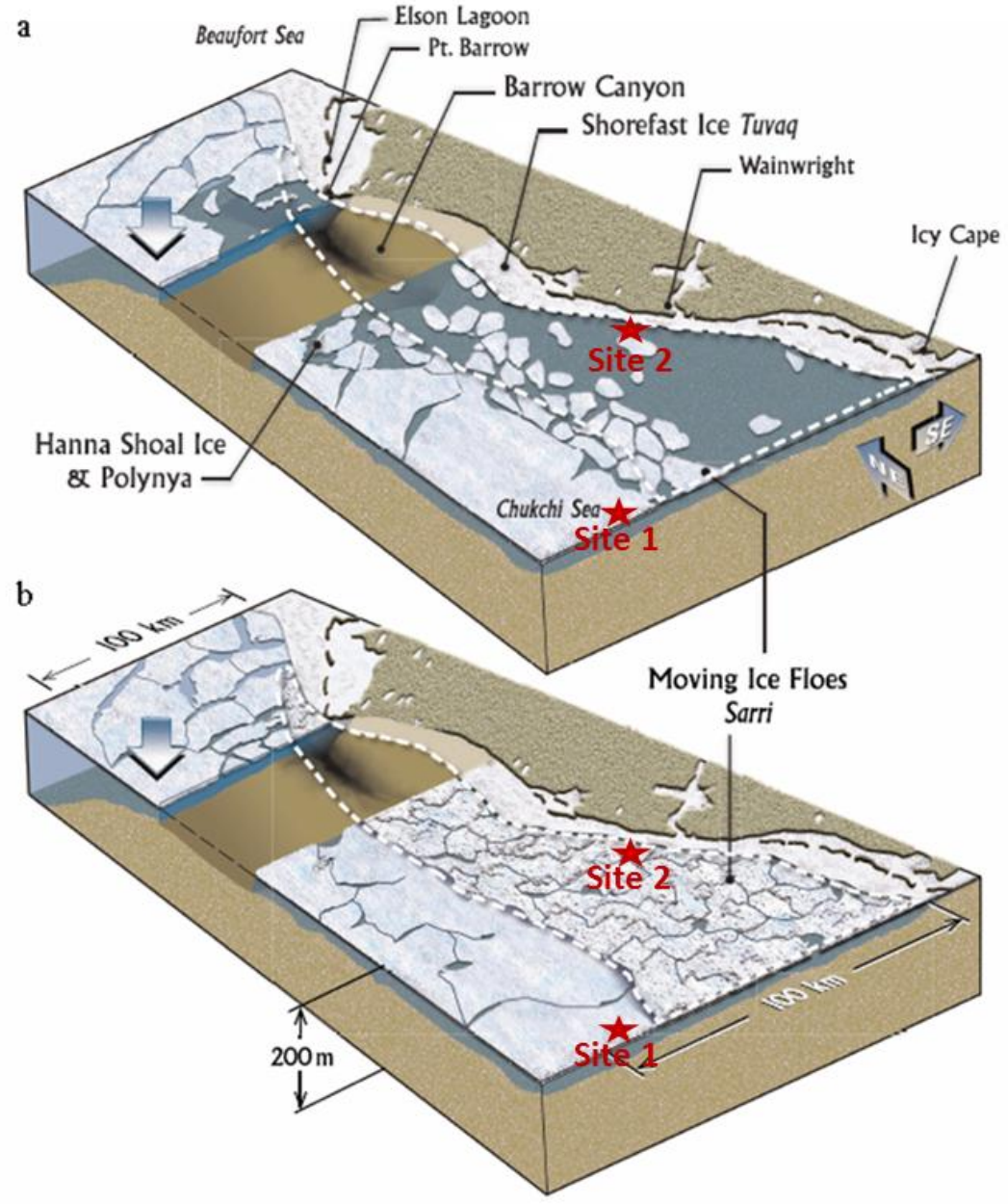

Figure 1-2. Ice dynamics in the Chukchi Sea (Norton and Gaylord, 2004). The dashed white line indicates Alaska's northern Chukchi Sea flaw zone from Icy Cape to the western edge of the Beaufort Sea. a) Ice moving to the southwest and b) ice moving to the northeast. Approximate locations of CPAI's Site 1 and Site 2 are also shown.

New ice formation in the Chukchi Sea begins in nearshore areas in early October while the outer edge of the offshore ice pack edge can be several hundred kilometers north of the coastline. Growth is characterized by outward extension and thickening of the nearshore ice cover. Simultaneously, new growth also appears in the offshore pack, primarily in areas of open water and thin ice.

Breakup of landfast ice near Barrow since 2000 has usually occurred in a period from mid-June to early July. In 2011, the landfast ice broke up through June while the sea ice was mostly cleared in the CPAI lease area by the first week of June, except for a few occasional ice keels passing through the area until mid-July. Prior to that, open water was encountered over short periods of time at Site 2, which is located in the Chukchi Flaw zone (in April and May) but not at Site 1, which is located further offshore in the pack ice zone. The flaw lead that started in the early May spread through eastern Chukchi Sea and the lease areas leading to clearing of the sea ice through June, with occasional ice floes passing through the area.

A notable difference between Beaufort Sea and Chukchi Sea ice features is the occurrence of floebergs, large masses of hummocky ice[1] or a group of hummocky ice frozen together, which are encountered frequently in the Beaufort Sea but not in Chukchi Sea, except for a large region of grounded ice on Hanna Shoal identified as Katie's Floeberg (Barrett and Stringer, 1978) and observed only in some years. In the Alaskan Beaufort Sea, floebergs have been observed to extend over distances of many kilometres parallel to the coastline with sail heights of 5 to 25 m.

[1] Hummocky sea ice is formed when individual ice floes impinge upon each other or push against weaker ice resulting in the "haphazard accumulation of ice blocks of a most irregular and formidable appearance" (Kovacs and Mellor, 1974).

1.3 ORGANIZATION OF THE REPORT

This report is organized into several sections reflecting the various phases of the study.

- Section 2 presents a summary of the data collection program, including the field operations (Deployment and Recovery) and the instrumentation and methodology used for data collection.
- Section 3 presents summaries of the data processing results for each type of data collected.
- Section 4 presents an overview of the ice conditions during the measurement period (July 2010 – July 2011) the results of the analysis of the ice draft data set involving detailed statistical summaries, and the analysis of big keels and very large observed ice features. Analysis results are also presented for ice velocities and ocean waves.
- Section 5 presents a summary of the study analyses of the largest observed ice keels, ice velocity, ocean currents and waves.
- Finally, Section 6 lists literature and report citations used in the writing this report.

More detailed information, key study data sets and results derived from the data processing tasks of this study are provided in a Project Archive on an FTP site or upon request on DVD.

2 DATA COLLECTION

2.1 INSTRUMENTATION

The primary instruments utilized in this study were the Ice Profiling Sonar (IPS-5), manufactured by ASL Environmental Sciences Inc. (ASL), which allows detailed measurements of ice keel depths, and the Teledyne RDI Acoustic Doppler Current Profiler (ADCP), which measures ice and ocean current velocities.

The IPS and ADCP instruments were deployed using separate near-bottom taut line moorings at Site 1 and 2 (Figure 2-1). The two moorings were located within 130 metres of each other and their configurations were as shown in Figure 2-2. To provide additional speed of sound information, a self-contained conductivity/temperature sensor, a SeaBird model SBE37, was attached to the IPS-5 mooring frame at both sites (Figure 2-3). Recovery was carried out through use of acoustic release devices, which are activated by sonar signals transmitted from a command unit operated from the deck of the deployment/recovery vessel. Mooring details, including their location, depth, and deployment and recovery times are shown in Table 2-1.

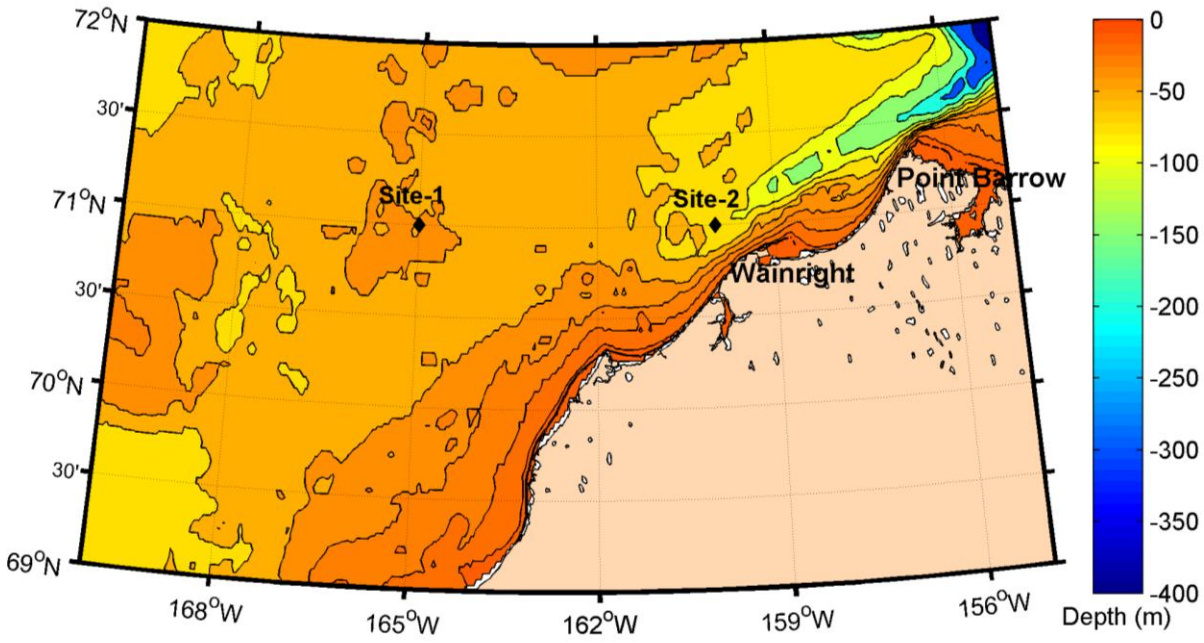

Figure 2-1. Map of mooring locations for IPS-5 and ADCP instruments at Site 1 (71˚N and 165˚W) and Site 2 (71˚N and 161˚W), 2009-2010 field program.

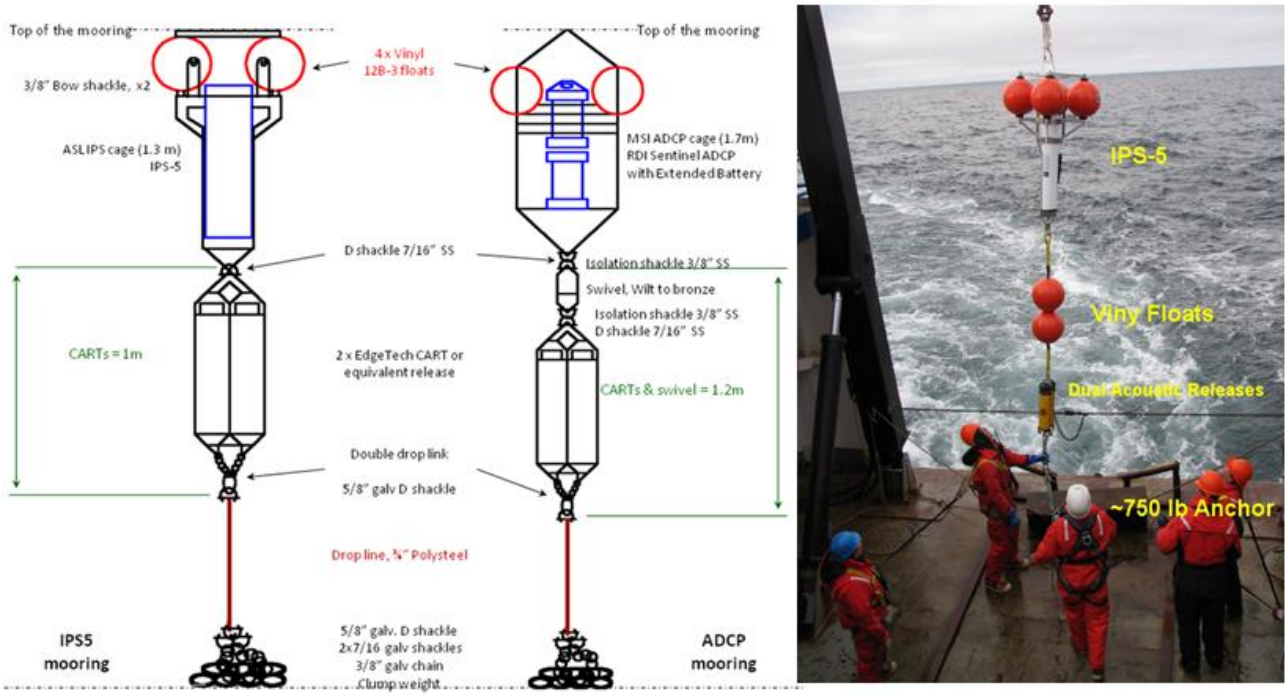

Figure 2-2. Left: A schematic diagram of the taut line moorings used for deployment of the IPS and ADCP instruments. Each instrument is at the upper end of the mooring supported by four plastic Vinyl floats. Two acoustic releases (ORE CART units) are located below. Right: IPS-5 mooring as it is being prepared for deployment, the same orientation as it would sit in the water column.

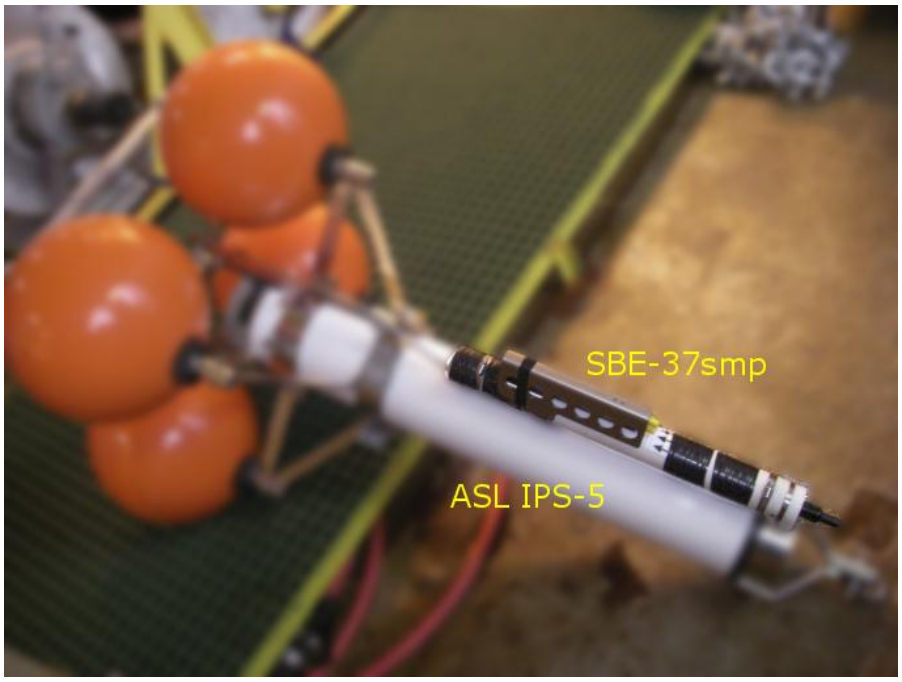

Figure 2-3. SBE 37-SMP mounted on IPS-5 frame. All of the image but the SBE 37 has been intentionally blurred.

The ASL IPS-5 provides a continuous over-winter record of ice draft at sampling rates of once every 1 or 2 seconds. In combination with ADCPs, used to measure ice velocities, ice draft time series acquired with IPS instruments can be converted to a spatial (distance) series equivalent. The IPS-5 also provided 2 Hz wave bursts during the ice-free season.

The instrumentation used in this study has been widely used in other parts of the world, including the greater Arctic Ocean region, where sea ice is present for nearly the entire year (Melling et al., 1995), and in marginal seasonal ice zones (Fissel et al., 2008).

Table 2-1. Instrumentation, locations, and deployment and recovery times for the moorings operated in the Chukchi Sea from July 2010 to July 2011. Further details are available in the Cruise Reports (Borg et al., 2010 and Borg et al., 2011).

Site	Instrument Type	Latitude	Longitude	Water Depth (m)	Deployment Date (UTC)	Recovery Date (UTC)
Site 1	IPS-5 51068	70°59.973' N	165°0.064' W	39	July 26, 2010 15:23	July 27, 2011 14:48
	ADCP WH-300	70°59.903' N	165°0.043' W	39	July 26, 2010 15:09	July 27, 2011 14:32
Site 2	IPS-5 51060	70°58.691' N	160°58.379' W	47	July 28, 2010 05:46	July 29, 2011 04:51
	ADCP WH-300	70°58.735' N	160°58.169' W	47	July 28, 2010 05:38	July 29, 2011 04:24

The use of two separate moorings at each monitoring site was dictated by a need to keep the instruments as close to the seabed as possible, whereas, in deeper waters, the IPS instrument is often located above the ADCP instrument on a single taut line mooring. It was expected that extremely large sea-ice keels could have keels nearly as deep as the water depth at the measurement locations, raising concerns that collisions with sea-ice could lead to loss of the instruments as well as of the collected data sets.

2.1.1 ICE PROFILING SONAR (IPS)

The IPS instrument is an upward-looking ice profiling sonar, which provides the high-quality ice thickness, or more correctly, ice draft data required for characterizing the winter oceanic environment. Originally, this instrument was designed by the Institute of Ocean Sciences, Victoria, BC, Canada, and has been further developed and subsequently manufactured by ASL Environmental Sciences Inc. of Victoria, BC, Canada. The ice keel depth is determined from the return travel time of an acoustic pulse (420 kHz; 1.8° beam at -3 dB) reflected off the underside of the sea ice. The return time is converted to an acoustic range value through use of the speed of sound in seawater.

The IPS-5 units were setup to run through various configurations (phases) to acquire the best data based on climatological conditions. Site 1 and Site 2 IPS-5 instruments were deployed with the same set-up parameters to collect ice and wave data. Out of the total

eight configured phases, five phases were utilized until the recovery of the two IPS-5 instruments in late July 2011. The basic setup parameters are shown in Table 2-2.

Table 2-2. Setup parameters for Site 1 and Site 2 IPS-5 instruments. Phase 1 starts with Site 1 (*) and Site 2 (**) deployment and Phase 5 ends with Site 1 (July 27, 2011, 14:48) and Site 2 (July 29, 2011, 04:51) recovery.

IPS-5 Settings	Phase 1	Phase 2	Phase 3	Phase 4	Phase 5
Start Date	July 26, 2010 15:23* July 28, 2010 05:46**	August 15, 2010 00:00:00	October 15, 2010 00:00:00	December 01, 2010 00:00:00	June 01, 2011 00:00:00
Phase Type	Wave	Wave	Ice	Ice	Ice
Ping Period	5 s	10 s	1 s	2 s	1 s
Base Ping Rate/Frequency	2 Hz	2 Hz	1 Hz	1 Hz	1 Hz
Burst Period	5400 s	5400 s	50 s	120 s	50 s
Burst Length	1024 s	2048 s	1 s	1 s	1 s

Phases 1 and 2 had 1024 and 2048 seconds of 2 Hz wave bursts, respectively, repeated every hour and a half (5400 s) in wave profiling mode that lasted until the middle of October. During phases 1 and 2, ice sampling was done at 5 and 10 second intervals, respectively. Phases 3, 4 and 5 collected data in ice profiling mode as there is little or no open water data exist during this period (mid-October to late July [recovery date]). IPS data collection during phases 3 through 5 had acoustic sampling rates of 1, 2, and 1 second(s) intervals, respectively.

A pressure sensor (Paroscientific Digiquartz), installed on each IPS unit, is used to measure water level changes due to tidal and wind forcing, as well as apparent water level changes arising from depression/tilt of the mooring. The measured acoustic range, after correction for instrument tilt, is subtracted from the water level in order to get an accurate computation of ice keel drafts. The IPS contains pitch/roll sensors, to permit additional data compensation for instrument tilt and also collects near-bottom ocean temperature measurements.

The newer generation of IPS instruments can take compact-flash cards (8 GB as deployed and a maximum 16 GB as of writing). This increased data storage allows for the recording of up to 5 targets per individual ping and a subset of the raw acoustic backscatter profiles. The IPS-5 also has a wave mode, allowing bursts of wave data to be collected at up to 2 Hz. The 122 Alkaline D-cell batteries provided the necessary power to collect over 30 million pings over a 1 year period.

Instrument specification sheets for the IPS-5 instruments used in this project are included in the Project Archive.

2.1.2 ACOUSTIC DOPPLER CURRENT PROFILER (ADCP)

The Acoustic Doppler Current Profiler (ADCP), Sentinel Workhorse series, manufactured by Teledyne RD Instruments of Poway, California, USA was used at Sites 1 and 2. The ADCP technology is widely used for oceanic environmental monitoring applications. Mounted near the sea bottom, the ADCP unit provides precise measurements of ocean currents (both the horizontal and vertical components) at levels within the water column, from near surface to near-bottom. In addition, the ADCP provides time series measurements of the velocity of the pack ice moving on the ocean's surface, as well as near-bottom ocean temperature data.

The ADCP instruments measure velocity by detecting the Doppler shift in acoustic frequency, arising from water current (or ice) movements, of the backscattered returns of upward (20° from vertical) transmitted acoustic pulses. The Doppler shift of the 300 kHz acoustic signals is used to determine water velocities at a vertical spacing of 2 m at Sites 1 and 2. Also, to ensure data returns in winter when there are fewer scatterers in the water column, the ADCPs were reverted to narrowband mode. The Sentinel ADCPs were modified by RDI in 1996 to use the Doppler shift from the ice bottom surface to measure ice velocity as well [this is now a standard option]. The sampling scheme involved 5-minute ensembles composed of 24 water-column pings, interleaved with 3 bottom-track pings.

The data measurements are stored internally on a PCMCIA recorder card(s). Because of the extended 12-month deployment, the internal alkaline battery packs were supplemented with external battery packs (doubles).

Instrument specification sheets for the ADCP instruments used in this project are included in the Project Archive.

2.1.3 CT SENSOR

An SBE-37SMP internal recording conductivity and temperature (CT) sensor was mounted on the IPS-5 frames at both Sites 1 and 2. These CT sensors provided continuous measurements of salinity and temperature for use in adjusting the speed of sound to provide more accurate acoustic ranges (Section 3.1).

Refer to the Project Archive for further specifications on the CT sensors.

2.2 DEPLOYMENT AND RECOVERY

Deployment of the IPS and ADCP moorings at Site 1 and 2 to start the 2010-2011 measurement program was performed in late July 2010, immediately following the recovery of the same pair of moorings to end the previous year's (2009-2010) measurement program, on board the same vessel, *M/V Norseman II*. ASL field personnel boarded the *M/V Norseman II* on July 20, 2010 in Nome, Alaska to carry out the recovery and deployment tasks, which included compass calibrations, instrument tests, and mooring frame assembly. Site 1 deployment was completed on July 27, 2010 by using the spare equipment that was readily available and Site 2 deployment was completed by July 28, 2010. A complete list of all the instruments attached to the mooring frames is given in Table 2-3.

Table 2-3.List of all the instruments (and their serial numbers, if available) placed on each mooring frame.

Site	Mooring Frame	List of instruments (Serial numbers)
Site 1	IPS	IPS-5 (51068); SBE 37SMP (7820); 27 kHz Pinger (2443); CART (30466 and 30973)
	ADCP	ADCP WH-300kHz (8944); ADCP External Battery (3953); 27 kHz Pinger (2885); CART (31374 and 31373)
Site 2	IPS	IPS-5 (51060); SBE 37SMP (6270); 27 kHz Pinger (45106); CART (32897 and 32898)
	ADCP	ADCP WH-300kHz (10985); ADCP External Battery (3441); 27 kHz Pinger (2708); CART (32900 and 32899)

Recovery of the data collected by the moored instruments was carried out in late July 2011 from *MV Westward Wind* (Figure 2-4). The ORE Coastal Acoustic Release Transponders (CARTs) were used to bring the IPS-5 and ADCP moorings to the surface. With a release load of 500 kg, a maximum depth rating of 1000 m and battery lifetime of 1.5 years, they are well suited for the deployments in the Chukchi Sea.

Figure 2-4. *MV Westward Wind*.

The recovery operations started at Site 1 on the morning of July 27, 2011. The ADCP was released and reached the surface around 14:32 (UTC) and the IPS-5 was released and reached the surface around 14:48 (UTC). A preliminary examination of the data indicated that the IPS recorded a full data record. The ADCP, on the other hand, stopped recording data on March 3, 2011 due to underwater connector corrosion on the external battery housing. The recovery operations started at Site 2 on the evening of July 29, 2011 local time. The ADCP was released and reached the surface around 04:24 (July 30, UTC) and the IPS-5 was released and reached the surface around 04:51 (July 30, UTC). The IPS-5 and ADCP recorded full data record at Site 2.

2.2.1 PRE-DEPLOYMENT INSTRUMENTATION CHECKOUT

All the instrumentation had undergone extensive testing at ASL facilities in Canada prior to shipment to the Arctic. The orientations of the ADCP-measured currents were determined at each instrument by using an internal magnetic flux-gate compass. Because of the close proximity of the measurement locations to the north magnetic pole in the Arctic Ocean, and the consequent weakness of the earth's horizontal magnetic field component, regional calibrations of the instrument compass must be carried out. These calibrations were carried out on the beach at the same location as previous year, in Nome, Alaska, away from metallic objects. Calibrations were completed on the first day after ASL field personnel boarded the *MV Westward Wind*, on July 20, 2011.

2.2.2 ON-SITE DATA DOWNLOADING

All 2010-2011 data sets were downloaded from the retrieved instruments onboard the vessel (*MV Westward Wind*), with timing checks made on the instrument clocks to measure the clock drift over the period of the deployment. A preliminary examination of the data indicated that the IPS-5 and ADCP instruments recorded full datasets at Site 2. The IPS-5 at Site 1 recorded a full dataset, while the ADCP stopped recording data prematurely on March 3, 2011 due to underwater connector corrosion on the external battery housing.

All data downloaded during the July 2011 cruise were initially inspected, and found to be of uniformly high quality.

3 DATA PROCESSING

3.1 ICE DRAFT

3.1.1 INTRODUCTION

The processing of the Ice Profiling Sonar (IPS) data involves the conversion of the time-of-travel measurement recorded internally by the IPS unit into a calibrated time-series of ice draft in units of meters at 1 or 2 second intervals. The ice draft time-series is then converted to a spatial (or distance) data series, i.e. the time coordinate is transformed to distance using the measured ice velocities (section 3.1.3). The general approach to the data processing follows that of Melling et al. (1995). The implementation of the procedures, along with many further refinements, have been developed and carried out by ASL personnel since 1997.

The raw data recorded by the IPS instrument consists of the following measured parameters: the time-of-travel to the selected target echo and the amplitude and persistence (duration above a threshold amplitude level) of the target echo. The basic operation of the IPS instrument is outlined briefly below; more details are provided in the IPS hardware and software manuals (ASL Environmental Sciences Inc., 2011a & 2011b). Essentially, the IPS operates in a pulsed mode with its acoustic beam directed toward zenith. A multi-faceted algorithm (Melling et al., 1995) identifies the echo, which is intended to be that of the bottom of the sea-ice, if present, or in the absence of sea-ice, from the ocean-atmosphere interface. The following describes the target selection algorithm:

- Select those echoes that are returned from beyond a minimum range but within a maximum range whose amplitudes and durations (persistence) exceed chosen minimum values (i.e. the echo start amplitude and the minimum persistence).
- From this initial selection, the echoes of longest duration are chosen (up to 5 targets). Choice of the control parameters must be carried out with a view to minimizing the likelihood that the algorithm will select echoes from sources within the water-column as opposed to the ice under-surface.

The time of travel value was converted to a one-way range by applying a first estimate of the speed of sound of seawater, c, in ms^{-1}. For this study the initial value of c was chosen to be 1440 ms^{-1}.

The IPS units when recovered had range data sets of approximately twelve months duration. Given the sampling intervals at Site 1 and Site 2, the total data record for an IPS unit over this time has nearly 18,000,000 logical records of acoustic range and amplitude data. The IPS units also provided measurements of near-bottom pressure, two-components (x and y) of instrument tilt, and the near-bottom ocean temperature.

As expected, the raw IPS data contain “drop-outs” for pings in which an acoustic target exceeding the threshold amplitude was not found. The number of occurrences of such drop-outs was notably higher in the winter months, with drop-out rates of up to 25 percent. Fortunately, the Ice Profiler Sonar model 5 (IPS-5) instruments have a feature where the range to the maximum amplitude value (index target) is also recorded. When drop-outs occur, the index target range value is then used. When a target does exceed the threshold amplitude, the range is calculated using the time of travel to the leading edge of the target profile, at the time when the amplitude reaches the threshold level. However, if a target is below the threshold amplitude, the range is then determined from the time of travel to the peak of the target profile, which would occur at a slightly longer time than the time to the leading edge of the increased amplitudes associated with the sea ice backscatter returns (see Figure 3-1). This bias was corrected for by removing 4 cm from the range when the index target value was used, as determined from empirical comparisons of the time of travel to the leading edge of the sea ice backscatter returns with the time of travel to the maximum amplitude value for many pings having relatively low maximum amplitudes just above the threshold amplitude.

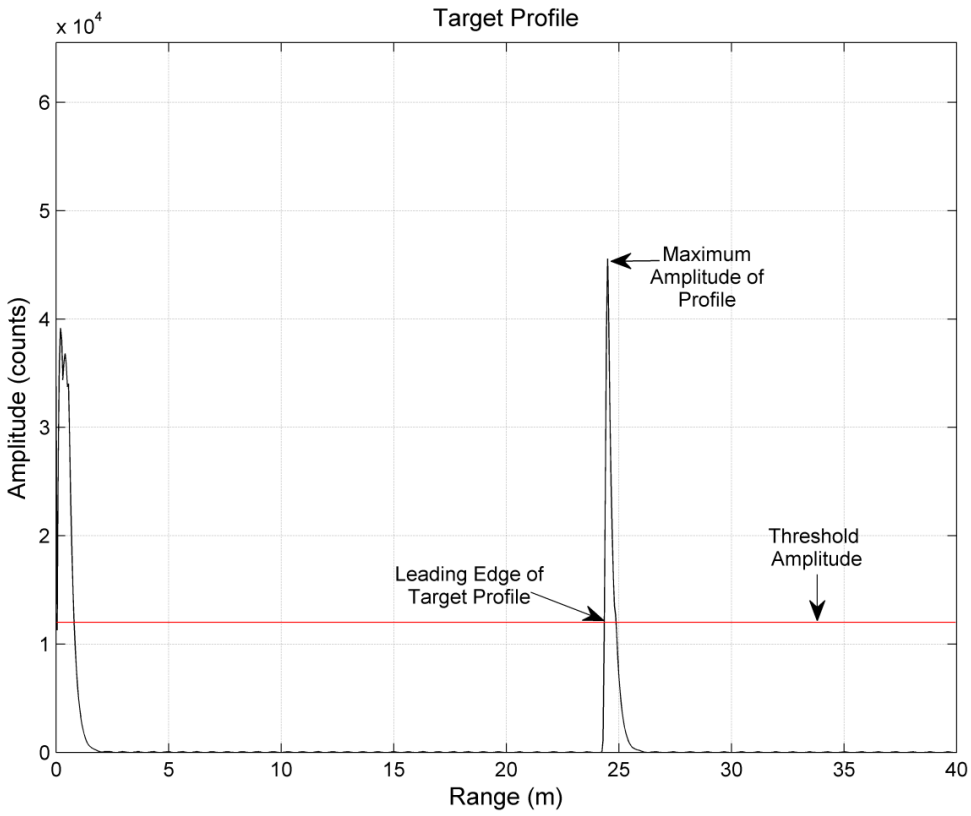

Figure 3-1. An example of a target profile that exceeds the threshold amplitude.

Less frequently, other types of erroneous values occurred in the form of ‘spikes’, i.e. one or a few data points that were markedly inconsistent with the measured neighbouring values. These were removed through automated programs that detected and replaced the erroneous values using linear interpolation. In the IPS datasets, some segments of

consecutive “drop-outs” were found. These segments contained more points than the threshold for allowing automatic interpolation during automated despiking. A method for removing most of these segments was developed (see following section) and a small number of segments that could not be edited automatically were reviewed manually.

3.1.2 PROCESSING OF ICE DRAFT TIME SERIES

The processing of IPS ice draft data uses a well-established methodology that has been developed from processing many dozens of IPS data sets over the past two decades (Melling et al., 1995 and Fissel et al, 2008). Based on this experience, ASL developed a suite of MATLAB data processing and analysis software (ASL Environmental Sciences Inc., 2011) which was used in the processing of the Site 1 and Site 2 IPS data sets from July 2010 to July 2011. Typical data processing consists of the following steps, all in accordance with the references given above, however, every data set is unique and the general processing procedures outlined below are occasionally customized as necessary.

1. Converting raw IPS data from the internal binary format in the instrument to nominal engineering units.
2. Correcting the timing characteristics of the IPS data files for the effects of instrument clock time drift. The correction is derived from a comparison of instrument start and stop times with times from an independent clock recorded on start-up and shut-down of the instrument. Clock drifts are typically small, i.e. 0 to 10 minutes over deployments of several months.
3. Manually reviewing time-series plots of all measured raw data. In addition to the anomalous data records in the raw data, the data have not yet been corrected for variations in water levels due to tides and other effects, changes in the speed of sound in the water column, and the effects of instrument tilt. This review is primarily focused on finding significant data issues including instrument failure, large data gaps, high fractions of anomalous data values and ice events within the lockout range.
4. Automatically correcting for double bounce effects. The acoustic signal transmitted by the IPS can transit the water column multiple times. Under certain deployment conditions, this effect is recorded resulting in range measurements that are too high. If available in the ping data, these records are replaced with more appropriate targets; otherwise, the range value is corrected arithmetically or by interpolation.
5. Removing unnecessary data at the start and end of the data record related to out-of-water time before deployment and after recovery.
6. Automated editing of range records associated with no targets. This step is performed with a combination of interpolation and replacement with the range corresponding to the maximum amplitude recorded during acoustic backscattering.
7. Automated removal of range values < 0.01 m to remove range drop-outs, and automated editing of range records with values considered to be too high. The detection threshold for high range values is calculated as: *instrument depth at high tide + buffer*. The *buffer* value avoids clipping of wave peaks and is determined through a manual review of the raw data.

8. Masking of segments of range data that show evidence of large waves. This prevents the records corresponding to the wave extremes from being identified as spikes in the later automated despiking steps.
9. Automated despiking of acoustic and ancillary data. This includes at least two iterations to remove anomalous features in the range data with lengths of one to four records. Appropriate detection thresholds are first estimated using a representative ice velocity. These thresholds are further refined through trial despiking iterations and reviews of the results.
10. Patching of the previously masked segments of range data back into the data record.
11. Manually reviewing the edited data set for any additional spikes or suspect values. These may include targets within the lockout range and short duration targets due to bubbles associated with strong winds and large waves. The amplitude data is often helpful in classification of range features during this step.
12. Calculating ice drafts using IPS range data, calculated water levels, and IPS tilt magnitudes. The ice drafts are then corrected for variations in the speed of sound.
13. Manually identifying and flagging segments of open water and segments of ice contaminated by waves. Manually identifying and flagging or interpolating sections of data contaminated by high tilts and/or surface wave effects.
14. Automatically identifying and interpolating negative ice draft spikes < -0.05 m.

Any manual or automated processing step that results in interpolation of range data points is restricted to interpolation over 10-30 seconds depending on the initial review of the data. Segments longer than these time spans undergo an extra step; if the neighbouring records differ by less than 10 cm than the segments and the segments are shorter than several minutes then the segment is interpolated. The remaining segments are investigated and edited manually. Due to the significantly smaller size of ancillary datasets, any manual or automated processing step that results in interpolation of ancillary data is manually reviewed. The numbers of erroneous data values detected and removed using the procedures described above are summarized in Table 3-1 and Table 3-2.

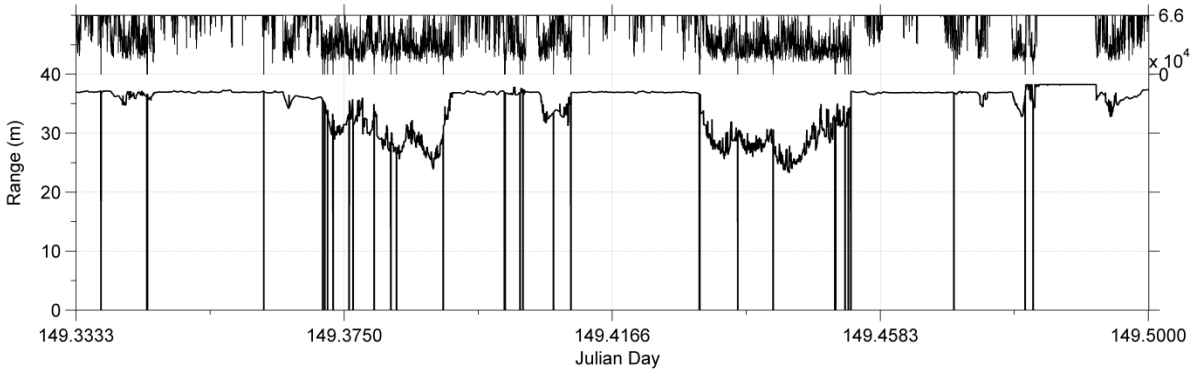

Figure 3-2. An example of the unedited range and amplitude (top panel) data measured by an IPS-5 showing a period characterized by sea-ice floes and some range "drop-outs".

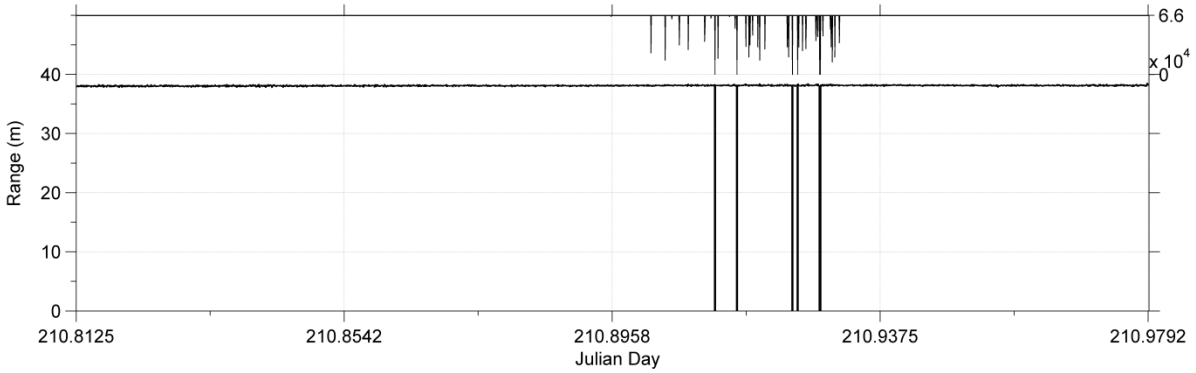

Figure 3-3. An example of the unedited range and amplitude (top panel) data measured by an IPS showing a period following the main part of the ice season. This is an example of 'rough open water' in which the returns obtained from targets below mean sea level are believed to result from the troughs of ocean waves and from bubbles located beneath the surface.

Table 3-1. Summary of the two main stages of ice draft data processing for Site 1, giving number of data records having errors that were detected and replaced or flagged. Where applicable, the number of segments of edited data and/or the percentage of the total number of points is provided in parentheses. The final number of replaced records excludes the drop-outs replaced by the target range value.

		Site 1				
	Phase	**1**	**2**	**3**	**4**	**5**
	Start date/time	26-Jul-2010 15:23:22	15-Aug-2010 00:00:41	15-Oct-2010 00:02:25	01-Dec-2010 00:03:45	01-Jun-2011 00:08:56
	Stop date/time	15-Aug-2010 00:00:38	15-Oct-2010 00:02:17	01-Dec-2010 00:03:45	01-Jun-2011 00:08:56	27-Jul-2011 14:32:53
	Sample interval	5.0000169	10.0000307	1.0000238	2.0000085	1.0000238
Range data	**# drop-outs**	7636	182	390,096	2,035,187	66,437
	# records as lower out-of-bound	0	0	0	0	0
	# records as upper out-of-bound	0	0	0	0	0
	# records as single negative spikes	0	0	8	1,256	52
	# records as single positive spikes	0	0	18	1,330	52
	# records as double negative spikes	0	0	0	60	0
	# records as double positive spikes	0	0	0	64	0
	# records as triple spikes	0	0	0	9	0
	# records as quadruple spikes	0	0	0	0	0
	# records replaced by manual editing	0	0	5	273	1
Ice draft data	**# records flagged as bad**	0	6	257	908	513
	# records replaced manually	0	0	0	12	6
	# records flagged as open water/thin ice	334,522 (100.00%)	527,040 (100.00%)	2,527,945 (62.25%)	48,680 (0.62%)	4,697,640 (96.06%)
	Total # of records	334,522	527,046	4,060,751	7,862,497	4,890,111
	Final # of replaced data records (excluding drop-outs and open water/thin ice)	0 (0.00%)	6 (0.001%)	288 (0.007%)	3,912 (0.05%)	624 (0.01%)

Table 3-2. Summary of the two main stages of ice draft data processing for Site 2, giving number of data records having errors that were detected and replaced or flagged. Where applicable, the number of segments of edited data and/or the percentage of the total number of points is provided in parentheses. The final number of replaced records excludes the drop-outs replaced by the target range value.

	Site 2					
	Phase	**1**	**2**	**3**	**4**	**5**
	Start date/time	28-Jul-2010 05:46:10	15-Aug-2010 00:00:30	15-Oct-2010 00:02:13	01-Dec-2010 00:03:32	01-Jun-2011 00:08:38
	Stop date/time	15-Aug-2010 00:00:30	15-Oct-2010 00:02:07	01-Dec-2010 00:03:31	01-Jun-2011 00:08:35	30-Jul-2011 04:50:46
	Sample interval	5.0000164	10.0000138	1.0000030	2.0000060	1.0000035
Range data	**# drop-outs**	6,281	1,472	76,710	330,702	62,375
	# records as lower out-of-bound	0	0	0	0	0
	# records as upper out-of-bound	0	0	0	0	0
	# records as single negative spikes	0	0	28	1,565	42
	# records as single positive spikes	0	0	29	1,873	65
	# records as double negative spikes	0	0	0	66	6
	# records as double positive spikes	0	0	0	86	8
	# records as triple spikes	0	0	0	0	0
	# records as quadruple spikes	0	0	0	0	0
	# records replaced by manual editing	0	0	196	302	0
Ice draft data	**# records flagged as bad**	0	0	0	27	56
	# records replaced manually	0	0	486	201	11
	# records flagged as open water/thin ice	306,890 (100.00%)	527,047 (100.00%)	2,036,516 (50.15%)	386,619 (4.92%)	4,993,567 (97.64%)
	Total # of records	306,890	527,047	4,060,852	7,862,525	5,114,507
	Final # of replaced data records (excluding drop-outs and open water/thin ice)	0 (0.00%)	0 (0.00%)	739 (0.02%)	4,120 (0.05%)	188 (0.004%)

3.1.2.1 COMPUTATION OF ICE DRAFT

The next stage of data processing deals with converting the measured ranges into ice drafts. The ice draft, *d*, is derived from the edited ice ranges, *r*, and the water level, η. η is computed from the measured ocean bottom pressure, P_{btm}, and atmospheric pressure, P_{atm}, as follows:

$$\eta = \frac{(P_{btm} - P_{atm})}{\rho \cdot g} \qquad (1)$$

where g is the calculated local acceleration due to gravity and ρ is the density of sea water. Table 3-3 lists the values of these parameters for the IPS measurement sites. Measurements of P_{atm} were obtained from Wainwright, Alaska. The ice draft, *d*, is then computed from the edited range data as:

$$d = \eta - \beta \cdot r - \Delta D \qquad (2)$$

where β is a calibration factor for the actual mean speed of sound in sea-water, *c*, relative to the initially assumed value of 1440 ms^{-1} and ΔD is the distance of the pressure sensor below the acoustic transducer. Note that the sign convention for ice draft is positive downwards, i.e. a draft of +5 m represents an ice keel which extends 5 m below sea level.

Table 3-3. Values used in the calculation of water level for Site 1 and Site 2.

Site	ρ (kg m^{-3})	g (m s^{-2})	ΔD (m)
Site 1	1026.20	9.826658	0.1686
Site 2	1026.47	9.826646	0.1854

The density values were derived from historical temperature-salinity-density data sets available for the Chukchi Sea and from the measured density values, as derived from the Conductivity-Temperature (CT) instrument data available at both Site 1 and Site 2 (section 3.5). The CT derived densities represent an upper bound of the actual water column density values due to density stratification of the water column, especially during summer and fall.

Corrections were also made for the effect of instrument tilt on the measured ranges. Generally, if not corrected for, this source of uncertainty would result in errors of a few centimetres or less on the ice drafts.

3.1.2.2 RANGE CORRECTION FACTOR

The factor, β, applied to the measured range in equation (2) represents the ratio of the actual sound speed to the nominal value of 1440 ms^{-1}. To determine β, open water segments in the range data set were selected (i.e. *d = 0* in equation 2 above) and β was empirically computed. The empirical values of β seem to follow reasonably well the variation in the local speed of sound as computed from the measured near-bottom temperatures obtained from the IPS values at the measurement locations.

A fit was made to determine the time varying β values over the full duration of the time series data based on:

- the empirical computations of β realized from periods of open water;
- the computed effect of near-bottom temperatures on c (using a fixed salinity and the speed of sound algorithm of Urick, 1983).

Plots of the time varying $\Delta\beta$ values are shown in Figure 3-4 and Figure 3-5 where:

$$\Delta\beta = (\beta - 1) \times 1000 \qquad (3)$$

The empirically derived values of β were applied through equation 2 to the edited range data to compute ice drafts.

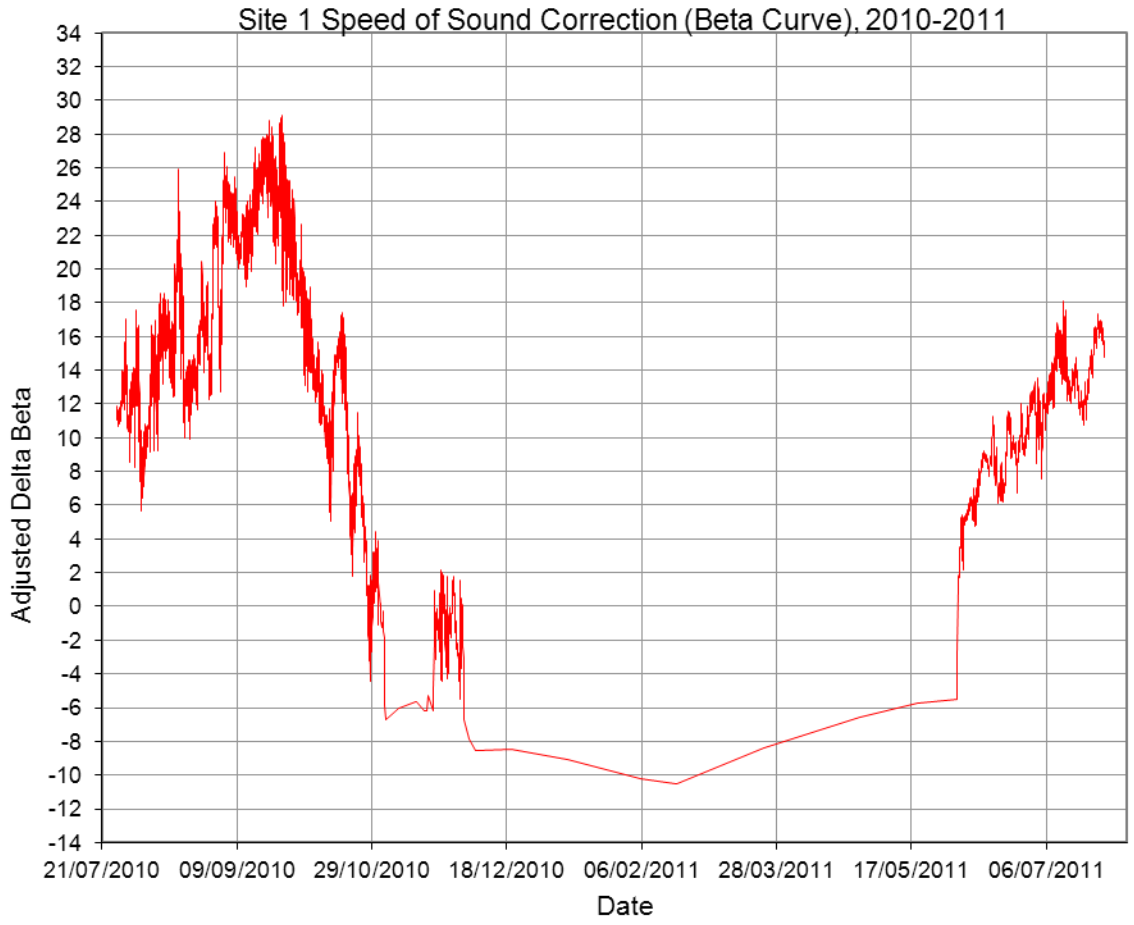

Figure 3-4. Plot of the time varying Δβ values for Site 1.

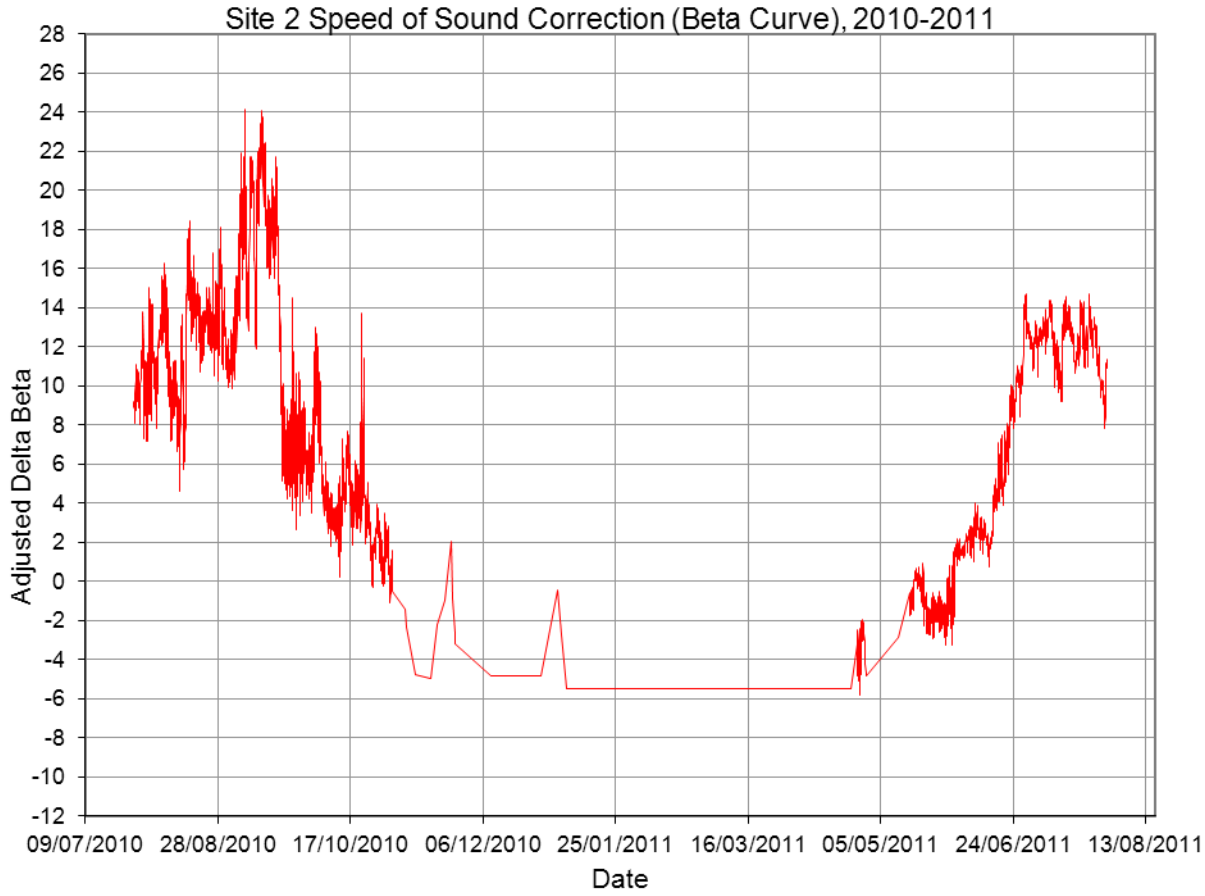

Figure 3-5. Plot of the time varying Δβ values for Site 2.

3.1.3 PROCESSING OF ICE DRAFT SPATIAL SERIES

The ice draft time series data sets were converted to a distance (or spatial) series using the processed ADCP ice velocities (Section 3.3). The resulting spatial data file contained east and north displacements and ice drafts beginning at zero distance, or ice path length. The cumulative distance was calculated using the east and north displacements for each sample, incrementing until the end of the file.

The ice draft was sampled at regular time intervals (once every 1 or 2 second[s]). However, due to the irregular motion of the ice cover, the resulting distance-series was unevenly spaced in distance. To account for this, the distance-series was interpolated to regular increments through the use of a double-weighted double-quadratic interpolation scheme. As shown in Figure 3-6, the value Y_1 represents the value obtained from a quadratic interpolation using two points to the left and one to the right of x_i {($y(u_{i-1})$, $y(u_i)$ and $y(u_{i+1})$} and Y_2 represents the interpolated value using two points to the right and one to the left of x_i {($y(u_i)$, $y(u_{i+1})$ and $y(u_{i+2})$}. In the figure, the desired regularly spaced interpolation point is x_i, and the measurement locations are given by u_{i-1}, u_i, u_{i+1} and u_{i+2}. The two interpolated values were then averaged using a weight based on the distance between points and on the

change in draft between points. The double weighting scheme, as shown in the equation, was adopted to avoid overshoots in areas of sudden draft changes.

In order to represent the ice drafts at low ice velocities, the draft data file was interpolated to 0.10 m distances then block averaged to 1.0 m distances. The 1.0 m spacing represents a distance slightly less than the width of the IPS sonar footprint at an average 30 m water depth and the smallest resolvable distance.

As part of reviewing the data for open water occurrences, a manual review was conducted to identify data segments which contain thin ice in waves (denoted as “waves in ice”). The flagging of long sections of open water occurred at times when air temperatures rose above 0 degrees, and low concentrations of sea-ice with only occasional large keel occurrences being detected.

$$y(x_i) = \frac{Y_1[y(u_{i+2}) - y(u_{i+1})][x_i - x(u_{i+1})] + Y_2[y(u_i) - y(u_{i-1})][x_i - x(u_i)]}{[y(u_{i+2}) - y(u_{i+1})][x_i - x(u_{i+1})] + [y(u_i) - y(u_{i-1})][x_i - x(u_i)]}$$

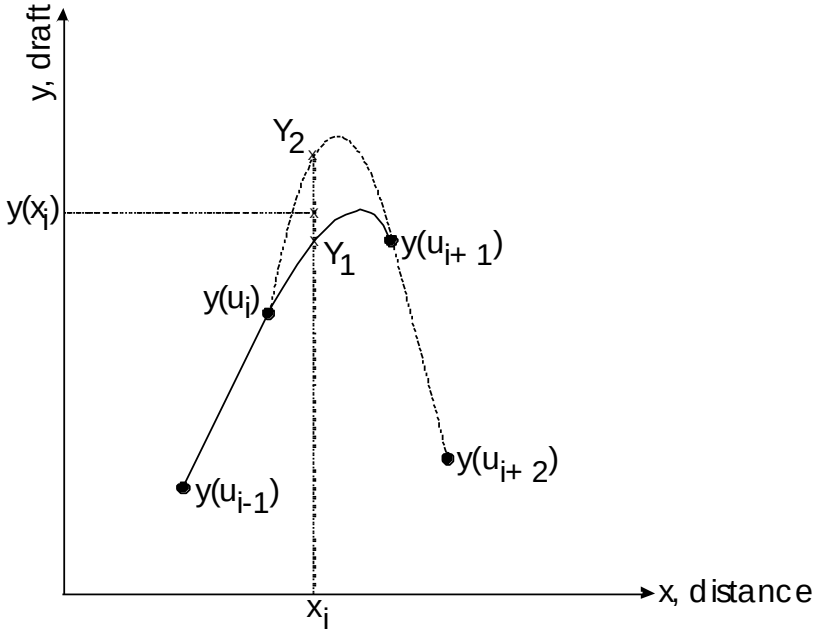

Figure 3-6. The double quadratic interpolation method used to convert the ice draft time series into a spatial series.

The final step in reviewing the spatial series was to search for unrealistic features. These features were generally located where the uncertainty in the ice velocities was largest. Modifications were made to the ice velocities, and the spatial series were recalculated.

3.1.4 SUMMARY OF ICE DRAFT

The measured acoustic range, pressure, and tilt data channels recorded by the IPS-5 instrument, combined with sea level pressure measurements, were processed and analyzed to compute time- and distance-series of ice keel drafts. Following a careful and thorough review of the ice drafts, final edited versions of ice draft time- and distance-series were created and plotted. The duration of the ice draft records with time and distance at the measurement sites are shown in Table 3-4 and Table 3-5.

Sea ice was first detected by the ADCP on November 2 at both sites. The ice had mostly disappeared after June 3 at Site 1 and after June 2 at Site 2, but a few ice keels were present on an intermittent basis until June 5 at Site 1 and June 14 at Site 2. Compared to the previous year (summer of 2010), ice clearing started at Site 1 around the same time (June 3, 2011 vs. June 2, 2010), followed by a few days of scattered ice keels transiting through the site. Clearing of the sea ice started at Site 2 a couple of weeks later (June 2, 2011 vs. May 16, 2010), however, the period of scattered keels transiting through the site was shortened by more than a month (June 14, 2011 vs. July 22, 2010), indicating a relatively sudden shift from ice-infested to ice-free conditions at both sites.

The distance-series of ice drafts have interruptions during periods of reduced ice concentrations, which results in unreliable ice velocity measurements.

Table 3-4. Final time-series and distance-series segments of valid data for Site 1.

Site 1		
Time-Series		
Phase	**Start Date / Time**	**Stop Date / Time**
1	26-Jul-2010 15:23:22	15-Aug-2010 00:00:38
2	15-Aug-2010 00:00:41	15-Oct-2010 00:02:17
3	15-Oct-2010 00:02:25	01-Dec-2010 00:03:45
4	01-Dec-2010 00:03:45	01-Jun-2011 00:08:56
5	01-Jun-2011 00:08:56	27-Jul-2011 14:32:53
Distance-Series **Note: ADCP stopped recording on March 2, 2011		
Segment	**Start Date/Time**	**Stop Date/Time**
1	02-Nov-2010 18:17:59	21-Nov-2010 04:03:27
2	02-Dec-2010 02:03:55	02-Mar-2011 04:36:16

Table 3-5. Final time-series and distance-series segments of valid data for Site 2.

Site 2		
Time-Series		
Phase	**Start Date / Time**	**Stop Date / Time**
1	28-Jul-2010 05:46:10	15-Aug-2010 00:00:30
2	15-Aug-2010 00:00:30	15-Oct-2010 00:02:07
3	15-Oct-2010 00:02:13	01-Dec-2010 00:03:32
4	01-Dec-2010 00:03:32	01-Jun-2011 00:08:35
5	01-Jun-2011 00:08:38	30-Jul-2011 04:50:46
Distance-Series		
Segment	**Start Date/Time**	**Stop Date/Time**
1	02-Nov-2010 15:16:28	23-Nov-2010 11:46:47
2	24-Nov-2010 22:31:48	02-Jan-2011 15:32:23
3	04-Jan-2011 00:32:24	28-Apr-2011 13:19:07
4	29-Apr-2011 17:34:08	18-May-2011 10:49:25
5	22-May-2011 05:19:29	02-Jun-2011 15:34:39

The final versions of the ice draft data series (Project Archive) are considered to be generally accurate to within 0.3 m for the largest keel features and to somewhat better accuracies, to as good as 0.05 to 0.1 m, for typical ice drafts, based on the estimated uncertainties in the various stages of data processing. These accuracy estimates are consistent with inspections of the final edited data sets for data segments consisting of open water intervals when the ice draft, after allowing for any ocean wave effects, should be identically zero.

The processed ice draft data files are provided as part of the Project Archive, both as time-series data and as distance-series data. Plots of the distance-series ice drafts are also provided in the Project Archive for each of the segments of continuous good ice velocities. In the ice draft data files, segments containing waves in ice were flagged to -500, segments containing open water were flagged to -200, and segments of bad data were flagged to -9999.

3.2 OCEAN WAVE DATA DERIVED FROM ICE PROFILER

The range data from the ASL Ice Profiler was used to derive information on ocean waves when sea ice was not present. The processing of the IPS-5 data sets involved the conversion of the time-of-travel measurement recorded internally by the instrument, to an edited time series of wave heights. Wave autospectra were computed using the Fast Fourier Transform (FFT) technique. Two quantities, or non-directional wave parameters, were then computed from the autospectra: the significant wave height (H_s), calculated as four times the square root of the area under the autospectral curve; and the peak period (T_p), calculated as the corresponding period at which the autospectra reaches its maximum. A third parameter, H_{max}, was obtained from the time-series by using the largest crest to trough distance in the segment.

The data was collected in five phases consisting of different sampling intervals. Wave data for phase 1 (July 26/July 28, 2010 [Site 1/ Site 2] to Aug 15, 2010) and phase 2 (Aug 15, 2010 to October 15, 2010) were collected in wave burst mode at 2 Hz. The burst size was 2048 points sampled at 2 Hz for phase 1 and 4096 points sampled at 2 Hz for phase 2 (every 1.5 hours). The significant wave height (H_s) and the peak period (T_p) were computed from the autospectra using cutoffs of 20 seconds (0.05 Hz) to 1 second (1 Hz) using all of the 2048 or 4096 points.

Wave data for phase 3 (October 15, 2010 to December 1, 2010), phase 4 (December 1, 2010 to June 1, 2011) and phase 5 (June 1, 2011 to July 27/July 30, 2011 [Site 1/Site 2]) were collected in ice profiling mode. The data for phases 3 and 5 was sampled at 1 Hz and the smallest resolvable period was 2 seconds (0.5 Hz). For phase 4, when waves are unlikely to be present, the ranges were sampled at 2 second intervals (0.5 Hz) and the smallest resolvable period was 4 seconds (0.25 Hz). Wave parameters were calculated using 3600 points (hourly intervals for phases 3 and 5; 2 hour intervals for phase 4) for these ice profiling mode phases.

Ocean waves occurred throughout most of phase 5, part of phase 3, with interruptions caused by ice in the area, and during the first day of phase 4 and on January 3, 2011. During phase 3 and phase 4, the high frequency content in most of the spectra was damped out, likely due to ice in the region.

For both data sets, the acoustic travel time was converted to a one-way range (distance from the IPS-5 to the air/water interface) by applying an estimated speed of sound in seawater of 1440 m/sec. Steps in the data processing consisted of:

1. Automated removal by linear interpolation of erroneous values that occur with the following attributes:
   - Out-of-range values
   - Null values
   - Statistical outliers

2. Trimming the start and end dates corresponding to the start and end of good data.
3. Applying a tilt correction using the recorded tilt values. For phases 1 and 2, the range and tilt were measured at 0.5 s intervals and each range was corrected using the corresponding tilt value. In Phases 3, and 5, the tilt values were recorded at 50 second intervals and was smoothed using a 31 point running average to reduce the effects of aliasing. The tilts were then interpolated to the 1-second range sampling interval. In Phase 4, the tilt values were recorded at 120 second intervals, smoothed using a 15 point running average, and then interpolated to the 2-second range sampling interval.
4. Manual examination of the time series plots for remaining spikes, bubble clouds, and ice. Spikes were replaced by linear interpolation and bubble clouds were replaced with 'flag' values (-9999). Ice data was also flagged.
5. Computing and plotting the autospectra using the 2048 and 4096 point bursts (~17 and ~34 minute) for phases 1 and 2 at 1.5 hour intervals. For phases 3, 4, and 5, 3600 points (1, 2, and 1 hours) were used to compute the autospectra. The significant wave height (H_s) and the peak period (T_p) were computed from the autospectra. If more than 50% of the data in a burst was flagged, the H_s and T_p values are set to –9999. For all phases, the peak period was flagged if the significant wave height was less than 0.1 m.
6. Manually reviewing each autospectral curve and the computed values for H_s and T_p.
7. Manually reviewing the Hmax values, and where necessary, reviewing and editing the time series of tilt corrected ranges.

Detailed processed results for each of the study sites are presented in Section 4.5 and are also included in the Project Archive.

3.3 ICE VELOCITY

3.3.1 INTRODUCTION

Ice velocity measurements were made with an Acoustic Doppler Current Profiler (ADCP) operated from the seabed (section 2.1.2), using the "Bottom-Track Upgrade" feature of the Teledyne RD Instruments Sentinel Workhorse. The ADCP's at Site 1 and Site 2 recorded ice velocities at 5 minute sample intervals. Each measurement was derived using the observed Doppler shifts as realized from the four individual acoustic beams (each beam was oriented at a 20 degree angle from the vertical). Each 5 minute water velocity sample is an ensemble average of multiple acoustic water column pings. Each 5 minute ice velocity sample is an ensemble average of special "bottom tracking" pings which are used only for ice tracking and not for water column ocean current profiles. The details of the number of ADCP pings for each measurement ensemble are given in Table 3-6.

Table 3-6. Summary of ADCP configurations.

	Site 1	Site 2
	2010-2011	
Water Pings	24	24
Bottom Pings	3	3
Cell Size (m)	2	2
Processing Bandwidth	Narrow Band	Narrow Band

According to the manufacturer, the accuracy of the "bottom track" velocity measurements is:

0.7 cm s^{-1}/(no. of pings per ensemble)$^{1/2}$. The accuracy of ice velocity measurements may be degraded because of the weak scattering coefficient from sea ice (Garrison et al., 1991); scattering energy from the seabed, which the manufacturers' specification is based on, is expected to be generally larger than that from sea-ice. However, the ADCP instruments have been demonstrated to effectively track ice velocities under at least some ice conditions (Belliveau et al., 1990; Melling et al., 1995).

Use of the ADCP for ice velocity measurements presents some special problems not encountered when used for bottom tracking (Melling et al., 1995):

Open water conditions: poorer accuracies for measurements of ice velocities under largely open-water conditions; under these conditions, the ADCP measurements are too noisy to be meaningful due to the rapid movement of the new targets (air bubbles and very short, capillary waves on the ocean surface) in response to the energetic motion of ocean waves. Due to the separation of the four acoustic beams, the wave-dominated velocities are unlikely to be equal within each beam. The assumption of uniform velocities among the four beams is fundamental to the operation of the ADCP instrument. As a result, the derived velocity is very noisy and has little information content. Such occurrences of noisy velocities associated with open water conditions are generally indicated by marked increases in the values of the vertical and error velocity components (the error velocity component is indicative of the degree of divergence in the Doppler velocities from each of the four acoustic beams).

Smooth ice: the occurrence of very weak echoes from smooth first year ice providing poor signal-to-noise ratio for velocities, so that the precision of the ice velocities is degraded.

Uncertainties from smooth ice were not found to be a problem in the present ice velocity data set. However, episodes of open water or very low ice concentrations were often apparent in the ice velocity data set.

3.3.2 PROCESSING ICE VELOCITIES

The procedures for processing the ice velocity data (using the oceanographic direction convention of motion towards rather than the wind direction convention) involved the following sequence of tasks, after applying the compass calibration corrections to the ADCP directional data:

1. The ice velocities were screened for Correlation < 64, Amplitude < 50 and Verror > 5 cm/s, compass corrected to geographic coordinates, and then averaged from 5 minute to 15 minute sampling intervals.
2. Prepare plots of raw east, north, vertical and error velocity channels.
3. Identify periods of probable open water for each data record using the plots from step (1) and other available information, including ice profiling sonar records supplemented by ice charts, and satellite imagery. For these periods, set the values of the horizontal velocity components to flag values of –9999. The first part of the time series records, when sea ice had not yet entered the area, or was of very low concentration, is also flagged.
4. Identify horizontal velocity values exceeding the out-of-bound threshold in absolute value (120 cms^{-1}).
5. Identify horizontal velocity values associated with error velocities exceeding 10 cm/s in absolute value.
6. Identify single point ‘spikes’ in each component of the horizontal velocities. A single point spike is where two successive first difference values exceed a 4 cm/s single point threshold and are opposite in sign.
7. Identify ‘double spikes’ exceeding a double spike threshold in each component of the horizontal velocities. A double spike consists of two consecutive points, both of which are either larger or smaller than the preceding and following points by more than the double spike threshold of 5 cm/s.
8. Identify ‘triple spikes’ exceeding a triple spike threshold in each component of the horizontal velocities. A triple spike consists of three consecutive points which are smaller than the preceding and following points by more than triple spike threshold, 6 cm/s, but whose middle points may not change by more than one third of the triple spike threshold from their respective leading neighbours.
9. Identify ‘quadruple spikes’ exceeding a quadruple spike threshold in each component of the horizontal velocities. A quadruple spike consists of four consecutive points which are smaller than the preceding and following points by more than quadruple spike threshold, 7 cm/s, but whose middle points may not change by more than one third of the quadruple spike threshold from their respective leading neighbours.
10. For all suspect values found as above in items 4 to 9, the values are replaced by linear interpolation, over all individual segments with durations of less than three hours (one eighth the duration of the tidal signal which is predominantly diurnal). For

longer segments of erroneous or suspect data, the values are replaced with flag values (-9999) and reviewed again in step 11.

11. Plots of the edited data sets (following step 10) are prepared and manually reviewed. Any remaining suspect values are manually edited using the ASL_EDIT display/editing software package. These suspect values are generally determined as being anomalous from adjoining values at nearby times and at nearby velocity bins containing data consistent with measurements on either side of the values in question.
12. Identify data segments where low ice concentrations increase the uncertainties in the ice velocities to unacceptable levels by further examination of the now-edited ice velocity times series, ice profiling sonar range plots and ice charts.
13. Reconstruct these sections, if possible, using nearby ice velocities or upper level ocean current measurements from the same site. If the ice velocities cannot be reconstructed, then flag the values as unreliable using –9999.
14. Plot the fully edited ice velocity data file to evaluate and continue editing, as required.

At Site 1 and Site 2, open water was encountered until the ice finally started to form in early November. There was then a period of open water or low ice concentrations which lasted over a week at site 1 until the ice formed again in early December. The ice remained at Site 1 until early March, which is when the Site 1 ice velocity instrument failed. At Site 2, the open water interval in November was only a few days in duration. Similarly, there were open water intervals of a few days in duration in January, April, and May. Open water in the form of low ice concentrations arrived on 2 June, 2011 and remained through the end of the data record. A summary by site of the start and end times of the periods of valid ice velocity measurements is given in Table 3-7.

Time series plots of the ice velocities are presented in Figure 3-7 and Figure 3-8. The plots show the major and minor components at Site 1 and Site 2, respectively. Segments of bad data/open water are denoted by gaps in the time series. The direction of the major ice drift component, including the positive major component, is tabulated in Table 3-8. At Site 1, the ice motion was oriented from 65° to 245° (245º positive) and at Site 2 the motion was oriented from 78° to 258° (258º positive). This rotation is optimized to maximize the variance in the major current component. The minor current component is perpendicular to the major current component.

Table 3-7. Summary of segments of the ice velocity data sets that were judged to be reliable or unreliable. Unreliable data includes open water.

Site 1 **Note: ADCP stopped recording on March 2, 2011			
Valid Date Start	**Valid Data End**	**Bad Data Start**	**Bad Data End**
		26-Jul-2010 15:15	02-Nov-2010 18:02
02-Nov-2010 18:17	21-Nov-2010 03:48	21-Nov-2010 04:03	02-Dec-2010 01:48
02-Dec-2010 02:03	02-Mar-2011 04:21		
10565 bad data points out of 20982 total for entire record (50.4%)			
1049 bad data points out of 11466 total from first ice to last ice (9.1%)			
Site 2			
Valid Date Start	**Valid Data End**	**Bad Data Start**	**Bad Data End**
		28-Jul-2010 06:15	02-Nov-2010 15:01
02-Nov-2010 15:16	23-Nov-2010 11:46	23-Nov-2010 12:01	24-Nov-2010 22:16
24-Nov-2010 22:31	02-Jan-2011 15:32	02-Jan-2011 15:47	04-Jan-2011 00:17
04-Jan-2011 00:32	28-Apr-2011 13:19	28-Apr-2011 13:34	29-Apr-2011 17:19
29-Apr-2011 17:34	18-May-2011 10:49	18-May-2011 11:04	22-May-2011 05:04
22-May-2011 05:19	02-Jun-2011 15:34	02-Jun-2011 15:49	30-Jul-2011 03:05
15608 bad data points out of 35220 total for entire record (44.3%)			
742 bad data points out of 20354 total from first ice to last ice (3.6%)			

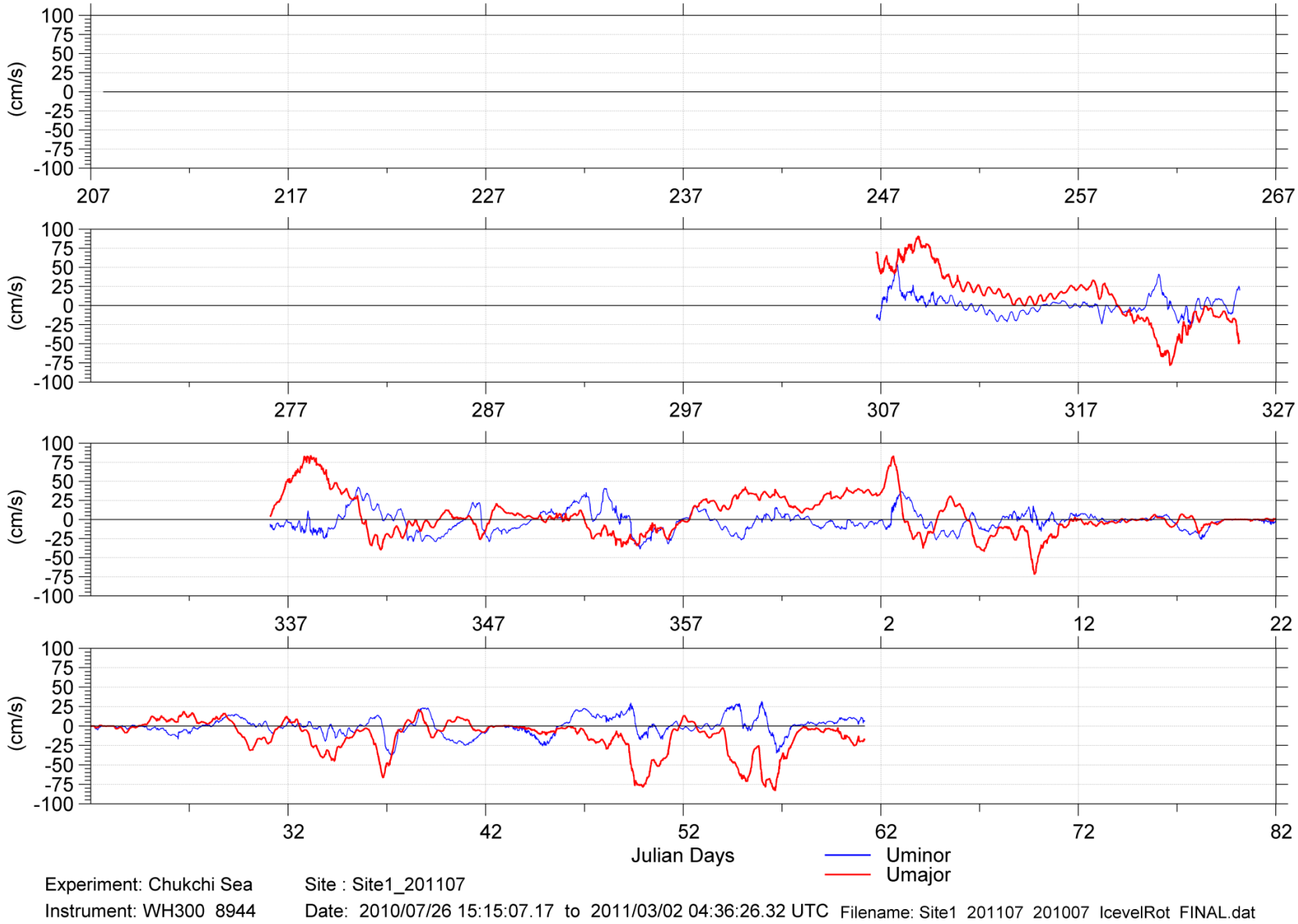

Figure 3-7. Plot of the edited ice velocity for Site 1 as a time series of the major and minor components of the ice velocity.

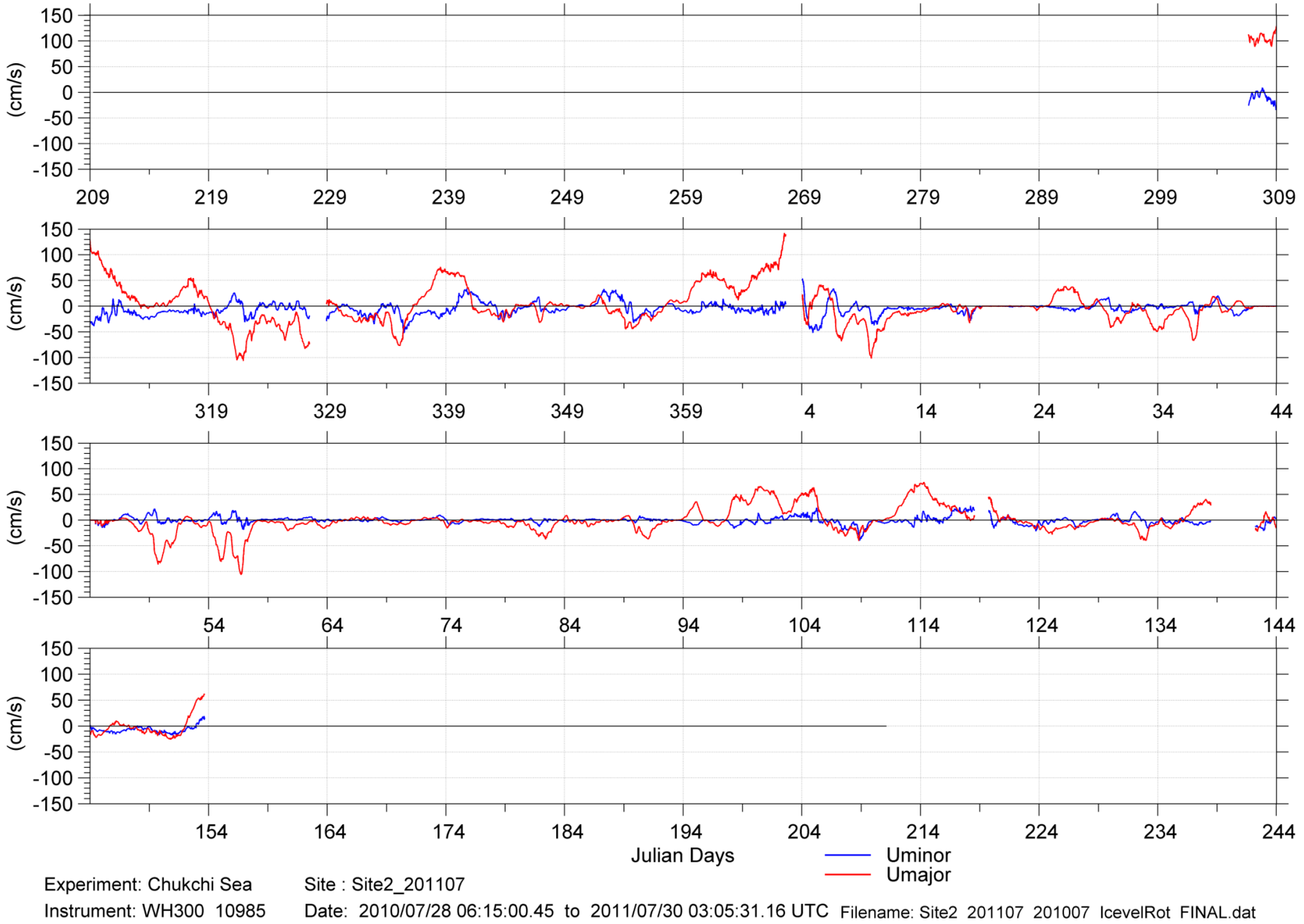

Figure 3-8. Plot of the edited ice velocity for Site 2 as a time series of the major and minor components of the ice velocity.

Table 3-8. Summary of the major current direction for the ice velocities at each site.

	Current Direction (°)	Heading of Positive Umajor (°)
Site 1	65 - 245	245
Site 2	78 - 258	258

Table 3-9. Summary of the number of ice velocity points that were edited at each site.

	Site 1		Site 2	
	East/ West	North/ South	East/ West	North/ South
Interpolated, Verr > 10 cm/s	6	6	108	133
Out of Range	2	0	50	4
Single Spike	113	117	237	268
Double Spike	72	68	210	206
Triple Spike	6	6	24	18
Quad. Spike	8	0	16	24
Manual Edit	944	1086	1326	1281
# Points Edited (%)	1151 (5.5%)	1283 (6.1%)	1971 (5.6%)	1934 (5.5%)
# Flags in Raw Data (%)	6538 (31.2%)		4176 (11.9%)	
# Flags Final (%)	10565 (50.4%)		15609 (44.3%)	
Total Pts	20982		35220	

3.3.3 SUMMARY OF ICE VELOCITY

Reliable ice velocity measurements were obtained at both measurement sites starting from November 2010, when new sea-ice formation began. At Site 1, the ADCP was recovered on July 27, 2011, but was not pinging at recovery. The last recorded data record was on March 2, 2011 and an examination of the battery pack determined that there was underwater connector corrosion. At Site 2, there were no issues with the ADCP and the instrument collected a full data record.

The ice velocities at the measurement sites exhibited coherent variations, as can be seen by the many similarities between the time series plots (Figure 3-7 and Figure 3-8). During the fall season the ice is constantly moving while ice is forming and high winds are prevalent, compared with the winter and spring where periods of slow-motion events are observed. The number of slow-motion points in each month is summarized in Table 3-10. A MATLAB function was written to locate slow motion events. To qualify as an event, a sequence of points had to be less than 0.5 cm/s at every point, and the duration had to exceed 4 hours. The proportion of slow-motion observations reaches a maximum of 16.8% in February at Site 2. For the same month, there was slow-motion at Site 1 for 8.1% of the time.

Table 3-10. Summary of the number of slow-motion points encountered at each site from July 2010 to July 2011. Note that the ice velocity data at Site 1 ended on March 2, 2011.

	Site 1				Site 2			
Month	**# non-flag points**	**# events**	**# slow points**	**% slow points**	**# non-flag points**	**# events**	**# slow points**	**% slow points**
Jul-2010	0	0	0	0	0	0	0	0
Aug-2010	0	0	0	0	0	0	0	0
Sep-2010	0	0	0	0	0	0	0	0
Oct-2010	0	0	0	0	0	0	0	0
Nov-2010	1767	0	0	0	2585	0	0	0
Dec-2010	2872	0	0	0	2976	3	75	2.52
Jan-2011	2976	4	215	7.22	2844	4	297	10.44
Feb-2011	2688	1	52	1.93	2688	5	258	9.6
Mar-2011	-	-	-	-	2976	0	0	0
Apr-2011	-	-	-	-	2768	3	88	3.18
May-2011	-	-	-	-	2615	0	0	0
Jun-2011	-	-	-	-	159	0	0	0
Jul-2011	-	-	-	-	0	0	0	0

Monthly statistics are given in Table 3-11 and Table 3-12 for Site 1 and Site 2 respectively. The number of valid points *versus* the total number of points for each month shows which months have smaller numbers of valid ice velocity samples, and thus less reliability. The largest ice speeds were measured at Site 2, where the maximum speed reached 142.3 cm/s. At Site 1, the maximum ice speed reached was 91.2 cm/s. The mean speeds of the entire deployment were 23.6 and 23.8 cm/s at Site 1 and Site 2 respectively.

The ice velocities are further illustrated through compass plots, which show the speed and direction joint frequency distribution. The color of each segment denotes its speed interval. The radial length of each segment denotes the proportion of measurements within the illustrated speed and direction interval. The maximum and mean are illustrated through the second radial scale as the red and green lines respectively for clear viewing. The speed and direction distributions are shown for the full deployment in Figure 3-11 while the monthly compass plots of ice velocity are shown in Figure 3-12 through Figure 3-14.

The full set of joint frequency tabulations of Ice Speed vs. Ice Direction for each site (full record plus each individual month) are provided as part of the Project Archive on ASL's FTP site.

Table 3-11. Statistical summary of measured ice velocities by month at Site 1.

Site 1	chan	min	1%	5%	25%	50%	mean	75%	95%	99%	std	max	# valid	total #
Time	cm/s													
26-Jul-2010	Uminor	-	-	-	-	-	-	-	-	-	-	-	0	515
-	Umajor	-	-	-	-	-	-	-	-	-	-	-	0	515
31-Jul-2010	Speed	-	-	-	-	-	-	-	-	-	-	-	0	515
01-Aug-2010	Uminor	-	-	-	-	-	-	-	-	-	-	-	0	2976
-	Umajor	-	-	-	-	-	-	-	-	-	-	-	0	2976
31-Aug-2010	Speed	-	-	-	-	-	-	-	-	-	-	-	0	2976
01-Sep-2010	Uminor	-	-	-	-	-	-	-	-	-	-	-	0	2880
-	Umajor	-	-	-	-	-	-	-	-	-	-	-	0	2880
30-Sep-2010	Speed	-	-	-	-	-	-	-	-	-	-	-	0	2880
01-Oct-2010	Uminor	-	-	-	-	-	-	-	-	-	-	-	0	2976
-	Umajor	-	-	-	-	-	-	-	-	-	-	-	0	2976
31-Oct-2010	Speed	-	-	-	-	-	-	-	-	-	-	-	-	2976
01-Nov-2010	Uminor	-25.2	-22.6	-18.6	-6.8	-0.2	0.8	6.8	23.2	41.1	12.5	57.3	1767	2880
-	Umajor	-78.6	-69.1	-52.0	-12.2	13.6	11.7	27.3	75.6	84.9	34.6	91.1	1767	2880
30-Nov-2010	Speed	1.5	2.9	6.9	15.4	23.3	31.6	46.3	77.4	85.3	22.3	91.2	1767	2880
01-Dec-2010	Uminor	-38.9	-32.4	-25.7	-12.9	-2.7	-2.5	6.5	26.0	37.8	15.5	42.4	2872	2976
-	Umajor	-40.0	-34.1	-26.0	-8.3	7.4	10.5	28.8	59.7	79.9	25.5	84.2	2872	2976
31-Dec-2010	Speed	0.5	1.5	4.9	17.5	25.2	27.4	35.3	61.9	81.1	15.9	85.9	2872	2976
01-Jan-2011	Uminor	-26.7	-23.6	-17.6	-5.3	-0.9	-1.4	2.2	13.5	30.8	9.4	36.7	2976	2976
-	Umajor	-72.1	-52.8	-31.2	-9.7	-0.8	-1.5	4.9	33.3	69.8	19.3	83.4	2976	2976
31-Jan-2011	Speed	0.0	0.0	0.1	4.0	11.0	15.3	22.4	41.5	71.5	15.1	85.0	2976	2976
01-Feb-2011	Uminor	-37.6	-34.0	-23.0	-8.2	-0.4	-0.8	5.7	22.1	26.7	12.9	31.9	2688	2688
-	Umajor	-83.2	-76.9	-68.9	-28.5	-8.0	-17.4	-2.7	7.9	15.4	22.9	21.2	2688	2688
28-Feb-2011	Speed	0.0	0.0	2.0	7.2	18.1	23.7	30.3	69.9	78.5	20.9	85.8	2688	2688
01-Mar-2011	Uminor	2.1	2.1	5.1	7.7	9.0	8.7	10.2	11.0	11.2	2.0	11.3	114	115
-	Umajor	-25.7	-25.7	-24.9	-20.4	-18.4	-18.3	-15.3	-12.9	-11.8	3.7	-11.4	114	115
02-Mar-2011	Speed	12.7	12.7	14.6	18.0	20.3	20.4	22.6	26.7	27.2	3.5	27.3	114	115
Entire	Uminor	-38.9	-29.8	-22.5	-8.7	-0.8	-1.1	5.2	22.2	33.7	12.8	57.3	10417	20982
-	Umajor	-83.2	-73.1	-46.1	-14.6	-1.3	-0.2	12.5	49.2	78.5	27.6	91.1	10417	20982
Record	Speed	0.0	0.0	1.4	8.9	19.9	23.6	31.3	67.8	80.7	19.1	91.2	10417	20982

Table 3-12. Statistical summary of measured ice velocities by month at Site 2.

Site 2	chan	min	1%	5%	25%	50%	mean	75%	95%	99%	std	max	# valid	total #
Time	cm/s													
01-Aug-2010	Uminor	-	-	-	-	-	-	-	-	-	-	-	0	2976
-	Umajor	-	-	-	-	-	-	-	-	-	-	-	0	2976
31-Aug-2010	Speed	-	-	-	-	-	-	-	-	-	-	-	0	2976
01-Sep-2010	Uminor	-	-	-	-	-	-	-	-	-	-	-	0	2880
-	Umajor	-	-	-	-	-	-	-	-	-	-	-	0	2880
30-Sep-2010	Speed	-	-	-	-	-	-	-	-	-	-	-	0	2880
01-Oct-2010	Uminor	-	-	-	-	-	-	-	-	-	-	-	0	2976
-	Umajor	-	-	-	-	-	-	-	-	-	-	-	0	2976
31-Oct-2010	Speed	-	-	-	-	-	-	-	-	-	-	-	0	2976
01-Nov-2010	Uminor	-38.7	-33.5	-25.7	-15.9	-9.5	-8.9	-1.9	8.5	19.5	10.6	26.3	2585	2880
-	Umajor	-106.5	-98.9	-76.0	-30.7	-4.4	2.1	27.3	104.4	115.4	52.1	129.4	2585	2880
30-Nov-2010	Speed	3.1	8.0	11.6	21.1	32.3	44.3	61.3	107.1	118.2	30.9	133.7	2585	2880
01-Dec-2010	Uminor	-52.0	-41.0	-24.8	-11.2	-4.6	-3.2	3.1	24.5	29.5	13.7	34.0	2976	2976
-	Umajor	-76.8	-64.7	-32.4	-10.3	3.4	11.9	36.6	65.9	72.8	31.7	83.9	2976	2976
31-Dec-2010	Speed	0.0	0.1	1.4	11.3	24.9	29.6	47.6	68.6	76.0	21.6	84.0	2976	2976
01-Jan-2011	Uminor	-51.7	-45.3	-30.6	-7.5	-3.3	-4.7	0.0	13.0	30.3	12.1	53.7	2844	2976
-	Umajor	-101.7	-84.8	-49.2	-16.0	-1.4	-1.9	3.8	72.6	113.7	32.7	142.3	2844	2976
31-Jan-2011	Speed	0.0	0.0	0.0	4.5	15.7	24.2	34.6	80.3	114.0	25.6	142.3	2844	2976
01-Feb-2011	Uminor	-19.2	-17.5	-10.9	-3.0	0.0	0.0	1.9	12.9	18.3	6.7	22.3	2688	2688
-	Umajor	-106.1	-93.3	-73.0	-26.8	-6.7	-16.9	-0.2	6.7	16.1	24.6	19.7	2688	2688
28-Feb-2011	Speed	0.0	0.0	0.1	4.3	10.8	20.3	27.9	74.1	92.8	22.9	106.1	2688	2688
01-Mar-2011	Uminor	-12.5	-8.5	-4.9	-0.6	0.4	0.4	1.7	5.0	7.8	2.8	10.2	2976	2976
-	Umajor	-37.2	-32.6	-24.6	-8.3	-3.2	-5.3	0.1	4.9	8.3	8.4	9.6	2976	2976
31-Mar-2011	Speed	0.0	0.1	0.5	2.6	5.8	7.5	9.0	24.8	32.7	7.2	37.3	2976	2976
01-Apr-2011	Uminor	-39.7	-30.5	-15.3	-4.2	-0.4	-0.2	3.1	17.9	22.3	9.2	28.0	2768	2880
-	Umajor	-40.2	-32.1	-21.4	-2.1	14.9	18.1	40.6	62.9	70.8	26.8	73.8	2768	2880
30-Apr-2011	Speed	0.0	0.1	0.8	8.3	24.8	27.0	41.9	63.6	71.1	19.9	75.8	2768	2880
01-May-2011	Uminor	-21.6	-17.5	-14.3	-9.7	-4.4	-4.5	-0.3	7.1	13.9	6.6	17.6	2615	2976
-	Umajor	-39.8	-36.2	-23.3	-13.9	-7.3	-5.9	0.6	26.1	36.0	13.2	41.0	2615	2976
31-May-2011	Speed	0.1	1.4	2.8	7.7	12.9	14.1	18.9	32.6	38.6	8.6	41.4	2615	2976
01-Jun-2011	Uminor	-9.7	-9.2	-6.3	-4.1	-1.4	2.4	10.8	16.2	18.0	8.1	19.2	159	2880
-	Umajor	-0.8	-0.2	3.1	19.5	39.7	36.3	52.6	58.0	61.0	18.4	62.2	159	2880
30-Jun-2011	Speed	6.2	6.3	7.8	19.9	39.8	37.4	53.3	60.2	63.3	18.1	63.8	159	2880
01-Jul-2011	Uminor	-	-	-	-	-	-	-	-	-	-	-	0	2797
-	Umajor	-	-	-	-	-	-	-	-	-	-	-	0	2797
30-Jul-2011	Speed	-	-	-	-	-	-	-	-	-	-	-	0	2797
Entire	Uminor	-52.0	-34.0	-19.7	-7.7	-1.5	-2.9	1.3	13.2	25.3	10.0	53.7	19611	35220
-	Umajor	-106.5	-80.5	-45.6	-13.9	-1.9	0.7	8.0	61.9	102.8	31.8	142.3	19611	35220
Record	Speed	0.0	0.0	0.5	6.4	16.1	23.8	33.2	72.0	104.9	23.6	142.3	19611	35220

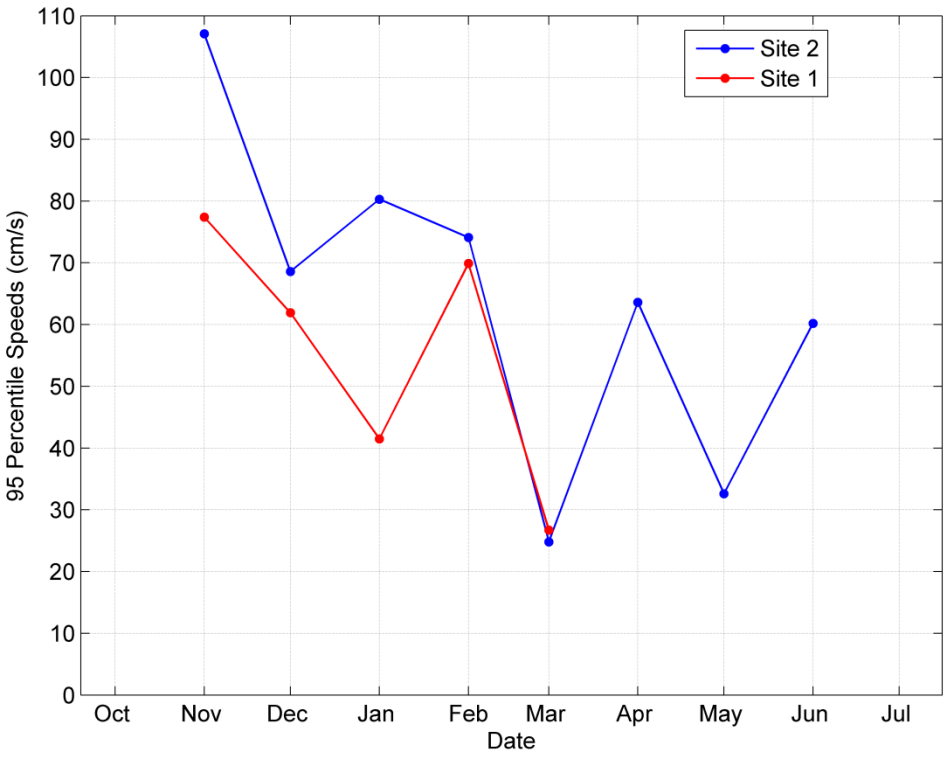

Figure 3-9. The 95 percentile speeds (cm/s) by month at Sites 1 and 2.

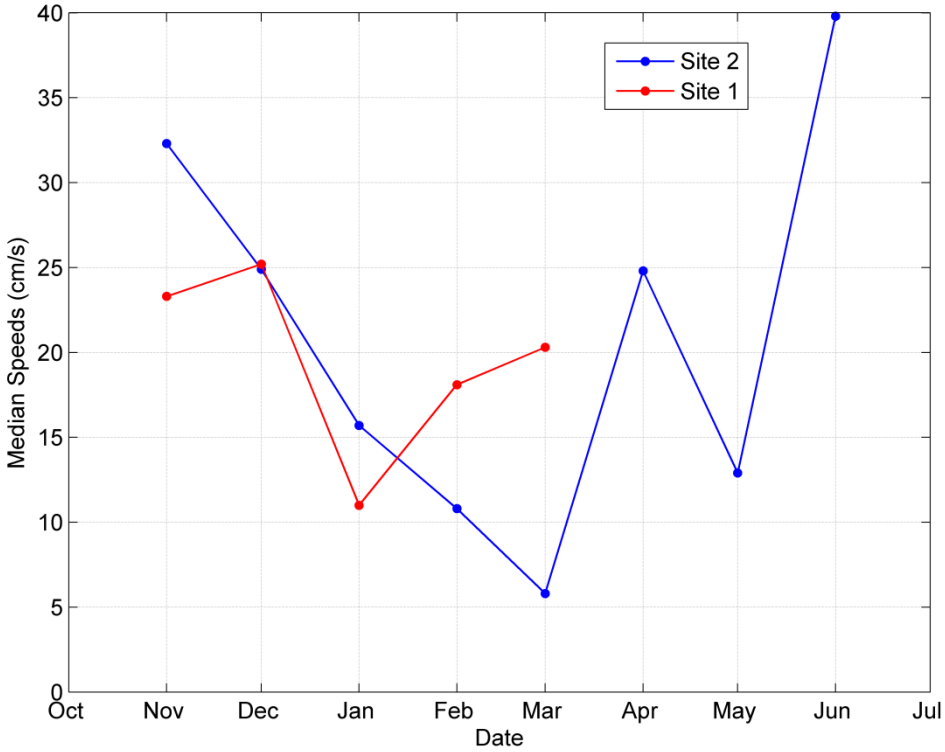

Figure 3-10. The median speeds (cm/s) by month at Sites 1 and 2.

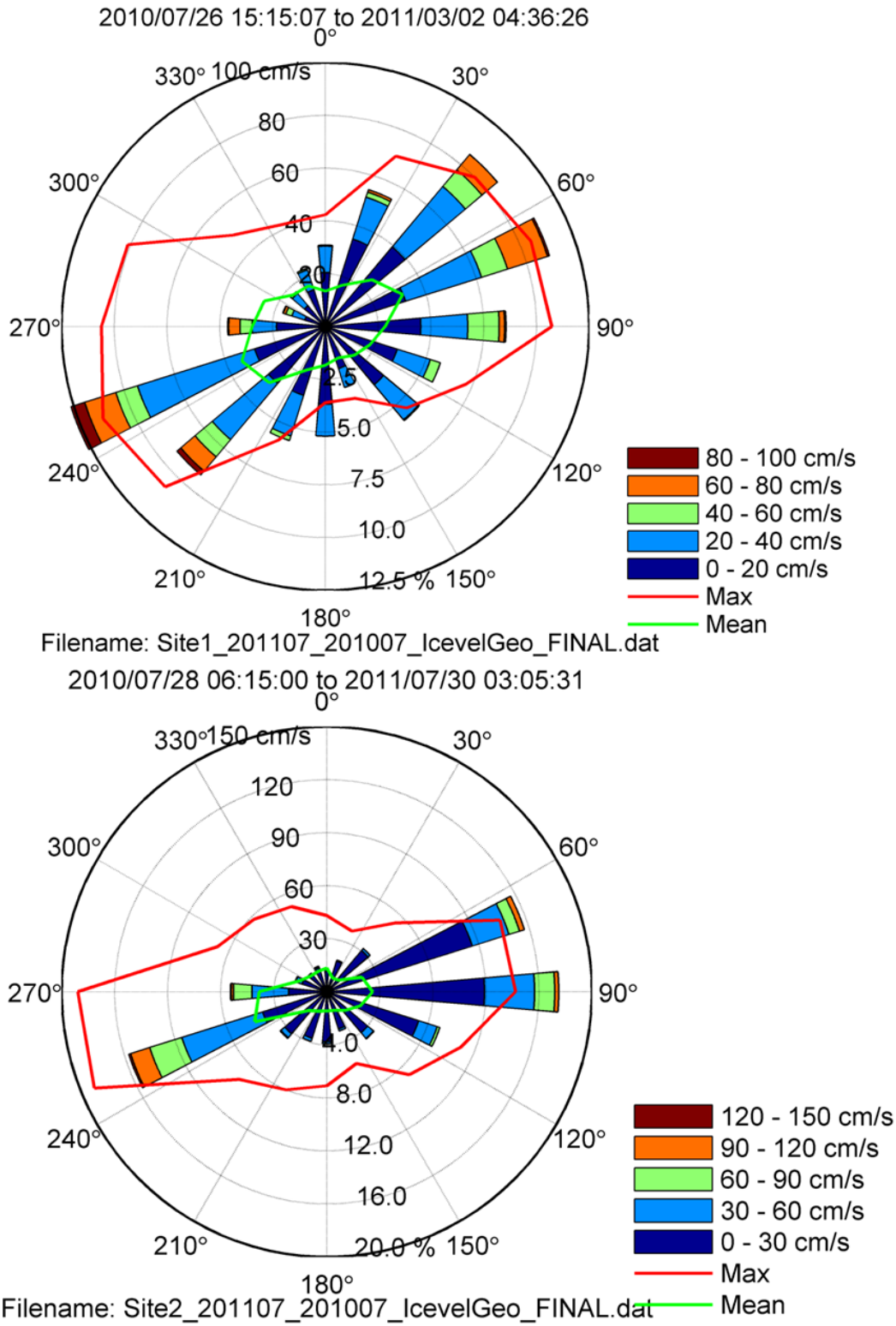

Figure 3-11. Compass plots of the directional (towards) distribution of the observed ice velocity over the full deployment for Site 1 (top) and Site 2 (bottom). The next pages contain the monthly compass plots for each site.

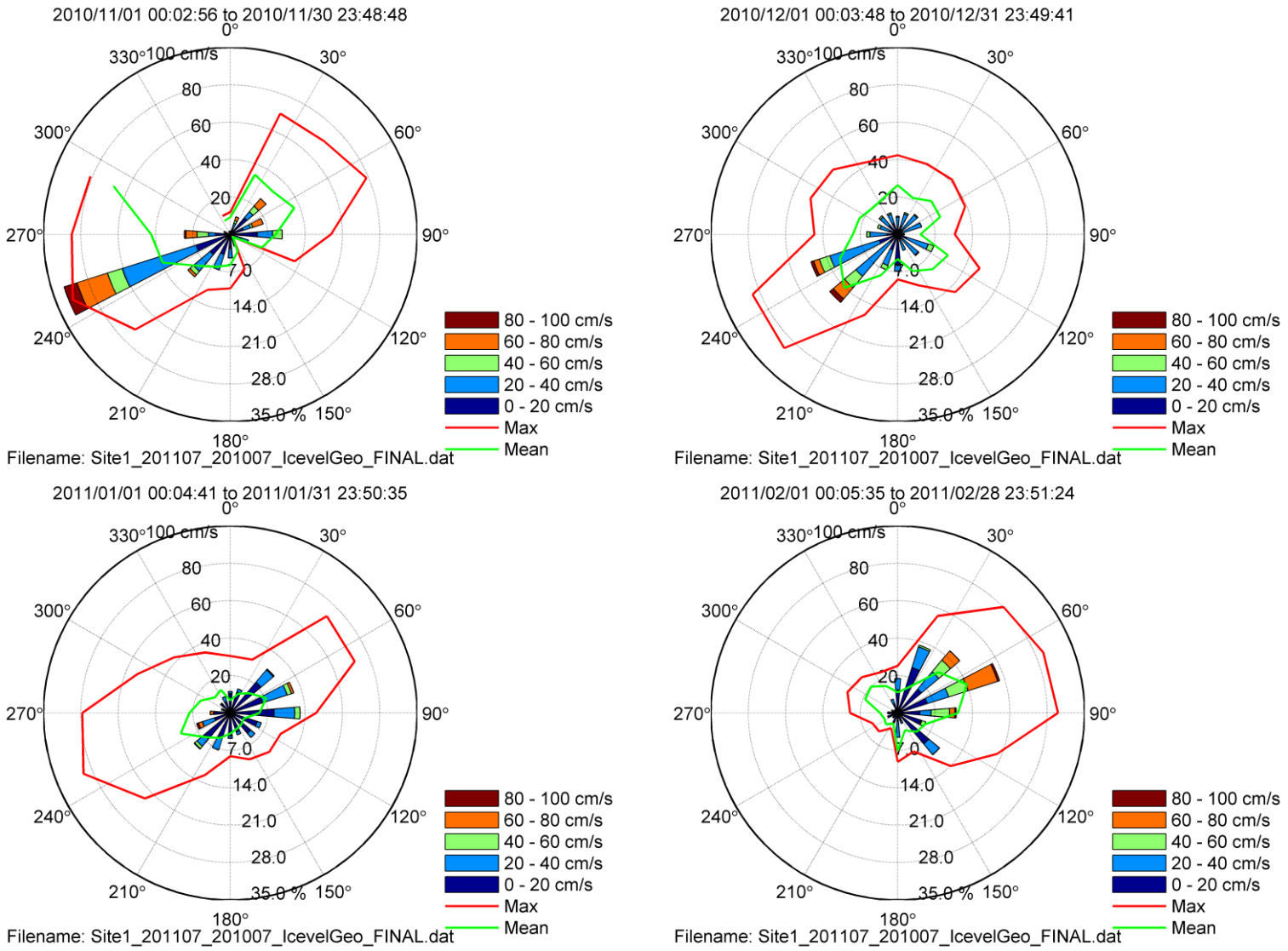

Figure 3-12. Monthly compass plots of the directional (towards) distribution of ice velocities at Site 1 from November 2010 to February 2011.

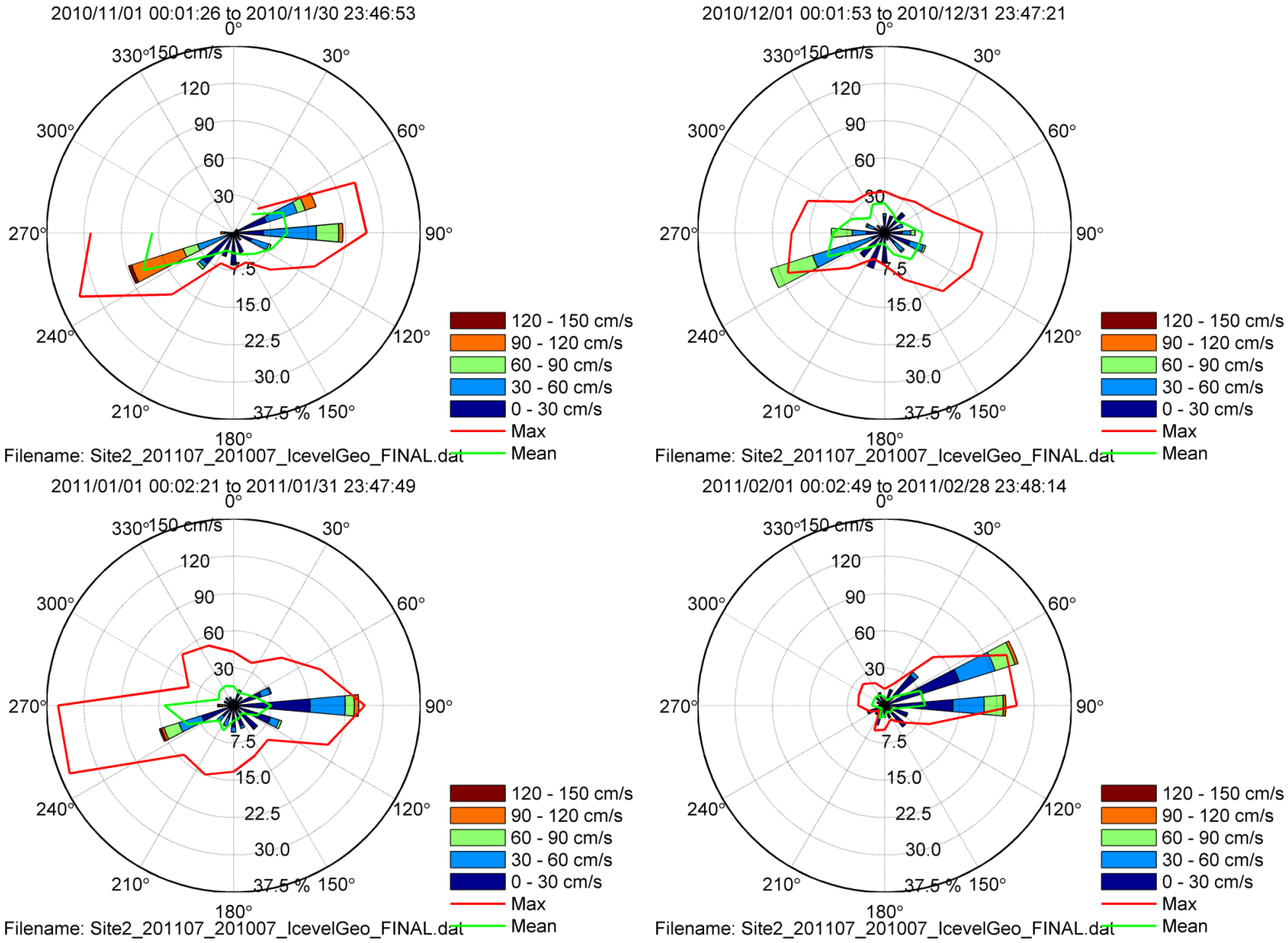

Figure 3-13. Monthly compass plots of the directional (towards) distribution of ice velocities at Site 2 from November 2010 to February 2011.

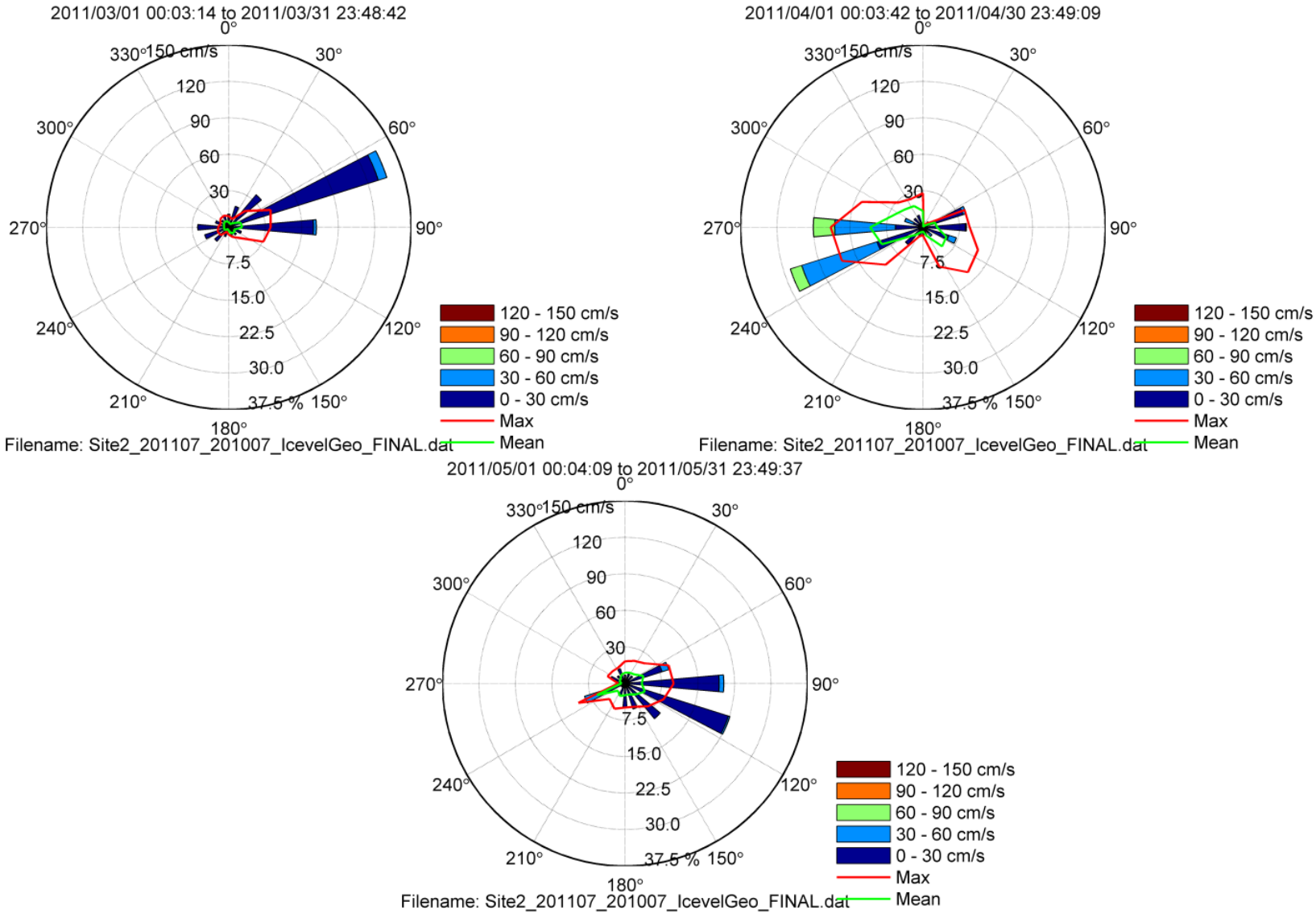

Figure 3-14. Monthly compass plots of the directional (towards) distribution of ice velocities at Site 2 from March 2011 to May 2011.

3.4 OCEAN CURRENT DATA

3.4.1 PROCESSING CURRENT PROFILER DATA

The Acoustic Doppler Current Profiler (ADCP) instrument, operating in the conventional water column data acquisition mode, provided time series measurements of three dimensional ocean currents, at 5 minute sampling intervals and with a vertical resolution of 2 m at Site 1 and Site 2. The near-bottom ADCP measurements correspond to measurements about 4 m above the instrument due to the blanking distance associated with the instrument. Table 3-13 tabulates several of the measurement parameters associated with the water column measurements as well as the acoustic bins which yielded useful data.

The data from the instrument at Site 1 ended on March 2, 2011 due to underwater connector corrosion on the external battery pack. A time check showed the ADCP at this site to be 10 minutes 43 second slow. At Site 2, the ADCP collected a full data record ending July 30, 2011 and was found to be 5 minutes 32 seconds slow.

Horizontal velocities were analyzed from three levels, near surface, mid-depth and near bottom. The mid and near bottom level currents were derived from single ADCP bins. However, the ADCP currents in bins near the water-air interface are at times contaminated by waves. Similarly, the currents in the upper-most bins near the ice-water interface are at times contaminated by the presence of ice keels. A semi-automated methodology was developed to identify the first uncontaminated bin nearest the air-water interface for open water conditions or nearest the ice-water interface for ice covered conditions. This involved the use of the ADCP's pressure and bottom track channels in the following way:

1. The pressure record and the pressure standard deviation record were extracted from the ADCP.
2. The depth of water in each beam at which the bottom track was located was extracted from the ADCP (i.e. the vertical component of the bottom track range in each beam).
3. Due to the possibility of acceptable three beam solutions of the ice velocity, an assumption was made that if ice was present in one of the beams, but not the other three, the built-in data rejection algorithms of the ADCP would discard the data in the blocked beam, and generate an acceptable solution. Therefore, the second deepest depth by beam was extracted.
4. The pressure was converted to approximate depth by multiplying by a density of 1.025 and the time series was plotted.
5. The second deepest bottom track depth time series was overlaid on the same plot. This time series will subsequently be referred to as the range time series for the rest of the description of the algorithm.
6. An offset to bring the range and pressure time series to the same level, in the absence of ice, was selected.

7. A sidelobe correction factor of 0.9397 (cos 20°) was applied to the ranges
8. An approximation of the significant wave height was found (4 * pressure standard deviation).
9. The deeper of the wave height and the sidelobe corrected ranges was chosen, and the bin corresponding to this depth was selected.
10. The time-series of selected bins and currents were examined. In cases where shear in the water column, and changing of bin-number seemed to be creating artefacts in the velocity time series, the selected bin was edited to remove the artefact.

The ADCP's *false target rejection* algorithm calculates a three-beam solution if the intensity from a single beam differs by a significant amount from the other beams. However, if more than one beam's intensity was significantly different from the other values or too small, no measured value was recorded. Time series plots of the depths chosen for the near surface bins at Site 1 and Site 2 are shown in Figure 3-15 and Figure 3-16.

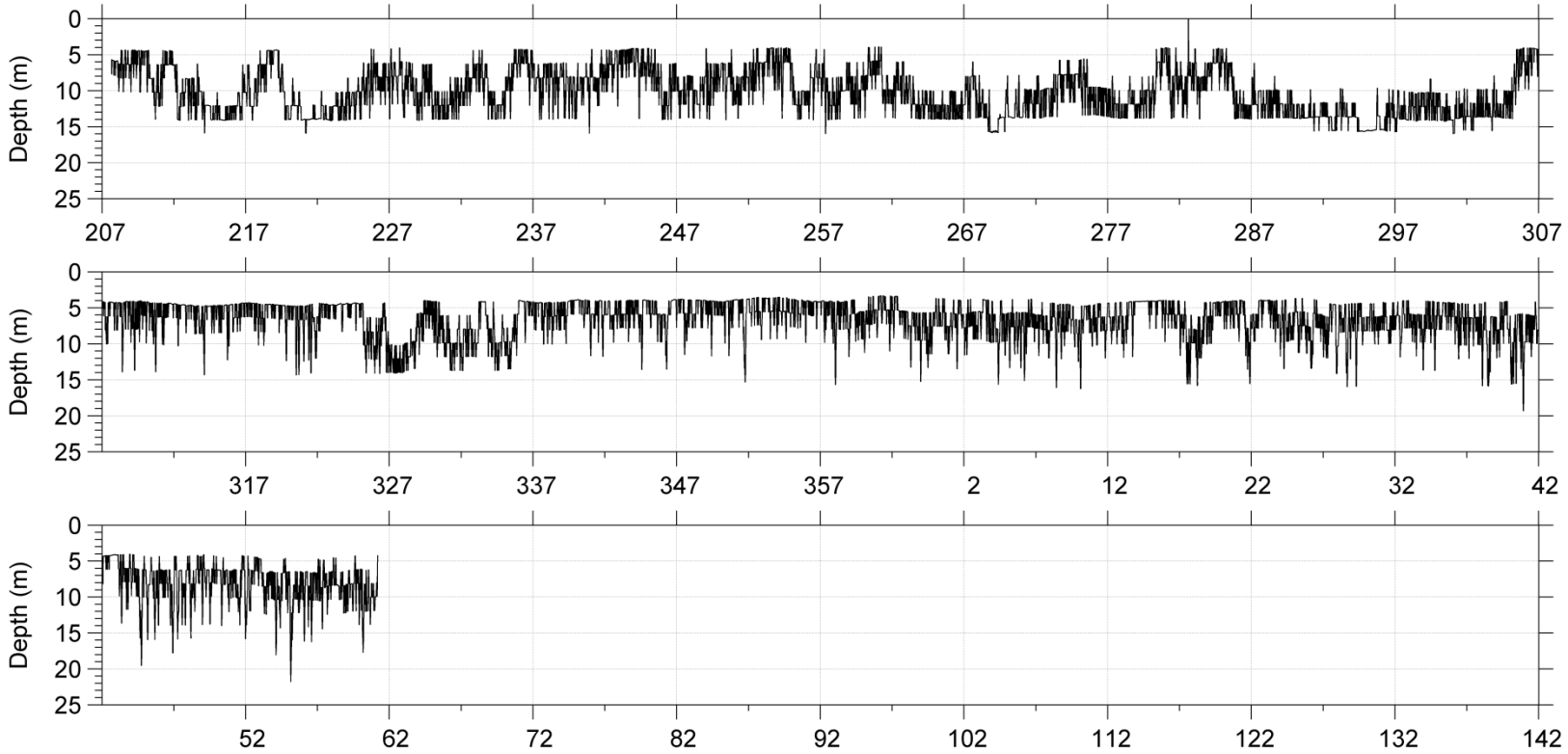

Experiment: Chukchi_Site1 Site : Site1
Instrument: Pr739 Date: 2010/07/26 15:10:07.17 to 2011/03/02 04:31:26.32 UTC Filename: Site1 201007 Nearsf ed12 despike.dat

Figure 3-15. Time series plot of the depth chosen for the near surface bin at Site 1.

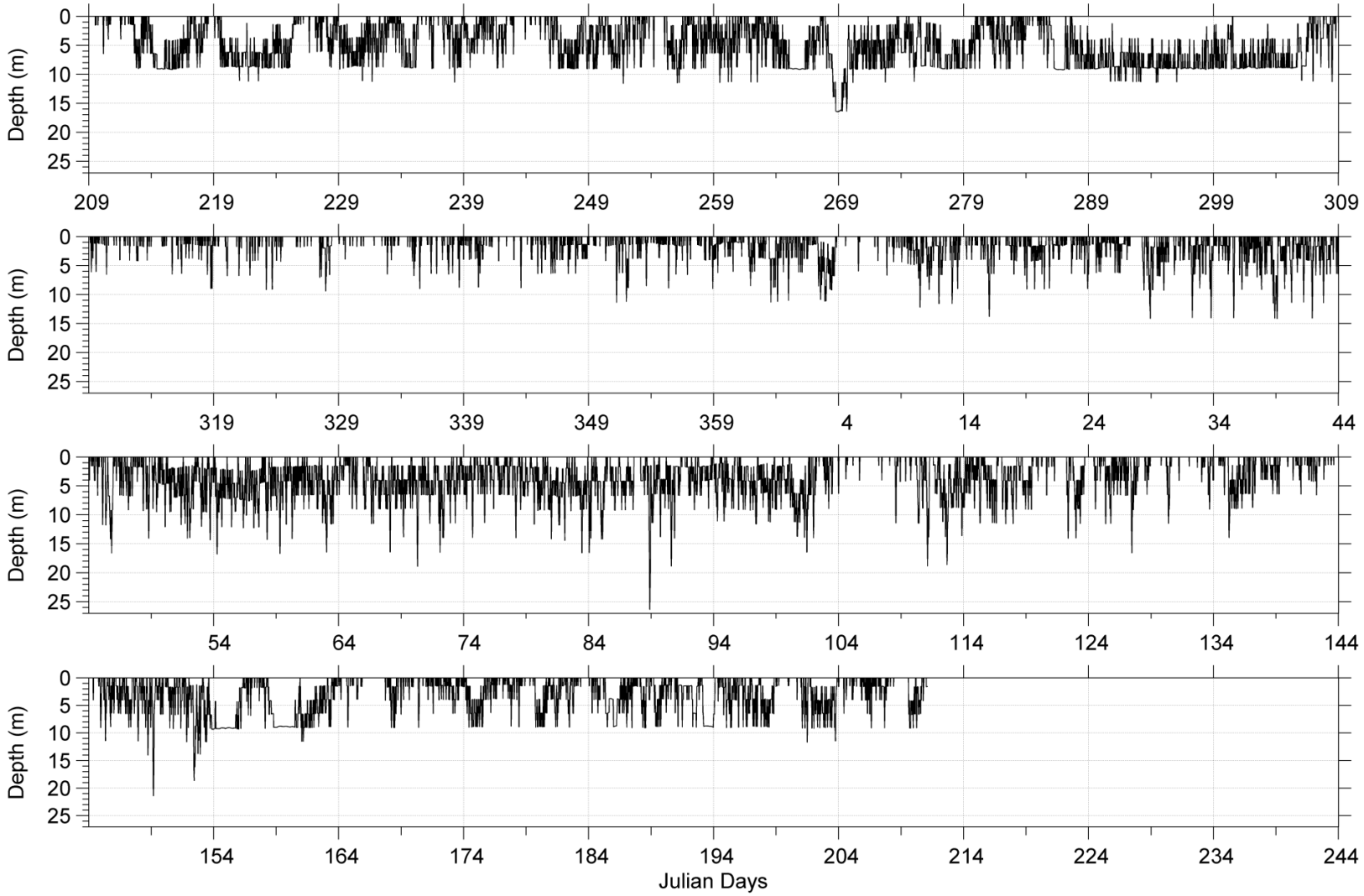

Figure 3-16. Time series plot of the depth chosen for the near surface bin at Site 2.

Table 3-13. Summary of current measurement parameters.

	Site 1	Site 2
Latitude	N 70° 59.911'	N 70° 58.723'
Longitude	W 164° 59.981'	W 160° 58.178'
Instrument Depth (m)	35	43
Bin Size (m)	2	2
Sample Interval, Prior to Time Averaging (min)	5	5
Number of Data Values	63,081	106,059
Instrument Bin Number	Measurement Depth (m)	
1	26	34
2	24	32
3	22	30
4	20	28
5	18	26
6	16	24
7	14	22
8	12	20
9	10	18
10	8	16
11	6	14
12	4	12
13	2	10
14	0	8
15	-	6
16	-	4
17	-	2
18	-	0

Each time series data set was subjected to quality control procedures. The steps in the error detection and removal procedures were applied as follows, after applying the compass calibration data to the ADCP directions:

1. The currents were screened for Correlation < 64, Amplitude < 50 and Verror > 5 cm/s, the currents were compass corrected to geographic coordinates, and then averaged from 5 minute to 15 minute sampling intervals.
2. Plots of all the raw data sets were prepared and reviewed, including the ADCP vertical and error velocities.
3. Values of measured horizontal components of current that had absolute values exceeding the out-of-bound threshold of 120 cm/s were selected.
4. Values of measured horizontal components of current with accompanying error velocities that exceeded 5 cm s^{-1} were selected.

5. Single point 'spikes' in each component of the horizontal velocities were identified. A single point spike consisted of two successive first difference values exceeding a single spike threshold of 4 cm/s and opposite in sign.
6. 'Double spikes' exceeding a double spike threshold in each component of the horizontal velocities were identified. A double spike consisted of two consecutive points, both of which were either larger or smaller than the preceding and following points by more than the double spike threshold, 5 cm/s.
7. 'Triple spikes' exceeding a triple spike threshold in each component of the horizontal velocities were identified. A triple spike consisted of three consecutive points which were smaller than the preceding and following points by more than the triple spike threshold, 6 cm/s, but whose middle points could not change by more than one third of the triple spike threshold from their respective leading neighbours.
8. 'Quadruple spikes' exceeding a quadruple spike threshold in each component of the horizontal velocities were identified. A quadruple spike consisted of four consecutive points which were smaller than the preceding and following points by more than the quadruple spike threshold, but whose middle points could not change by more than one third of the quadruple spike threshold, 7 cm/s, from their respective leading neighbours.
9. For all suspect values found as above in items 3 to 8, the values were replaced by linear interpolation, over all individual segments with durations of less than two and a half hours (approximately one eighth of the tidal signal which was predominantly diurnal). For longer segments of erroneous or suspect data, the values were replaced with flag values (-9999) and reviewed again in step 10.
10. Plots of the edited data sets (following step 9) were prepared and manually reviewed. Any remaining suspect values were manually edited. These suspect values were generally determined as being anomalous from adjoining values at nearby times or at adjacent bins above and below.
11. In cases where there were flags (from step 8), velocity data from neighbouring bins were used to reconstruct the segments.

The number of data points which were identified as suspect in accordance with the above methodology is summarized in Table 3-14.

Table 3-14. Summary of the number of points modified at Site 1 and Site 2 for selected bins.

	Veast			Vnorth		
	Near Surface	**16 m**	**26 m**	**Near Surface**	**16 m**	**26 m**
	Site 1					
Bad Verr	0	0	0	0	0	0
Out of Range	0	1	1	0	1	1
Single Spike	54	173	139	17	165	117
Double Spike	0	12	4	0	24	16
Triple Spike	3	6	0	0	0	3
Quad. Spike	0	0	0	0	4	0
Manual Edit	475	22	7	536	87	48
Total # Edited (%)	532 (2.54%)	214 (1.02%)	151 (0.72%)	553 (2.64%)	281 (1.34%)	185 (0.88%)
# Flagged	0	0	0	0	0	0
Total Pts	20982			20982		
	Veast			**Vnorth**		
	Near Surface	**22 m**	**34 m**	**Near Surface**	**22 m**	**34 m**
	Site 2					
Bad Verr	16	0	0	16	0	0
Out of Range	1	14	2	1	14	2
Single Spike	1,167	154	165	841	153	165
Double Spike	234	16	24	166	24	8
Triple Spike	54	3	0	42	6	6
Quad. Spike	16	4	4	16	0	0
Manual Edit	62	5	31	348	35	46
Total # Edited (%)	1534 (4.36%)	196 (0.56%)	226 (0.64%)	1414 (4.01%)	232 (0.66%)	227 (0.64%)
# Flagged	0	0	0	0	0	0
Total Pts	35220			35220		

3.4.2 PLOTS AND STATISTICAL SUMMARIES FOR NEAR-SURFACE, MID-DEPTH AND NEAR-BOTTOM MEASUREMENT LEVELS

A major/minor coordinate system (u-major and u-minor) was used, similar to the one already presented for the ice velocities in the previous section. Table 3-15 tabulates the direction axis that the currents at each depth were oriented along, and specifies the direction of positive u-major.

Table 3-15. Summary of the rotation applied at the near-surface, mid-depth, and near-bottom bins of each site to obtain the major/minor velocity components.

Site 1			
Bin	**Depth (m)**	**Current Direction (°)**	**Heading of Positive Umajor (°)**
Bin 1	26	73 - 253	253
Bin 6	16	81 - 261	261
Near Surface	variable	84 - 264	264
Site 2			
Bin	**Depth (m)**	**Current Direction (°)**	**Heading of Positive Umajor (°)**
Bin 1	34	83 - 263	263
Bin 7	22	92 - 272	272
Near Surface	variable	93 - 273	273

The final versions of the edited current meter data sets for the two sites are presented for the near-surface, mid-depth, and near-bottom as time series plots (Figure 3-17 through Figure 3-22).

Statistical summaries of the near-surface, mid-depth and near-bottom current speeds are given for the full deployment period in Table 3-16 and quarterly statistical tables are given in Table 3-17 through Table 3-22. The current speeds are further illustrated through compass plots (Figure 3-23), which show the speed and direction joint frequency distribution for the entire deployment. The color of each segment denotes its speed interval. The radial length of each segment denotes the proportion of measurements within the illustrated speed and direction interval. The maximum and mean are illustrated through the second radial scale as the red and green lines respectively.

The full set of joint frequency tabulations of current speed vs. current direction for each depth at each site (full record plus each individual month) are provided in the Project Archive to this report which can be downloaded from the ASL FTP site.

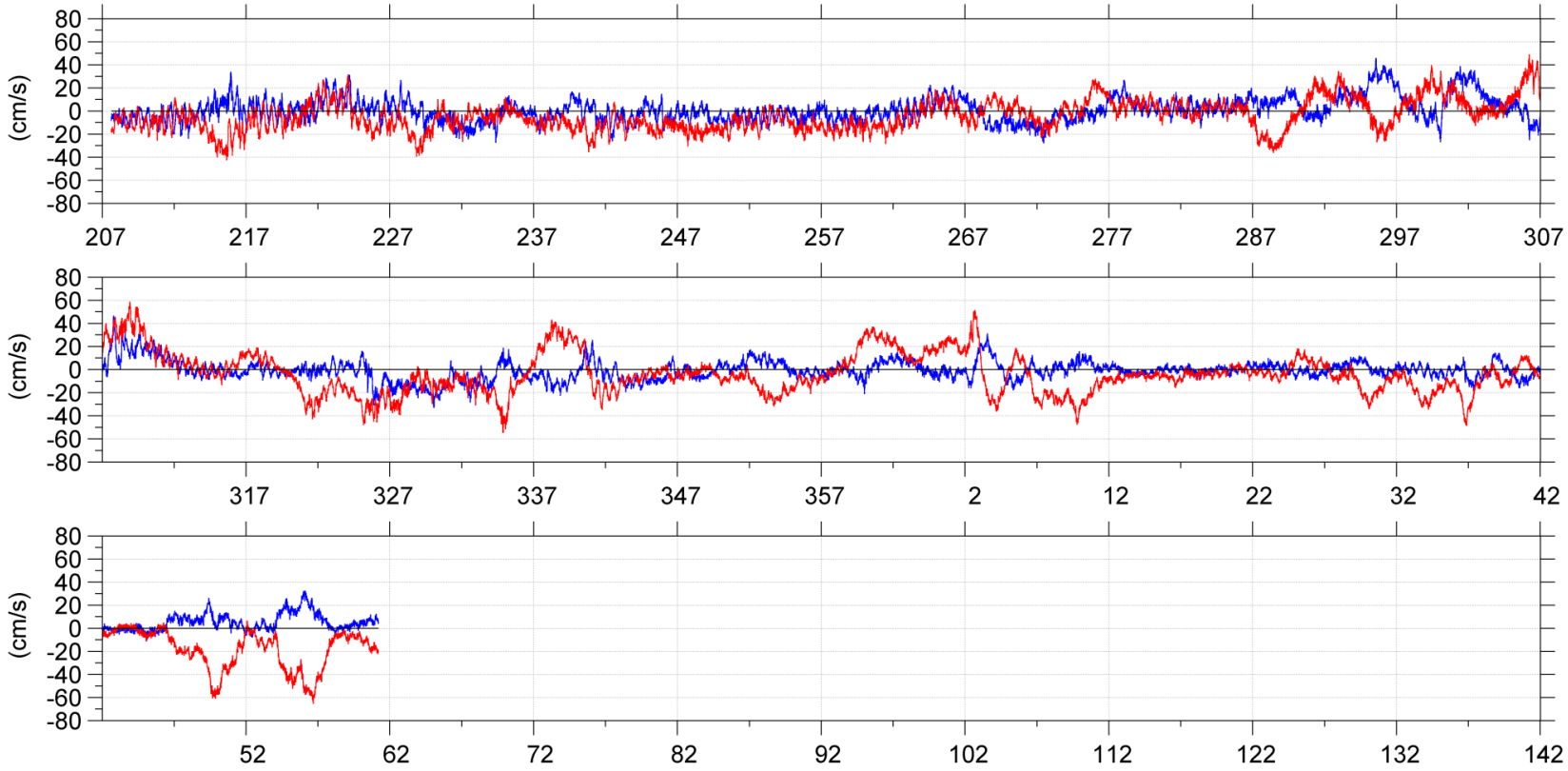

Figure 3-17. Plot of the near surface current measurements at Site 1.

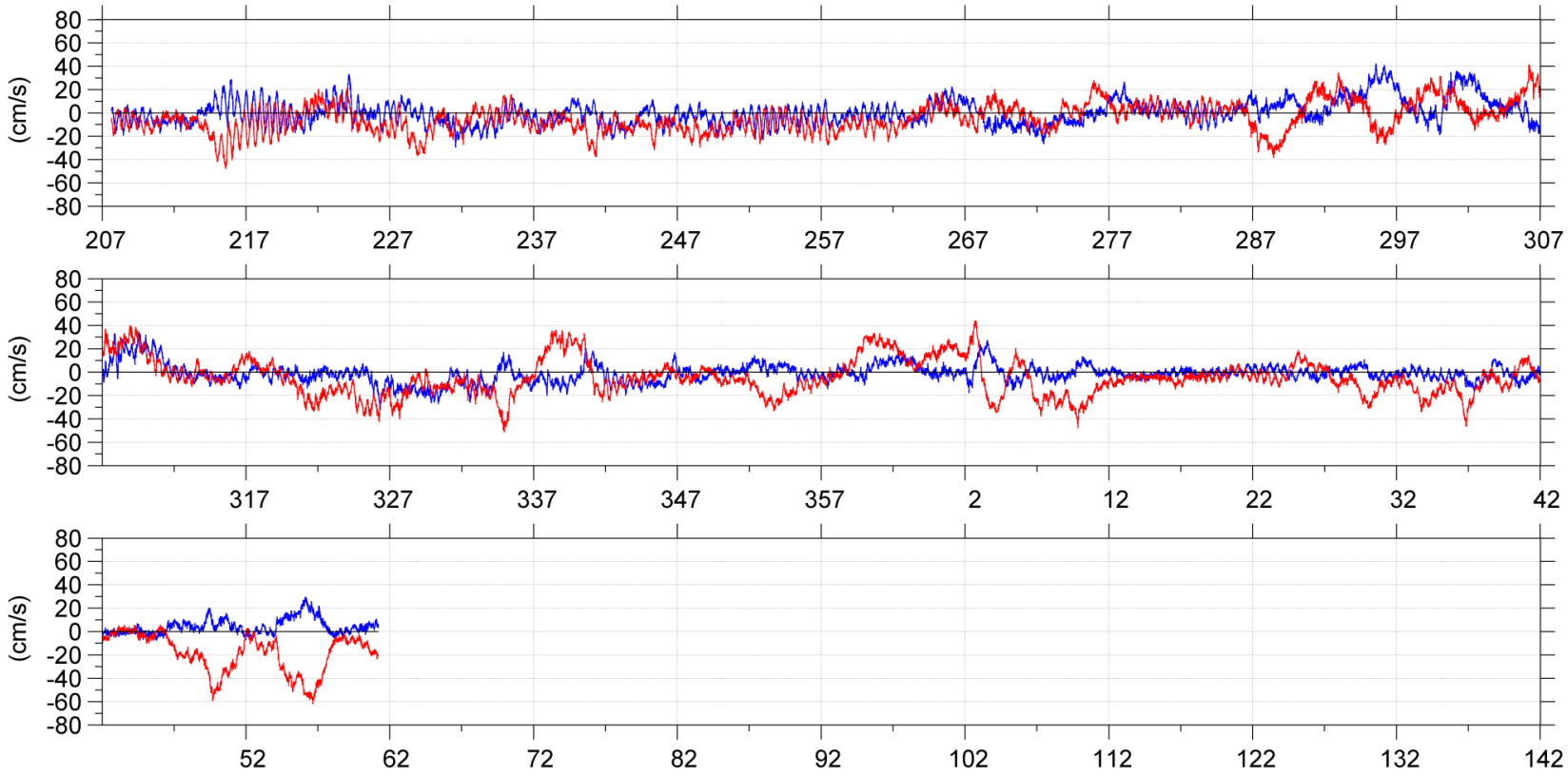

Figure 3-18. Plot of the mid-depth (16 m) current measurements at Site 1.

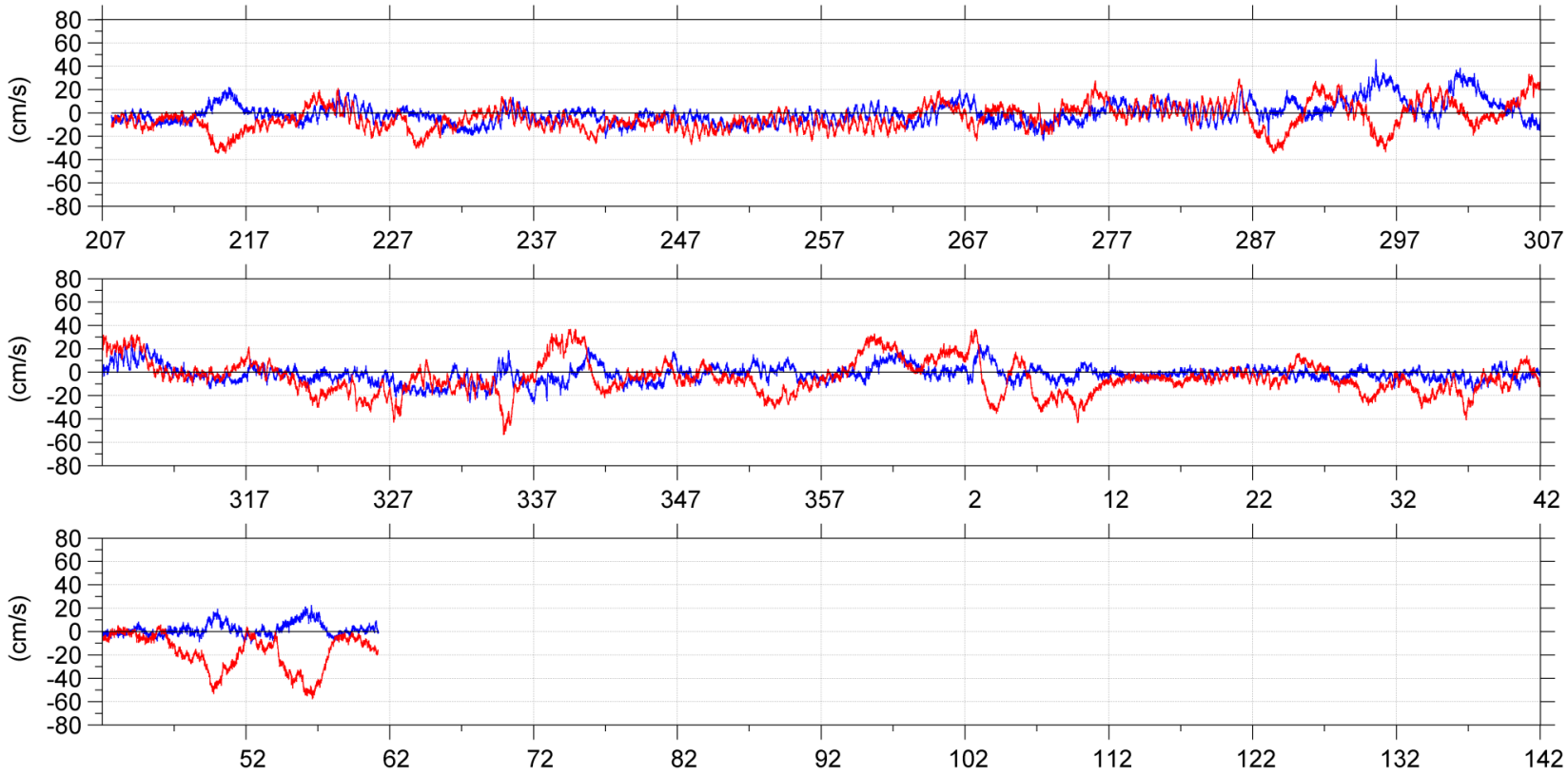

Figure 3-19. Plot of the near bottom (26 m) current measurements at Site 1.

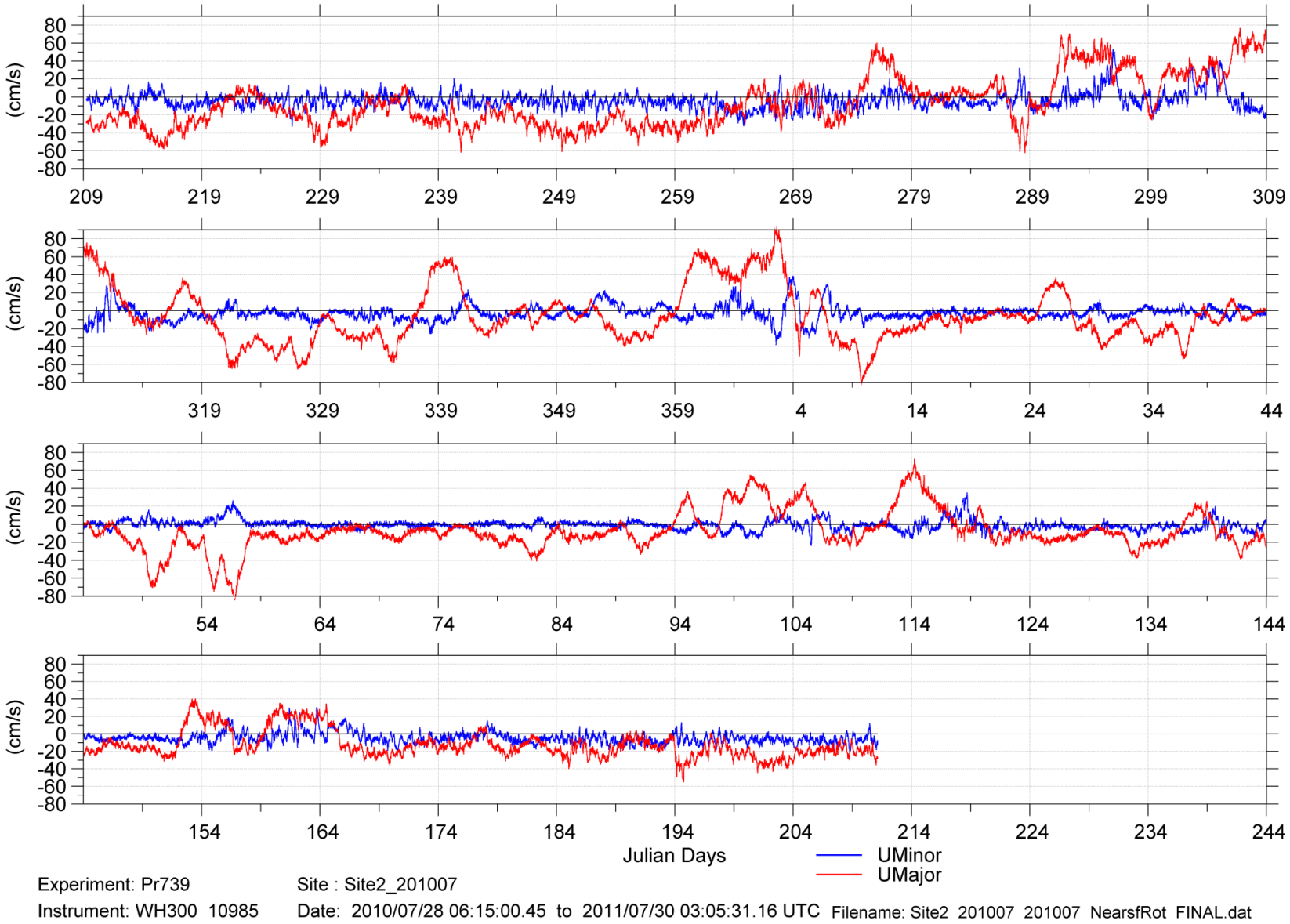

Figure 3-20: Plot of the near surface current measurements at Site 2.

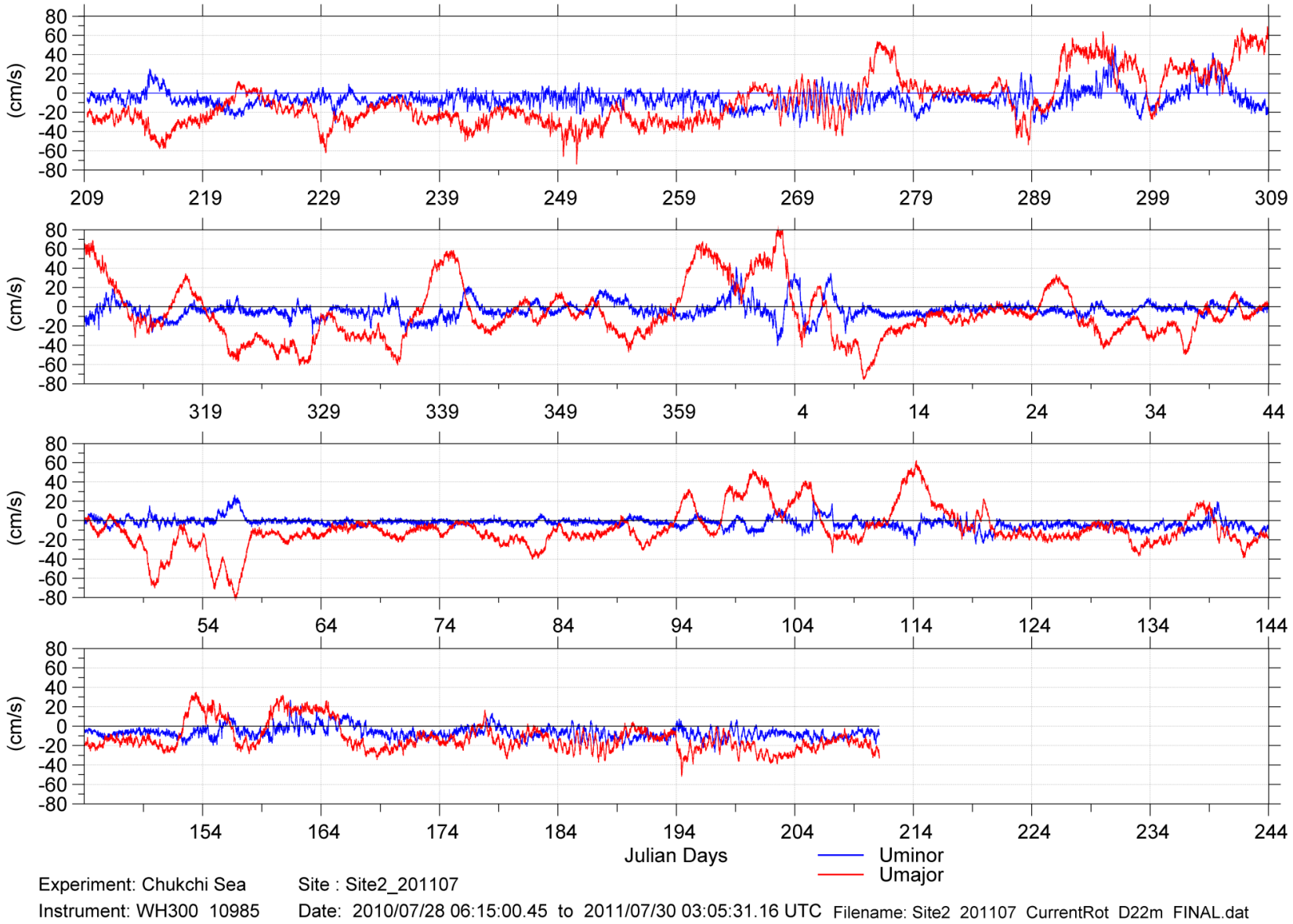

Figure 3-21: Plot of the mid-depth (22 m) current measurements at Site 2.

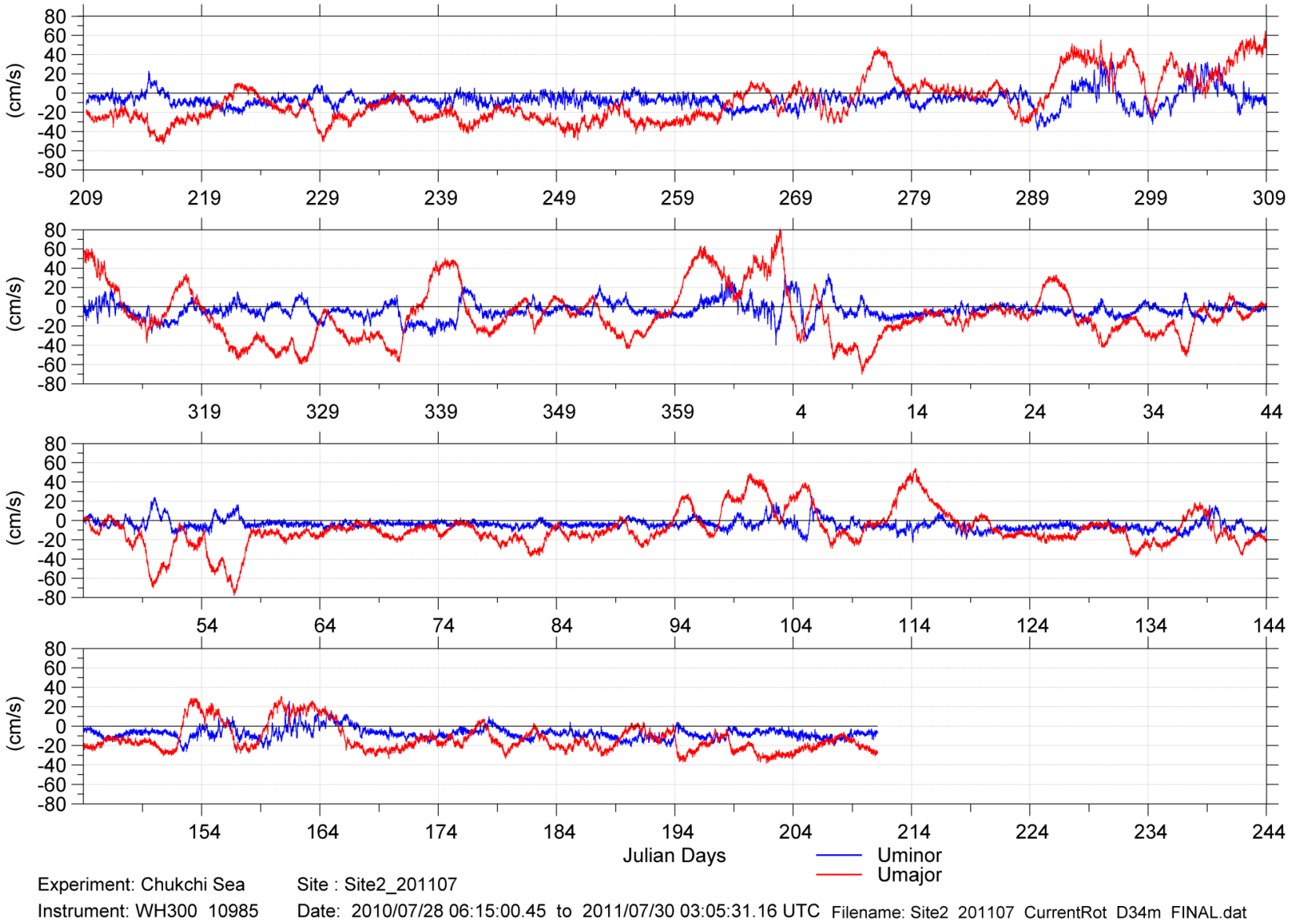

Figure 3-22. Plot of the near bottom (34 m) current measurements at Site 2.

Table 3-16. Statistical summary of current components and speeds at Site 1 and Site 2 for the entire deployment.

			Annual Statistics (cm/s)												
Site	Depth (m)	chan	min	1%	5%	2%	50%	mean	75%	95%	99%	std	max	# valid	total #
1	Near Surface	Uminor	-33.1	-20.9	-14.3	-5.4	-0.2	0.5	5.7	17.6	29.6	9.6	46.6	20982	20982
		Umajor	-65.4	-46.2	-30.7	-14.9	-6.0	-5.4	3.0	24.1	36.8	16.1	59.0	20982	20982
		Speed	0.0	1.4	3.3	8.2	14.2	16.3	21.8	36.5	51.3	10.7	67.2	20982	20982
	16	Uminor	-32.2	-19.6	-14.3	-5.8	-0.7	0.0	4.7	17.2	28.9	9.4	42.6	20982	20982
		Umajor	-62.2	-45.0	-30.1	-14.2	-6.0	-5.7	2.6	21.0	30.2	14.8	44.2	20982	20982
		Speed	0.1	1.4	3.3	8.2	13.4	15.6	20.9	34.0	47.0	9.9	64.2	20982	20982
	26	Uminor	-27.3	-17.4	-12.6	-5.8	-1.5	-0.7	3.3	14.3	26.2	8.2	46.1	20982	20982
		Umajor	-57.8	-43.1	-27.8	-13.0	-5.8	-5.6	1.7	18.8	28.3	13.6	37.2	20982	20982
		Speed	0.0	1.5	3.4	7.8	12.2	14.2	18.6	31.4	44.4	9.0	58.9	20982	20982
2	Near Surface	Uminor	-38.2	-21.2	-14.3	-7.4	-3.1	-2.8	0.8	10.0	24.3	7.9	53.3	35220	35220
		Umajor	-85.0	-59.7	-41.5	-23.0	-12.3	-7.8	1.9	45.0	62.2	25.2	93.5	35220	35220
		Speed	0.0	2.2	5.0	12.3	20.3	23.3	30.9	53.7	67.2	14.8	99.0	35220	35220
	22	Uminor	-40.6	-22.9	-16.6	-8.8	-4.6	-4.4	-0.7	8.3	21.5	7.9	49.3	35220	35220
		Umajor	-83.8	-58.5	-41.6	-23.1	-13.3	-9.0	0.6	41.5	57.1	23.6	84.6	35220	35220
		Speed	0.1	2.7	5.7	13.5	20.5	23.1	29.7	50.3	63.9	13.6	90.4	35220	35220
	34	Uminor	-39.9	-23.9	-16.7	-9.4	-5.7	-5.3	-2.0	8.5	19.7	7.7	35.4	35220	35220
		Umajor	-78.1	-53.8	-40.3	-23.1	-13.2	-9.2	0.6	36.7	50.9	22.0	83.7	35220	35220
		Speed	0.1	2.6	5.8	13.9	20.6	22.4	28.6	46.7	57.9	12.3	84.5	35220	35220

Table 3-17. Summary of ocean current quarterly statistics for Site 1 at the near-surface.

Site 1: Near Surface	chan	min	1%	5%	25%	50%	mean	75%	95%	99%	std	max	# valid	total #
Time	cm/s													
26-Jul-2010	Uminor	-27.8	-21.0	-15.8	-8.4	-2.8	-2.3	3.2	13.2	21.1	8.9	34.0	6372	6372
-	Umajor	-42.7	-33.4	-24.2	-15.3	-9.7	-8.8	-2.6	8.7	16.8	10.1	31.6	6372	6372
30-Sep-2010	Speed	0.2	2.0	4.3	9.8	14.3	14.7	18.7	27.0	35.2	6.9	42.8	6372	6372
01-Oct-2010	Uminor	-33.1	-22.4	-15.4	-5.3	0.7	1.7	7.8	22.5	33.1	11.1	46.6	8832	8832
-	Umajor	-54.6	-38.6	-28.2	-10.5	0.2	0.8	12.2	30.6	41.3	17.6	59.0	8832	8832
31-Dec-2010	Speed	0.1	1.6	3.8	8.9	15.9	17.8	25.2	37.7	48.5	10.9	61.4	8832	8832
01-Jan-2011	Uminor	-18.3	-13.0	-8.4	-2.5	0.7	1.7	5.0	15.4	24.1	7.1	32.6	5777	5777
-	Umajor	-65.4	-56.1	-41.2	-20.1	-7.7	-11.0	-2.0	11.2	27.8	15.9	51.4	5777	5777
02-Mar-2011	Speed	0.0	1.0	2.3	5.9	11.2	15.8	22.6	44.5	58.8	13.3	67.2	5777	5777

Table 3-18. Summary of ocean current quarterly statistics for Site 1 at mid-depth (16 m).

Site 1: 16 m	chan	min	1%	5%	25%	50%	mean	75%	95%	99%	std	max	# valid	total #
Time	cm/s													
26-Jul-2010	Uminor	-29.5	-20.7	-16.2	-9.3	-3.9	-3.1	2.4	12.5	19.8	8.8	33.4	6371	6371
-	Umajor	-47.9	-34.9	-24.7	-14.3	-8.5	-8.3	-2.0	8.5	14.1	9.9	21.7	6371	6371
30-Sep-2010	Speed	0.4	2.1	4.6	9.2	13.4	14.3	18.4	27.0	36.1	7.0	48.8	6371	6371
01-Oct-2010	Uminor	-32.2	-20.3	-14.5	-5.4	0.3	1.5	7.1	22.6	32.6	10.8	42.6	8832	8832
-	Umajor	-51.4	-35.6	-26.7	-10.5	-1.0	-0.3	10.2	26.2	32.4	15.7	41.7	8832	8832
31-Dec-2010	Speed	0.2	1.6	3.7	8.9	14.9	16.5	23.2	33.7	41.4	9.5	52.0	8832	8832
01-Jan-2011	Uminor	-17.8	-11.6	-7.7	-2.9	0.1	1.0	3.9	14.0	22.0	6.4	29.8	5779	5779
-	Umajor	-62.2	-53.1	-40.3	-19.8	-8.3	-11.2	-2.5	10.9	24.5	15.2	44.2	5779	5779
02-Mar-2011	Speed	0.1	1.1	2.5	6.1	11.0	15.4	21.8	42.3	56.4	12.6	64.2	5779	5779

Table 3-19. Summary of ocean current quarterly statistics for Site 1 at near-bottom (26 m).

Site 1: 26 m	chan	min	1%	5%	25%	50%	mean	75%	95%	99%	std	max	# valid	total #
Time	cm/s													
26-Jul-2010	Uminor	-23.9	-16.6	-13.6	-8.0	-3.8	-3.3	0.5	9.7	15.8	6.9	22.2	6371	6371
-	Umajor	-34.8	-29.4	-21.2	-12.6	-7.5	-7.3	-2.3	7.8	13.4	8.6	21.5	6371	6371
30-Sep-2010	Speed	0.1	2.1	4.3	8.3	11.6	12.3	15.4	22.3	32.2	5.8	38.1	6371	6371
01-Oct-2010	Uminor	-27.3	-19.2	-13.9	-5.5	0.0	1.0	6.4	19.1	30.1	9.9	46.1	8832	8832
-	Umajor	-53.6	-34.2	-25.2	-9.8	-1.5	-0.8	8.4	24.4	29.9	14.5	37.2	8832	8832
31-Dec-2010	Speed	0.0	1.6	3.6	8.4	13.6	15.3	21.2	31.1	39.6	8.8	54.1	8832	8832
01-Jan-2011	Uminor	-17.7	-11.2	-8.0	-3.8	-1.1	-0.4	2.0	11.2	17.4	5.6	24.2	5779	5779
-	Umajor	-57.8	-50.5	-37.8	-19.3	-8.5	-11.0	-2.8	10.3	23.0	14.1	37.1	5779	5779
02-Mar-2011	Speed	0.1	1.2	2.6	6.3	10.9	14.8	20.9	38.9	51.9	11.5	58.9	5779	5779

Table 3-20. Summary of ocean current quarterly statistics for Site 2 at the near-surface.

Site 2: Near Surface	chan	min	1%	5%	25%	50%	mean	75%	95%	99%	std	max	# valid	total #
Time	cm/s													
28-Jul-2010	Uminor	-32.9	-24.0	-18.2	-10.1	-5.5	-5.6	-0.8	6.4	12.5	7.4	24.3	6215	6215
-	Umajor	-61.7	-53.0	-45.1	-32.9	-24.3	-22.3	-12.6	5.4	12.7	15.0	20.2	6215	6215
30-Sep-2010	Speed	0.4	2.7	6.8	17.5	26.0	25.9	34.1	45.5	53.5	11.7	65.0	6215	6215
01-Oct-2010	Uminor	-25.8	-19.9	-14.9	-8.2	-3.5	-2.0	2.2	17.2	33.7	9.9	53.3	8832	8832
-	Umajor	-65.4	-58.6	-44.0	-17.9	2.5	6.0	33.4	58.5	67.1	31.9	76.9	8832	8832
31-Dec-2010	Speed	0.2	2.8	5.7	13.2	26.0	29.0	42.8	60.7	68.6	17.8	79.4	8832	8832
01-Jan-2011	Uminor	-38.2	-23.8	-9.0	-3.6	-0.8	-0.8	1.7	7.8	24.4	6.7	38.7	8640	8640
-	Umajor	-85.0	-70.7	-51.1	-21.9	-12.6	-13.5	-5.3	22.1	63.8	21.7	93.5	8640	8640
31-Mar-2011	Speed	0.0	1.5	3.5	8.5	15.2	20.3	26.4	58.8	79.1	16.8	99.0	8640	8640
01-Apr-2011	Uminor	-24.0	-15.1	-11.7	-6.6	-3.0	-2.3	0.7	10.2	17.7	6.7	35.5	8736	8736
-	Umajor	-38.8	-32.0	-24.8	-17.0	-9.4	-2.0	12.9	37.4	53.2	20.3	72.8	8736	8736
30-Jun-2011	Speed	0.5	2.7	5.7	12.3	17.6	19.0	23.5	38.1	53.8	10.1	72.9	8736	8736
01-Jul-2011	Uminor	-22.5	-17.6	-14.8	-10.4	-7.1	-7.0	-3.8	1.2	5.5	4.9	13.4	2796	2796
-	Umajor	-55.1	-41.9	-35.3	-26.1	-19.9	-19.8	-13.2	-4.4	-0.1	9.5	4.3	2796	2796
30-Jul-2011	Speed	1.0	4.2	8.5	16.1	21.6	22.0	27.5	36.1	42.7	8.5	56.4	2796	2796

Table 3-21. Summary of ocean current quarterly statistics for Site 2 at mid-depth (22 m).

Site 2: 22 m	chan	min	1%	5%	25%	50%	mean	75%	95%	99%	std	max	# valid	total #
Time	cm/s													
28-Jul-2010	Uminor	-36.1	-24.4	-19.8	-11.5	-7.0	-7.2	-3.0	4.8	13.9	7.4	25.5	6215	6215
-	Umajor	-74.0	-54.2	-44.5	-31.2	-23.9	-22.5	-14.4	3.3	9.6	13.7	20.3	6215	6215
30-Sep-2010	Speed	0.4	6.1	10.8	19.4	25.7	26.4	32.4	45.3	54.8	10.3	76.6	6215	6215
01-Oct-2010	Uminor	-32.6	-24.2	-18.2	-9.4	-4.5	-3.6	0.8	15.7	29.3	10.1	49.3	8832	8832
-	Umajor	-61.1	-55.2	-43.9	-18.9	0.9	3.3	26.8	53.6	61.2	30.0	69.4	8832	8832
31-Dec-2010	Speed	0.3	2.5	5.8	15.0	25.7	27.8	40.4	55.9	62.3	15.8	71.1	8832	8832
01-Jan-2011	Uminor	-40.6	-23.3	-10.0	-4.4	-1.8	-1.7	0.4	7.2	25.0	6.7	35.0	8640	8640
-	Umajor	-83.8	-69.5	-50.8	-22.7	-13.6	-14.6	-6.3	19.7	56.5	20.8	84.6	8640	8640
31-Mar-2011	Speed	0.1	1.7	4.0	9.6	16.1	20.8	26.4	57.4	76.4	16.1	90.4	8640	8640
01-Apr-2011	Uminor	-26.3	-17.7	-13.5	-8.4	-5.1	-4.6	-1.6	7.0	11.7	6.1	27.3	8736	8736
-	Umajor	-39.0	-31.2	-25.4	-17.6	-10.3	-3.3	10.7	34.9	49.8	19.2	62.6	8736	8736
30-Jun-2011	Speed	0.7	3.1	5.9	13.0	17.7	18.8	23.1	36.3	51.1	9.3	64.0	8736	8736
01-Jul-2011	Uminor	-27.0	-20.2	-16.8	-12.1	-9.0	-8.9	-5.8	-0.6	4.0	5.0	7.7	2797	2797
-	Umajor	-51.7	-37.0	-33.2	-24.8	-18.2	-18.4	-11.9	-3.8	0.2	9.0	4.7	2797	2797
30-Jul-2011	Speed	4.4	7.1	9.6	16.0	21.2	21.6	26.8	34.2	37.8	7.6	51.9	2797	2797

Table 3-22. Summary of ocean current quarterly statistics for Site 2 at the near-bottom (34 m).

Site 2: 34 m	chan	min	1%	5%	25%	50%	mean	75%	95%	99%	std	max	# valid	total #
Time	cm/s													
28-Jul-2010	Uminor	-28.3	-20.8	-17.4	-11.3	-7.7	-7.8	-4.3	1.7	8.7	5.8	23.3	6215	6215
-	Umajor	-53.3	-46.7	-38.6	-28.4	-22.4	-20.3	-13.0	4.0	9.0	12.4	13.2	6215	6215
30-Sep-2010	Speed	0.4	6.2	10.5	18.2	23.9	24.2	29.5	39.2	47.0	8.6	53.5	6215	6215
01-Oct-2010	Uminor	-39.2	-28.5	-21.2	-9.6	-4.8	-4.1	1.7	14.7	25.7	10.5	35.4	8832	8832
-	Umajor	-59.8	-53.2	-44.4	-19.4	1.4	2.2	25.4	47.3	55.3	28.1	64.6	8832	8832
31-Dec-2010	Speed	0.1	2.6	5.6	14.7	25.9	26.7	37.6	51.1	57.0	14.5	65.3	8832	8832
01-Jan-2011	Uminor	-39.9	-23.1	-11.4	-6.5	-3.8	-3.2	-1.0	7.9	22.3	6.7	34.6	8640	8640
-	Umajor	-78.1	-64.1	-49.4	-21.5	-13.4	-14.5	-6.4	18.4	52.5	19.6	83.7	8640	8640
31-Mar-2011	Speed	0.1	1.6	4.0	10.0	16.3	20.6	26.3	52.6	69.2	15.0	84.5	8640	8640
01-Apr-2011	Uminor	-26.4	-19.2	-14.3	-9.4	-6.2	-5.5	-2.6	6.5	12.7	6.2	25.9	8736	8736
-	Umajor	-38.3	-31.7	-26.3	-18.2	-10.7	-4.5	8.8	32.0	44.0	18.4	54.4	8736	8736
30-Jun-2011	Speed	0.5	3.1	6.1	13.5	18.4	18.9	23.5	34.6	44.6	8.4	55.3	8736	8736
01-Jul-2011	Uminor	-21.5	-18.5	-16.1	-12.1	-9.0	-9.3	-6.6	-2.9	-0.1	4.1	4.4	2797	2797
-	Umajor	-38.3	-35.0	-31.9	-25.1	-19.7	-18.7	-12.7	-2.9	1.2	8.7	4.5	2797	2797
30-Jul-2011	Speed	4.1	8.5	12.1	17.6	22.1	22.1	26.6	32.4	35.2	6.2	38.9	2797	2797

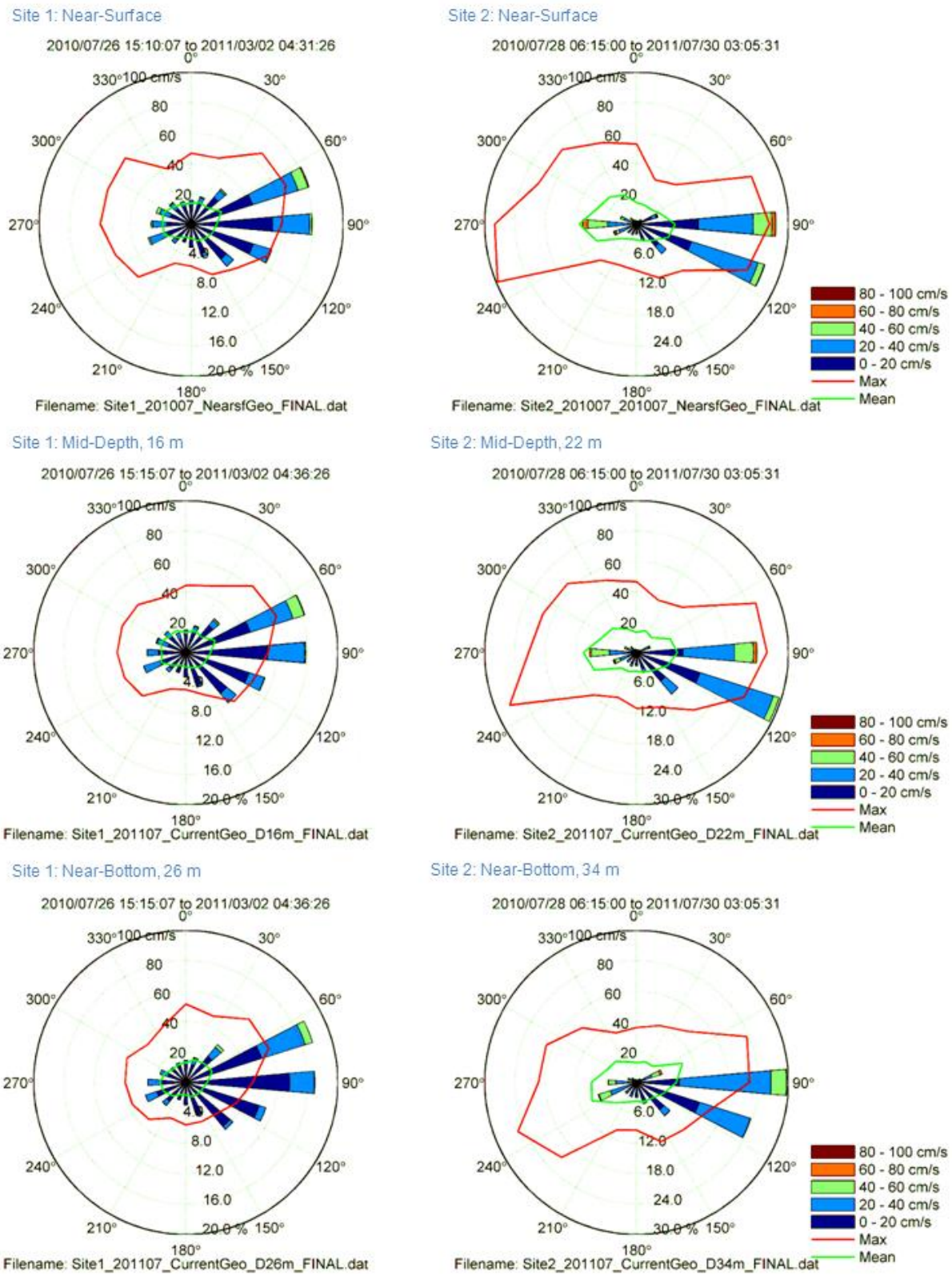

Figure 3-23. Compass plots of the directional distribution at the near-surface, mid-depth, and near-bottom at Site1 and Site 2 for the entire deployment period.

3.4.3 SUMMARY OF OCEAN CURRENTS

Continuous measurements of ocean current profiles were obtained at Site 1 for approximately 8 months, from July 26, 2010 to March 2, 2011. The instrument stopped recording data before its recovery on July 27, 2011 due to corrosion of the underwater connectors on the external battery pack. There were about 12 months of data collected at Site 2, where the instrument functioned properly for the entire deployment. At both sites, the quality of the data recorded was reasonably high with a small number of gaps where the instrument rejected data due to low backscatter amplitudes or inconsistencies between the beams.

The ocean currents were characterized by occasional events of large currents, particularly on January 2, 2011, where the site 2 near-surface speed reached 99 cm/s. The site 1 maximum in this time interval was only about 30 cm/s. It may be possible that the influence of waves or ice at site 2 (there was open water detected on 2 January at site 2) has driven the near-surface level selection algorithm to deeper bins than at site 1. This event corresponds to wind speeds close to 17 m/s at Wainwright, Alaska. Another instance of high current speeds was on February 25, 2011 where Site 1 peaked at 67.2 cm/s and Site 2 at 77 cm/s. The wind at this time was around 7 m/s at Wainwright. No wind data was available from Point Lay.

The average and maximum currents are somewhat larger at near-surface levels than at mid-depth and near-bottom levels. The average current speeds (and maximum speeds) at Site 1 were 16.3 (67.2) cm/s at the near-surface, 15.6 (64.2) cm/s at mid-depths (16 m) and 14.2 (58.9) cm/s at near-bottom (26 m) depths. At Site 2 the average (and maximum) current speeds are larger at 23.3 (99.0) cm/s at the near-surface, 23.1 (90.4) cm/s at mid-depths (22 m) and 22.4 (84.5) cm/s at near-bottom (34 m) depths.

3.5 BOTTOM TEMPERATURES, SALINITY AND DENSITY

The ADCP instruments were equipped with temperature sensors from which time series measurements of near bottom temperatures are available. Additionally, conductivity temperature (CT) instruments, model SBE37smp, were attached to the IPS-5 mooring cages at both Site 1 and Site 2. These instruments provide bottom temperature and conductivity data which could be used to derive a salinity and density time series. The ADCP and CT data sets require truncation of data values immediately after the instruments were deployed and on recovery to limit the time series to the in-water part of the deployment where the sensors were in thermal equilibrium with the ambient water.

The 2010-2011 temperature record at Site 2 (near shore site) indicate a sudden change in deep water temperatures (Figure 3-24), in contrast to last year's (2009-2010) Site 2 and to this year's Site 1 (the site further offshore) temperature record, which happened more gradually over a month (approximately from September 22, 2010 to October 26, 2010). Around September 22, 2010 the near-bottom ocean temperatures at Site 2 decreased suddenly from 4˚C to -1.3 over a two to three day period and stayed at near freezing temperatures with small variations until June 2, 2011, after which the water temperatures became gradually warmer reaching a seasonal maxima of 1˚C on July 5, 2011. The overall maximum water temperature at Site 2 for the 2010-2011 measurement period was recorded at 4.9˚C on September 6, 2010. A notable deep water warming event occurred over a 10-day period (December 30, 2010 – January 8, 2011) during the 8-month period of near freezing bottom temperatures at Site 2. Coincidentally, over this period partial open water conditions existed at Site 2, which can also be seen in (Figure 4-4). On average, the mean near bottom water temperatures were 0.47˚C colder than the previous year's temperature recorded at the same location, but caution should be taken when comparing point data sources such as these temperature observations as water characteristics can vary significantly over short distances in oceanographically dynamic areas.

As mentioned above, Site 1 near bottom temperatures presented a more gradual decrease towards the minimum water temperatures from late September to late October 2010 (Figure 3-24). After an initial period of appreciable variability in water temperatures through November and early December, they stayed within 0.3˚C of the yearly minimum from mid-December to early June, before reaching their seasonal maxima of 1.3˚C on June 19, 2011. Wave activity that was recorded by the Site 1 IPS-5 mooring around November 17 – 20, 2010 (after the freeze-up was recorded on November 1), followed by open water observations during November 23 to December 2, 2010, left a signature of high temperature variability and slightly higher than normal near bottom water temperatures during this period at both the CT and ADCP sensor data (Figure 3-24).

The salinity and density measurements at Site 1 (Figure 3-25) reveal increasing salinities from early November to early April which is likely associated with the formation of sea ice which extrudes salt into the water column. In the remainder of the winter and in spring, salinity varies between 30.9 PSU and 33.6 PSU as different water masses advected past the measurement site. Salinity variations are not as regular at Site 2 as they are at Site 1,

which implies that Site 2 is located in a more dynamic region. Site 2 salinities varied between 31.3 PSU and 34.6 PSU over the measurement period, presenting a slightly larger range than the Site 1 salinities. Statistical summaries are provided in Table 3-23, Table 3-24 and Table 3-25.

Table 3-23. Record-length statistics computed for the near-bottom temperature data at Sites 1 and 2.

Site	Instrument	Instrument Depth (m)	Water Depth (m)	Sample Interval (min)	Mean Temp (°C)	StdDev Temp (°C)	Min Temp (°C)	Max Temp (°C)
Site 1	ADCP #8944	35	39	5	-0.18	2.18	-1.90	6.38
	CT Sensor: SBE #7820	36	39	15	-0.57	1.87	-1.82	6.39
Site 2	ADCP #10985	43	47	5	-1.09	1.17	-1.83	4.66
	CT Sensor: SBE #6270	44	47	15	-1.08	1.18	-1.82	4.90

Table 3-24. Temperature, salinity and density statistics computed for the near bottom (36 m) at Site 1.

Site 1, SBE #7820 26-Jul-2010 16:00:00 to 27-Jul-2011 13:59:26													
Channel	**min**	**1%**	**5%**	**25%**	**50%**	**mean**	**75%**	**95%**	**99%**	**std**	**max**	**# valid**	**total #**
Temperature (°C)	-1.82	-1.81	-1.80	-1.77	-1.69	-0.57	0.15	3.95	5.27	1.87	6.39	35129	35129
Salinity (psu)	30.88	31.15	31.59	32.01	32.30	32.33	32.74	32.98	33.17	0.46	33.55	35114	35129
Density (kg/m^3)	1024.79	1025.15	1025.39	1025.81	1026.15	1026.13	1026.52	1026.70	1026.86	0.42	1027.17	35114	35129

Table 3-25. Temperature, salinity and density statistics computed for the near bottom (44 m) at Site 2.

Site 2, SBE #6270 28-Jul-2010 06:45:01 to 30-Jul-2011 04:30:06													
Channel	**min**	**1%**	**5%**	**25%**	**50%**	**mean**	**75%**	**95%**	**99%**	**std**	**max**	**# valid**	**total #**
Temperature (°C)	-1.82	-1.81	-1.80	-1.76	-1.67	-1.08	-0.86	0.94	4.05	1.18	4.90	35224	35224
Salinity (psu)	31.33	31.95	32.08	32.40	32.65	32.67	32.87	33.33	33.98	0.39	34.61	35224	35224
Density (kg/m^3)	1025.40	1025.67	1025.91	1026.27	1026.47	1026.47	1026.65	1027.03	1027.54	0.34	1028.05	35224	35224

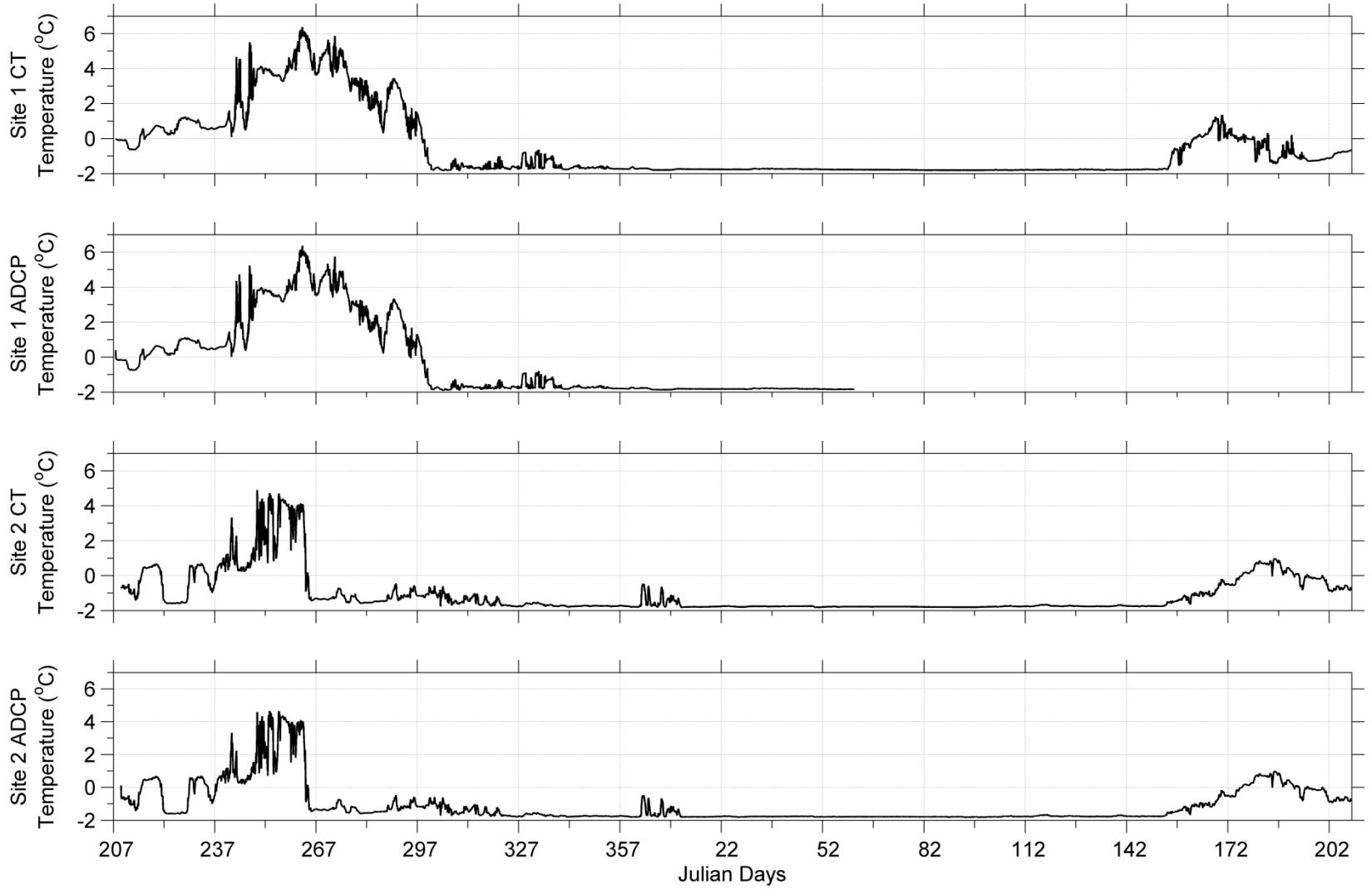

Figure 3-24. Near-bottom temperature data measured by ADCP and CT sensors at Sites 1 and 2.

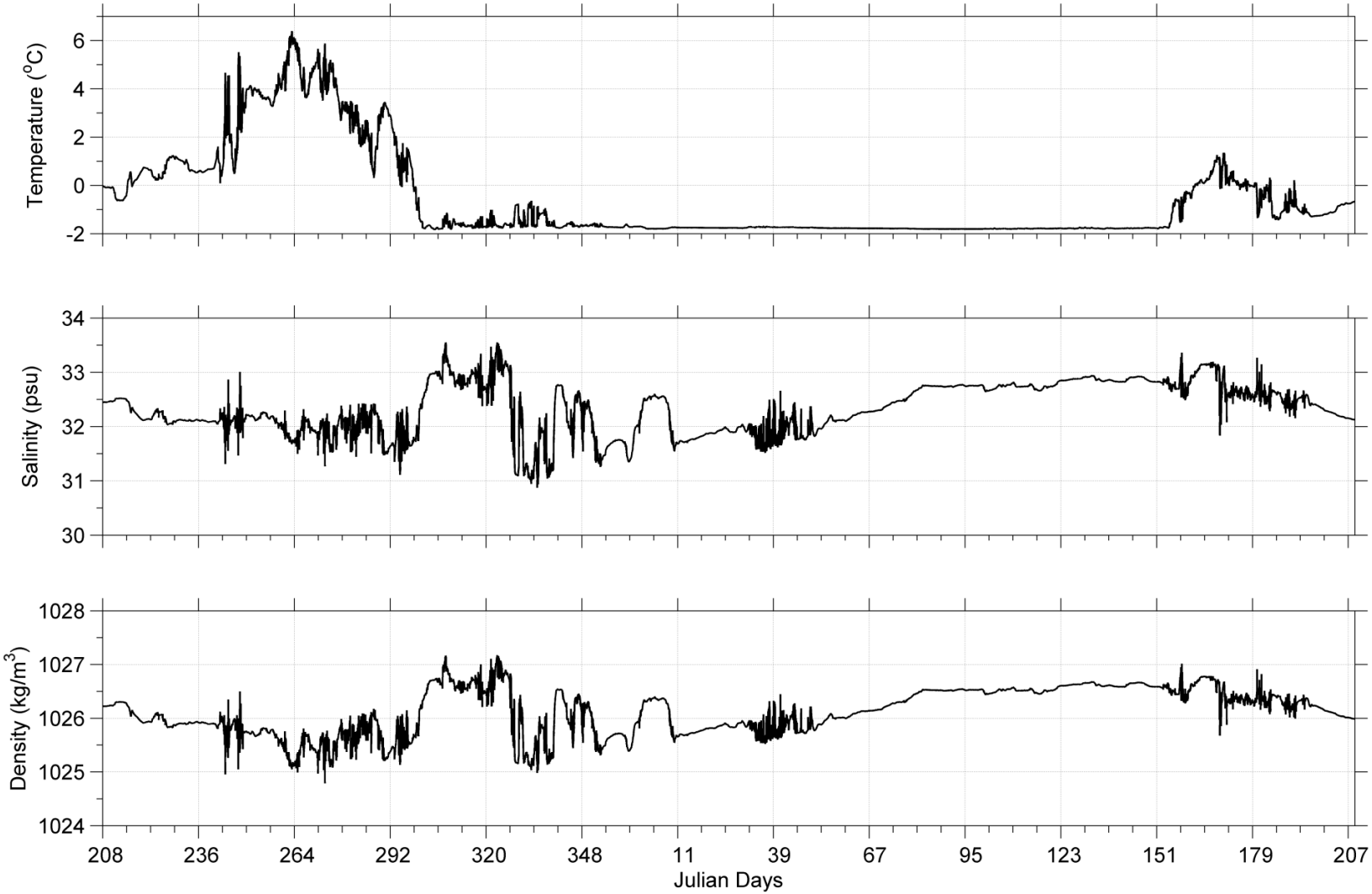

Figure 3-25: Near-bottom temperature, salinity, and density data measured by the CT sensor at Site 1.

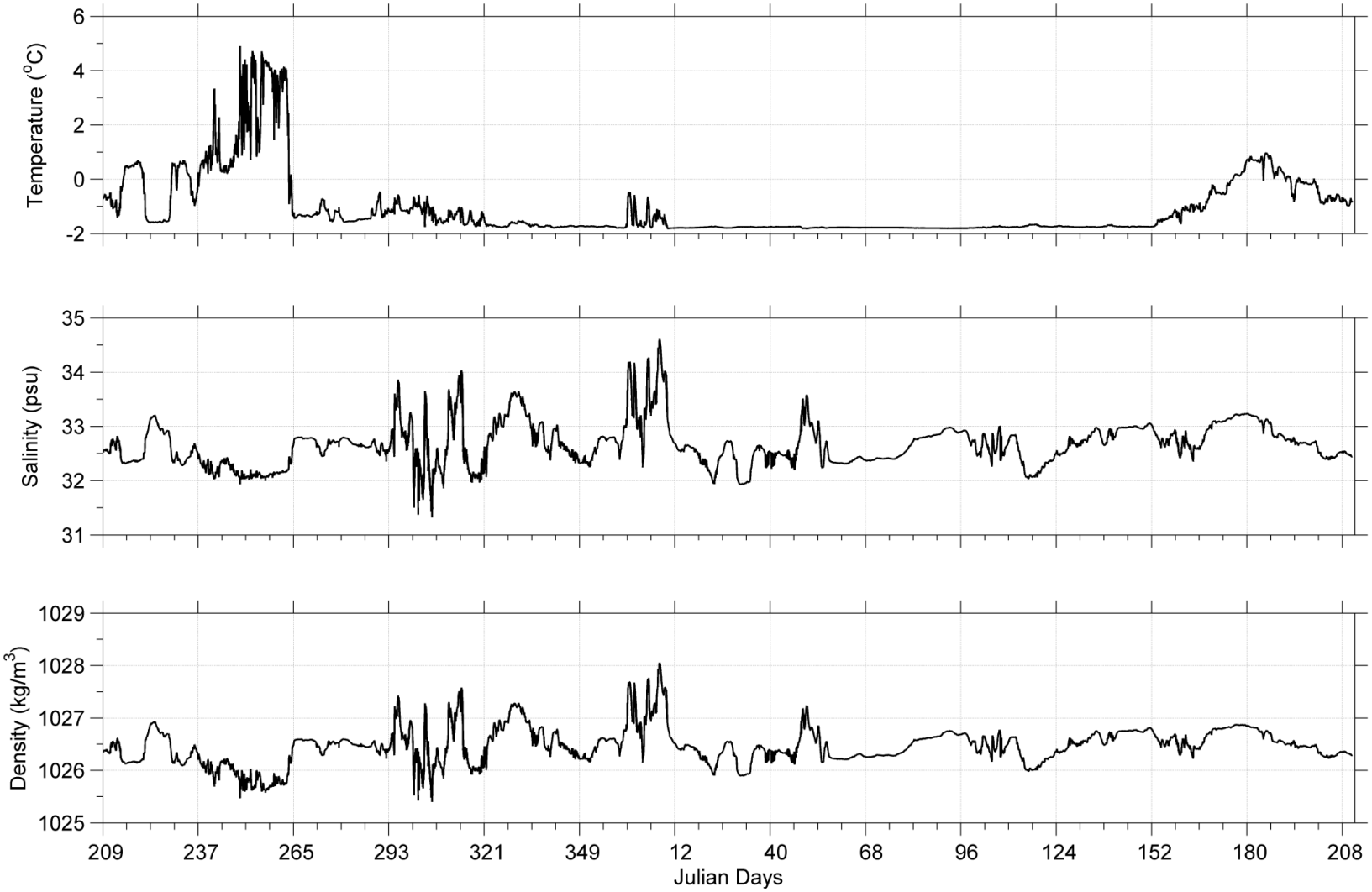

Figure 3-26. Near-bottom temperature, salinity, and density data measured by the CT sensor at Site 2.

3.6 METEOROLOGICAL DATA

Meteorological station measurements were obtained from Point Lay, and Wainwright, Alaska.

All of the measurements were obtained from the Weather Underground online weather service (*http://www.wunderground.com*). The wind data represents the standard 10 m anemometer height and represents mean wind values (1 minute or longer sampling duration) reported at hourly intervals.

The data from this site contained hourly- time series measurements of:

- atmospheric pressure (dbar)
- air temperature (°C)
- wind direction (°)
- wind speed ($m \cdot s^{-1}$)

The daily observations of wind speed and air temperature are shown in Figure 3-27. The meteorological observations were used to assist in interpreting and classifying ice keel features at the measurement site. The sea level pressure measurements (not illustrated) were also required to provide quantitative values for the purposes of computing ice drafts (Equation 1 in Section 3.1.2.1) for processing the ice profiling sonar data. Note that the air temperature and wind measurements obtained from Point Lay meteorological station have large data gaps approximately two and four months, respectively.

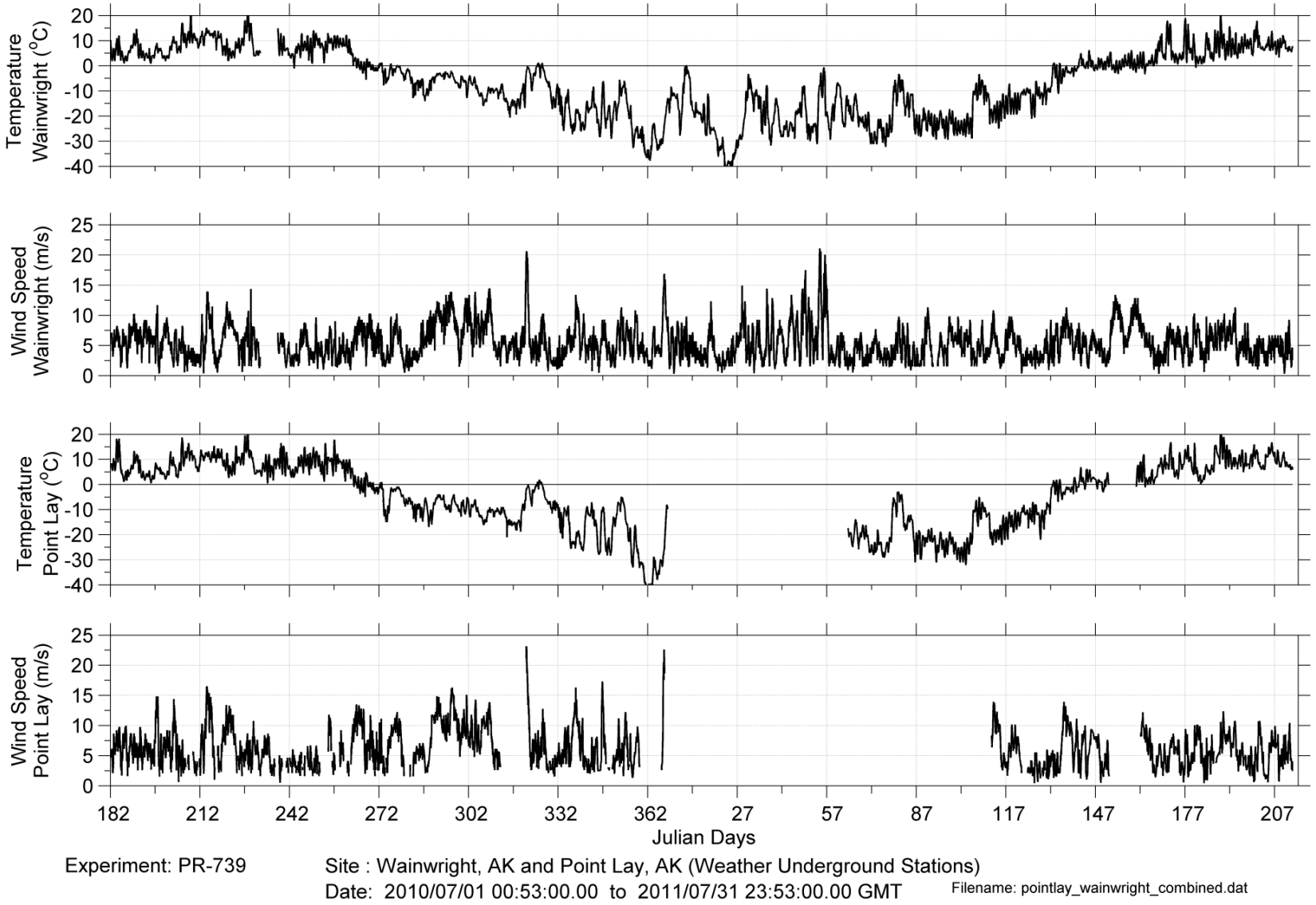

Figure 3-27. Daily air temperature and wind speed as observed at Wainwright and Point Lay weather stations from July 2010 to July 2011.

3.7 OTHER ICE DATA SETS

In addition to the underwater profiling measurements of ice keels collected at the measurement sites over the July 2010 to July 2011 period, other ice data were also obtained:

1. Weekly to sub-weekly ice charts prepared by the U.S. National Ice Service (http://www.natice.noaa.gov/) from the week of July 1, 2010 to the week of August 3, 2011.
2. Daily SSM/I passive microwave ice concentration data provided by NOAA (http://polar.ncep.noaa.gov/seaice/Analyses.html) from June 27, 2010 to August 1, 2011.

These ice data sets were used to assist in interpretation of the ice profiling sonar data set; in particular, for determining if very thin ice or open water was present to assist in making corrections for variations to the ice drafts due to changing sound speeds in the ocean.

A source book was created using all the above data types, as well as the weather measurements. It was circulated among ASL's in-house scientific analysts to aid in interpretation and verification of ice movements in the region and, specifically, at the monitoring sites.

3.8 PROJECT ARCHIVE

All data sets collected directly as part of the present study are provided on an FTP site or via DVD (upon request). The organization of the data, plots and other documentation is as shown in Figure 3-28.

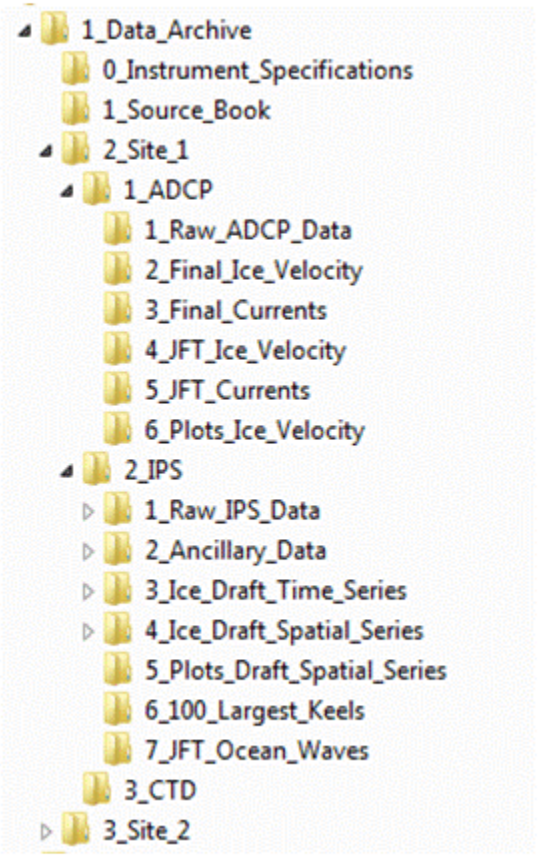

Figure 3-28. Directory tree of the Project Archive provided on ASL FTP site. Site 2 subdirectory branches are not shown as they are the same as Site 1 subdirectories.

Data are provided in ASL Standard Format: one data file, and header file pair for each dataset. The header file has the file extension '.hdr' and is a text file contains metadata for the data in the data file. The data file has the file extension '.dat' and is a text file that contains columns of data.

4 ANALYSIS RESULTS

4.1 OVERVIEW OF SEA ICE CONDITIONS IN 2010-2011

In recent years, the fall season in Arctic Ocean was characterized by a major retreat north of the edge of the pack ice (Figure 4-1). The Arctic Ocean ice extent was at a historic low in 2007, with the second lowest mean September ice extent happening this year, in 2011 since the beginning of observations in 1979. As indicated in Table 4-1, the last decade has seen so many yearly minimum sea ice extent that even the long-term mean (1979-2000 versus 1979-2010) is lowered significantly (7.04×10^6 km^2 vs. 6.52×10^6 km^2) when it includes the data from this decade. The retreat of the minimal sea ice extent was particularly pronounced in the western Arctic Ocean in all four years.

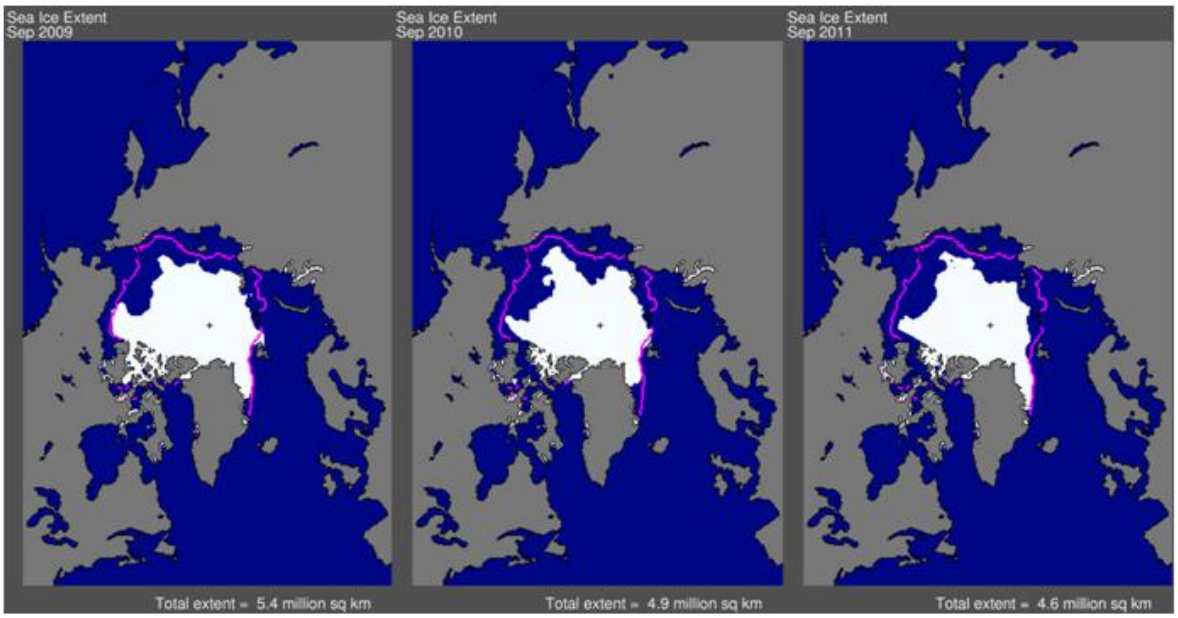

Figure 4-1. September sea ice extent concentrations for 2009 to 2011. (http://nsidc.org/).

Table 4-1. Previous Arctic sea ice extents for the month of September.

	2005	2006	2007	2008	2009	2010	2011
Monthly mean ($x10^6$ km^2)	5.60	5.90	4.30	4.67	5.36	4.90	4.61
1979-2000 mean	7.04						
1979-2010 mean	6.52						

4.1.1 FREEZE-UP PATTERNS: OF FALL 2010

As in previous measurement years, in the fall of 2010, pack ice was for the most part located well offshore in the northern Chukchi Sea with the ice edge extending well beyond the continental shelf and slope waters to northerly latitudes (Figure 4-1).

Ice formation began along the coast in October 2010 (Figure 4-2) following the usual seasonal pattern, however, no ice was recorded at Site 1 and Site 2 until November 1st (Figure 4-3). The freeze-up period at Site 1 and Site 2 started with new ice at concentrations of 4 - 6 tenths, as shown in the ice chart of November 1, it progressed quickly and by the end of first week in November (image from November 8) ice concentrations attained values of 9+ tenths for both sites. Although Site 2 (near shore site) was covered with high concentrations (9+ tenths) of ice during most of November, ice free waters remained in the proximity of Site 1 (offshore site), where waves and open water conditions were recorded by the Site 1 IPS instrument in mid to late November. The large pool of water with low ice concentrations (1-3 tenths) adjacent to Site 1 can also be seen in the ice chart of November 29, which extended towards the coast, influencing the ice concentrations at Site 2 for a few days in late November. By early December (Figure 4-4, image from December 6) almost all of Chukchi Sea, including the Sites 1 and 2 were covered with 9+ tenths of ice.

Although Site 1 stayed covered with high concentrations of ice (9+) until the sea ice break-up started in early June, Site 2 experienced a few short episodes of low ice concentration as seen in Figure 4-4, associated with the opening -and closing- of the polynya next to the landfast ice, which can extend towards Site 2, occasionally (images from January 3 and May 2, 2011).

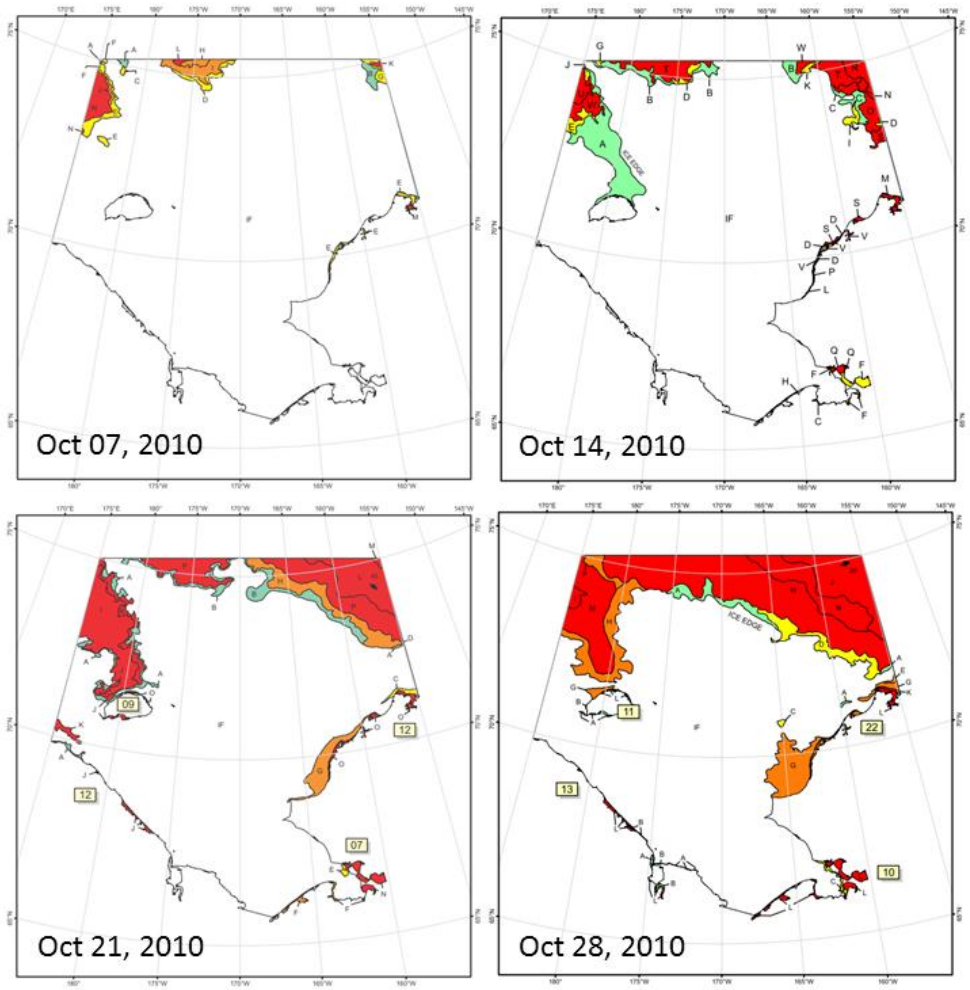

Figure 4-2. Fall 2010 freeze-up patterns. Ice charts are presented for selected days during October 2010 in the Chukchi Sea. Site 1 is located approximately at 71 ˚N, 165 ˚W and Site 2 is located at 71 ˚N, 161 ˚W.

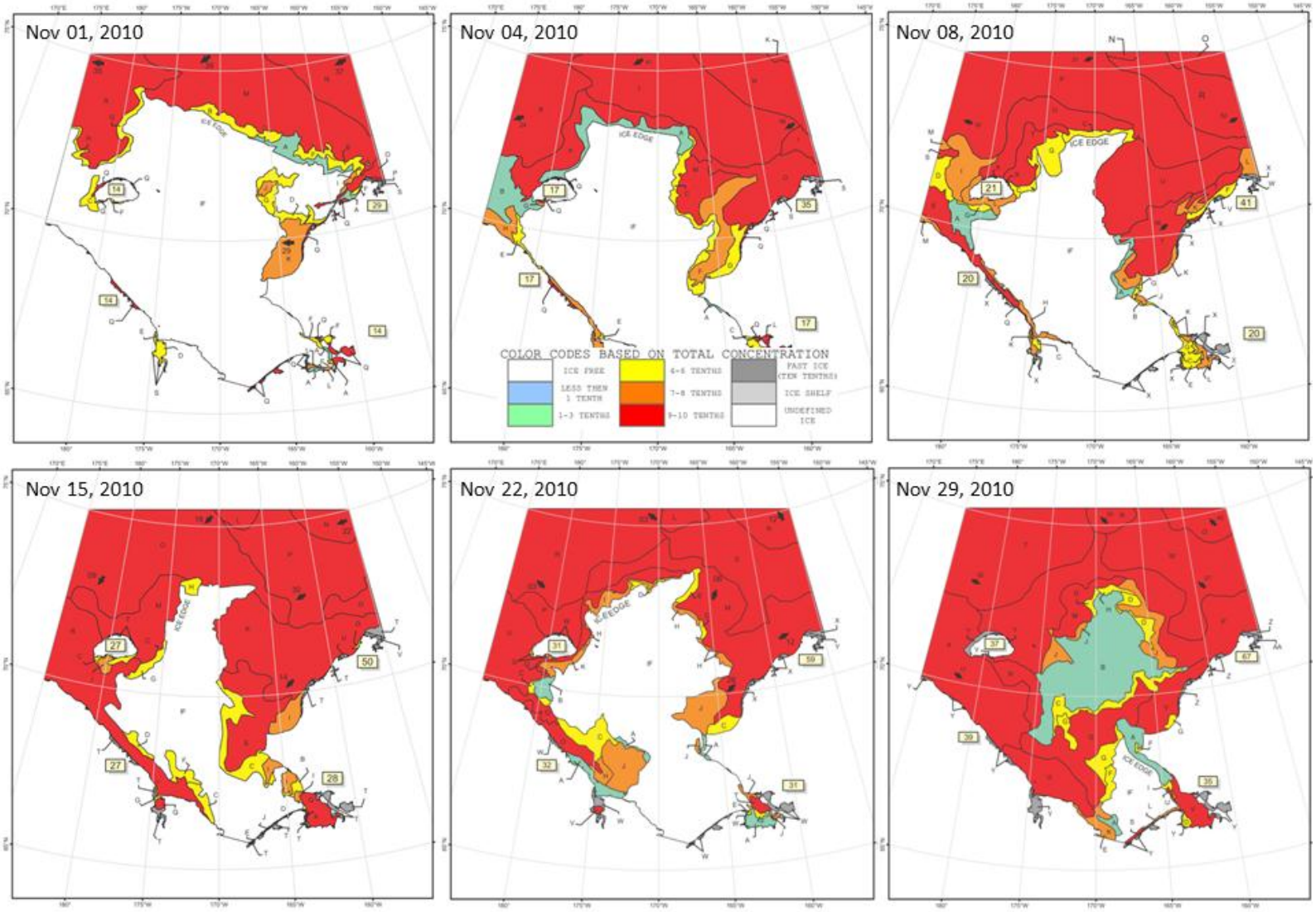

Figure 4-3. Fall 2010 freeze-up patterns. Ice charts are presented for selected days during November 2010 in the Chukchi Sea. Site 1 is located at 71 ˚N, 165 ˚W and Site 2 is located at 71 ˚N, 161 ˚W.

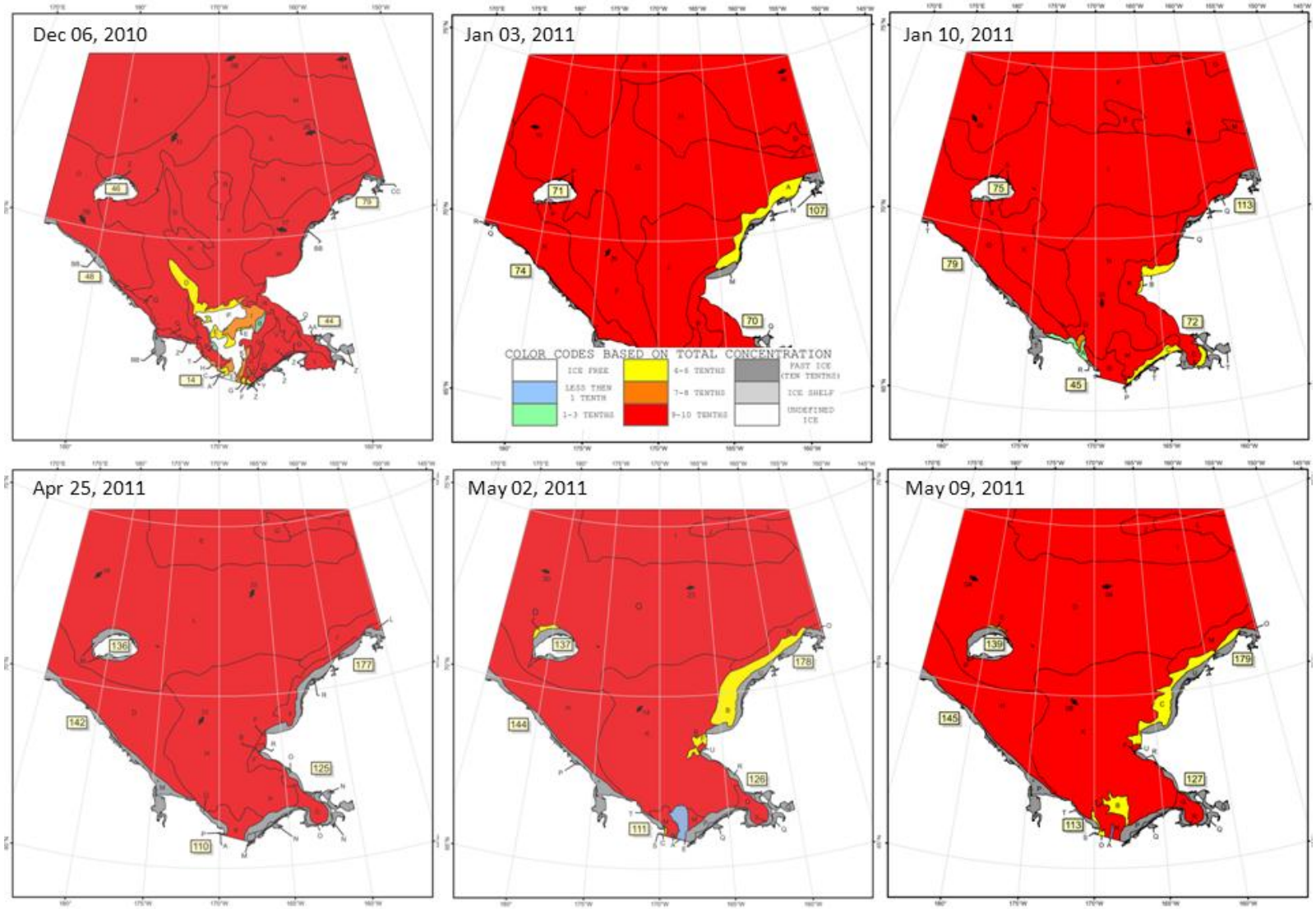

Figure 4-4. Progress of 2010-11 freeze-up patterns. Ice charts are presented for the period of December 6, 2010 to May 9, 2011 in the Chukchi Sea. Site 1 is located at 71 ˚N, 165 ˚W and Site 2 is located at 71 ˚N, 161 ˚W.

4.1.2 BREAK-UP PATTERNS: SUMMER 2011

In the summer of 2011 (Figure 4-4 and Figure 4-5), ice began to clear along the Alaskan coastline in early May (Figure 4-4, ice chart from May 2) with an extensive flaw lead present from south of Nome to Pt. Barrow, however, the ice concentrations stayed relatively high until mid-May at Site 2, which is located in the proximity of the flaw lead, as the flaw lead retreated towards the coast after its initial opening (Figure 4-4, ice chart from May 9). Site 1, further offshore, was heavily covered by ice during this period.

By mid-May (Figure 4-5, image from May 16) ice concentration at Site 2 were reduced sharply to 1-3 tenths due to the flaw lead. From this point on the break-up of ice progressed very quickly and large areas of Chukchi was ice-free before the end of May, 2-3 weeks earlier than the previous years. Both Site 1 and Site 2 IPS instruments recorded mostly ice-free waters on June 2, 2011. Even though a narrow, long strip of landfast ice persisted along the coast well into July following the seasonal ice break-up pattern, Site 1 and 2 became ice–free rapidly. As compared to the previous measurement year (2009-2010) where occasional ice floes originating to the north from the pack ice edge (just north of 72°N) continued to pass the measurement sites until well into July, the period of scattered keels transiting through the sites was much shorter this year (2010-2011). No ice keels were recorded by Site 1 IPS instrument after June 5 (after June 14 for Site 2)

The clearing of the sea ice in the eastern Chukchi Sea was approximately 3 to 5 weeks earlier in 2011 than in 2010, which was earlier than 2009. The ice conditions in the northern and western Chukchi Sea were also much milder than the previous year reaching the same level of open water conditions, approximately one month before the summer of 2010, by the end of June 2011.

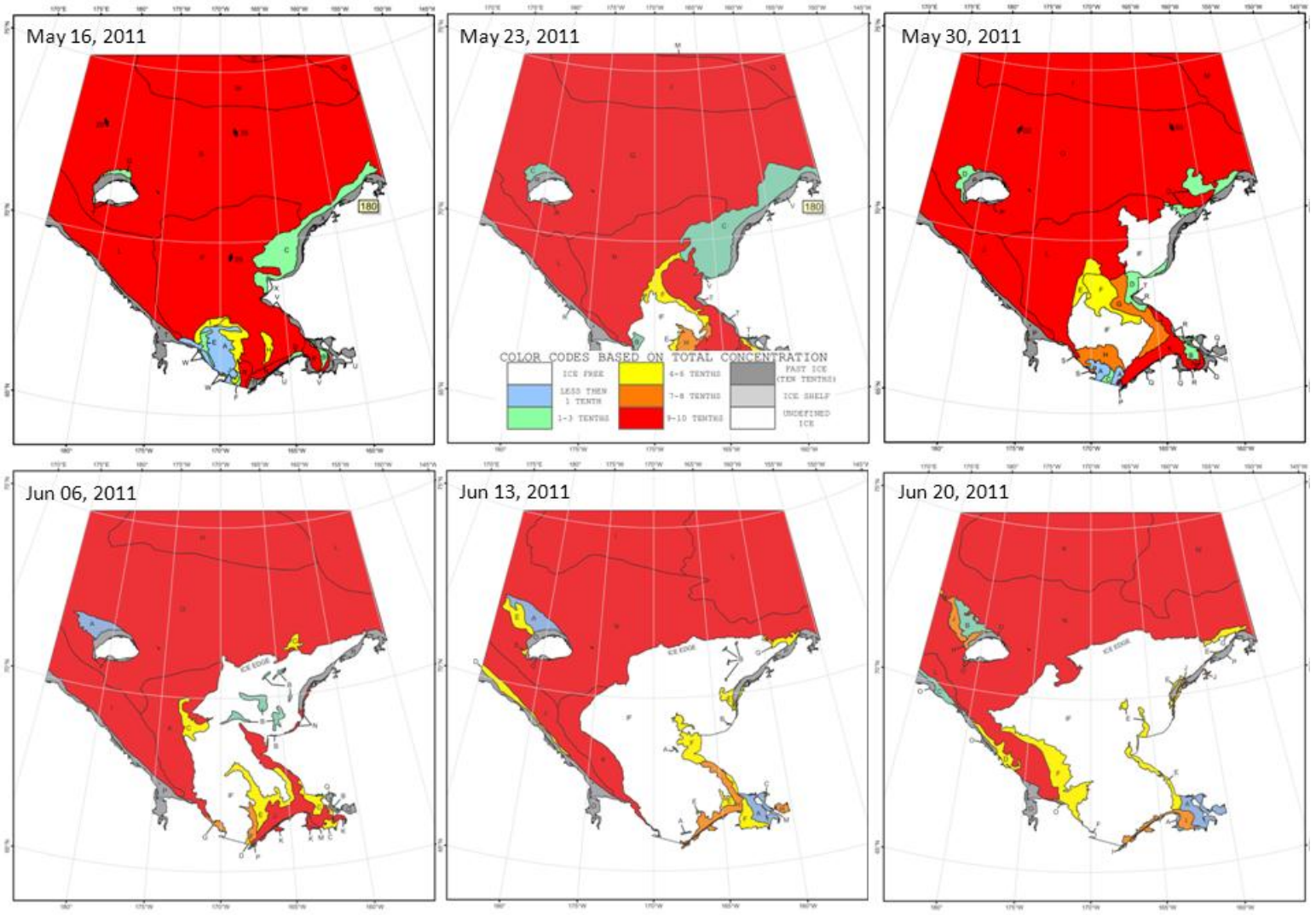

Figure 4-5. Summer 2011 break-up patterns. Ice charts are presented for the period of May 16 to June 20 in the Chukchi Sea. Site 1 is located at 71 ˚N, 165 ˚W and Site 2 is located at 71 ˚N, 161 ˚W.

4.2 ICE KEEL STATISTICS

4.2.1 METHODOLOGY FOR IDENTIFYING ICE KEELS

Ice keels that exceeded 5, 8, and 11 m were identified using either a Rayleigh criterion (α = 0.5), or a lower threshold of 2 m to end a feature. The keel detection algorithm was based on "Criterion A" as described in Vaudrey (1987). The algorithm found the start and end of individual ice features using three thresholds, as shown in Figure 4-6. For illustrative purposes, a 13 m starting threshold was used. A keel started, shown as "Start Point" in the figure, once the draft exceeded the "Start Threshold". The keel ended if it crossed the "End Threshold" at 2 m, or if it reversed slope at a point less than a threshold given by (1 - α)*Maximum Draft, where α = 0.5 is the Rayleigh criterion.

The beginning of the keel is then found by scanning backwards from the previously designated "Start Point". The earlier keel start was found at a point that crossed the "End Threshold," or reversed slope, at a point less than the threshold given by (1 - α)*Maximum Draft. Unlike the forward search to find the keel endpoint, the maximum draft was not updated; instead the value found for the forward search was used.

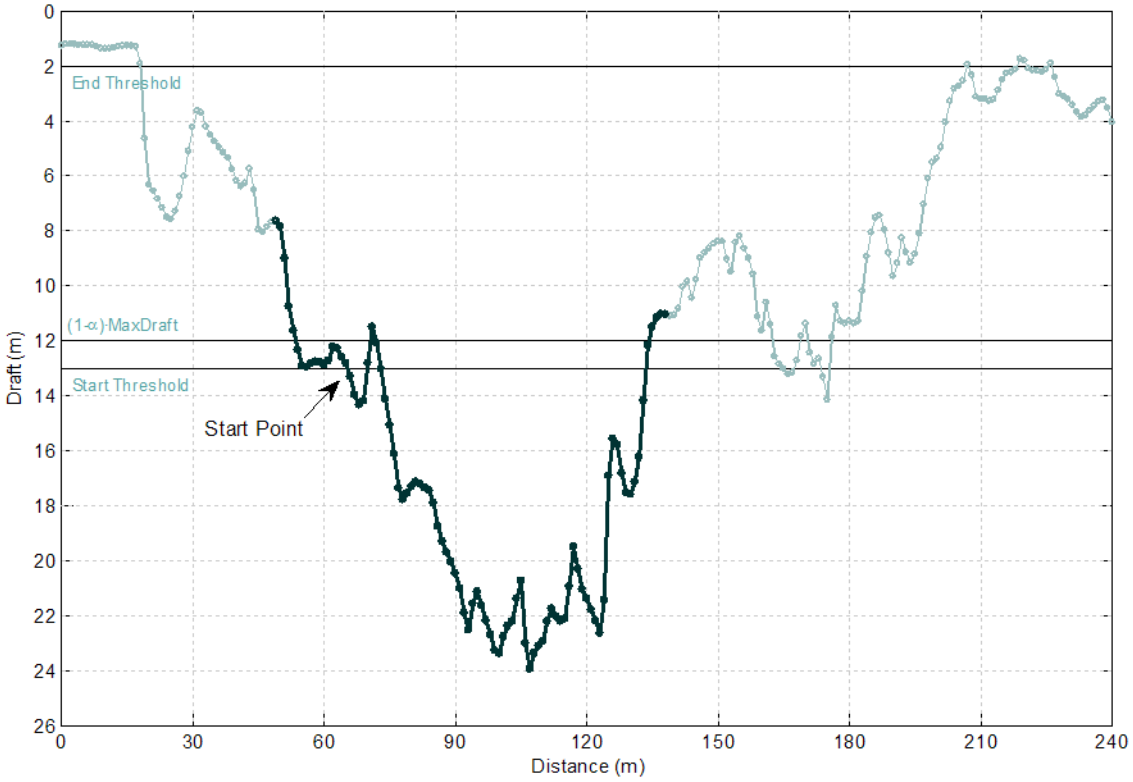

Figure 4-6. An example of the thresholds used by the keel identification algorithm. The keel was found using a 13 m start threshold, 2 m end threshold, and α equal to 0.5.

4.2.2 OVERLAPPING FEATURES

The backwards search technique used to find the start of a keel can result in overlapping keel features when a keel with a larger maximum draft was followed by one with a lower maximum draft. In the backwards search on the second lower draft keel, the beginning of the keel can extend past the beginning of the first keel since the lower draft means a lower α threshold. It is also possible that the second keel can overlap with more than one previous feature. After the preliminary keels were selected, they were re-processed and the overlapping features were combined into a single event by using the start of the first keel in the overlap and the end of the last keel in the overlap.

An example of this type of overlap and the resulting combined feature is shown in Figure 4-7. For illustrative purposes, a 13 m starting threshold was used and applied to the ice keel shown in Figure 4-6. Figure 4-7 shows an overlap with the feature in Figure 4-6, and the effect of combining the two features.

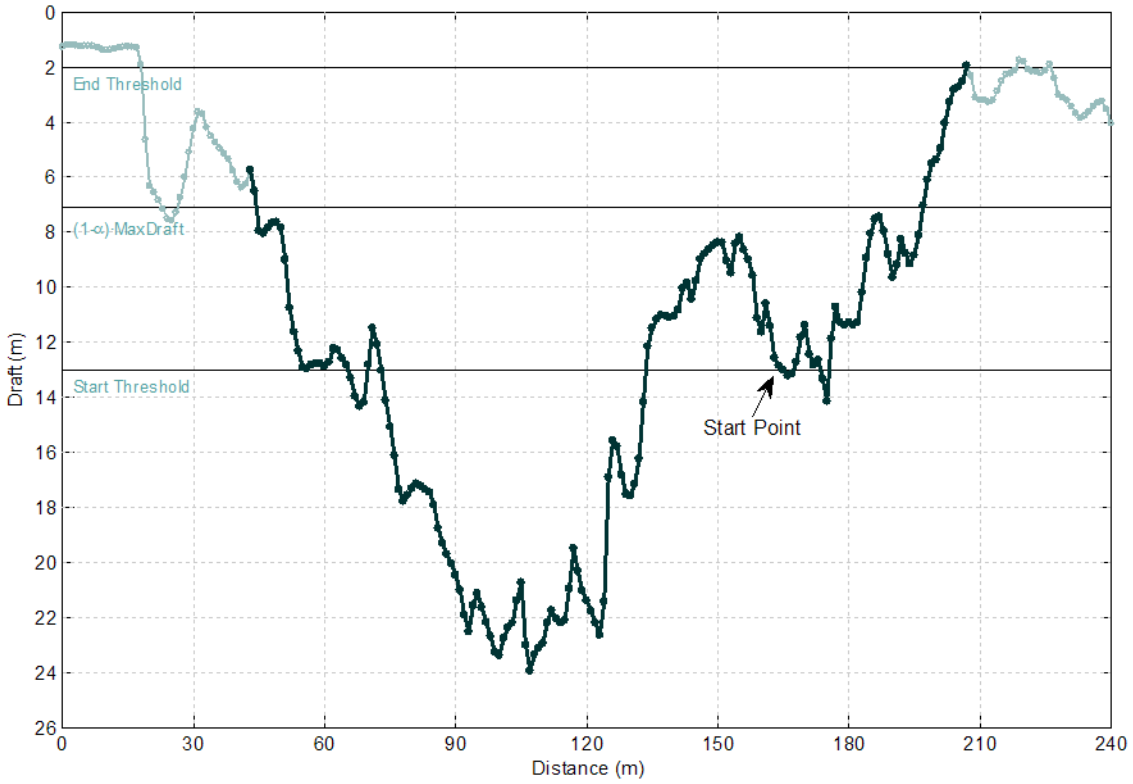

Figure 4-7. An example of a keel feature extending from the “Start Point” beyond the feature shown in Figure 4-6.

4.2.3 DESCRIPTION OF THE DATABASE OF KEEL FEATURES

A database of keel features was constructed using starting thresholds of 5, 8, and 11 m, an end threshold of 2 m and a Rayleigh criterion (α = 0.5). For each site and starting threshold, a data file was created containing the start time, end time, start distance, end distance, width, mean draft, maximum draft, minimum draft and the standard deviation of the draft for each keel feature. A description of each of the fields is provided in Table 4-2.

Statistical results are given over monthly and ice season time periods. For each starting threshold, a data file was created containing the start time of the statistic segment, the end time of the statistic segment, the minimum, mean, maximum and standard deviation of the maximum draft, the mean and standard deviation of the mean draft, the minimum, mean, maximum and standard deviation of the width, the total ice distance (sum of all ice distances for the time period), the total waves in ice and open water distance (sum of all waves in ice + open water distances for the time period), the total distance (sum of all ice + waves in ice + open water + data flagged as bad distances for this time period), the sum of all keel widths for this time period, the sum of all keel areas (sum of the product of each keel segment width and mean draft) and the number of keels in this time period. If a keel feature occurred on the boundary of consecutive monthly time segments, the keel was considered to be in the month where it had the greatest width. A description of each of the fields is provided in Table 4-3. In the ice keel statistical results, the average keel width is typically over 30 m. The widest keels may represent an amalgamation of individual keels or a rubbled ice field.

Table 4-2. A description of each field in the keel feature data file.

Name	Description
Start Time	The start time of the segment
End Time	The end time of the segment
Start Distance	The keel start distance (km)
End Distance	The keel end distance (km).
Width	The width of the keel feature (m).
Mean Draft	The mean draft value of the keel feature (m).
Maximum Draft	The maximum draft value of the keel feature (m).
Minimum Draft	The minimum draft value of the keel feature (m).
Std Dev of Draft	The standard deviation of the draft of the keel feature (m).

Table 4-3. A description of each field in the keel statistics (monthly and ice season) data file.

Name	Description
Start Time	The start time of the statistic segment.
End Time	The end time of the statistic segment.
Min of Max Draft	The minimum of all the maximum keel segment drafts in the time period (m).
Mean of Max Draft	The mean of all the maximum keel segment drafts in the time period (m).
Max of Max Draft	The maximum of all the maximum keel segment drafts in the time period (m).
Std of Max Draft	The standard deviation of all the maximum keel segment drafts in the time period (m).
Mean of Mean Draft	The mean of all the mean keel segment drafts in the time period (m).
Std of Mean Draft	The standard deviation of all the mean keel segment drafts in the time period (m).
Min Width	The minimum of all the keel segment widths in the time period (m).
Mean Width	The mean of all the keel segment widths in the time period (m).
Max Width	The maximum of all the keel segment widths in the time period (m).
Std of Width	The standard deviation of all the keel segment widths in the time period (m).
Total Ice Distance	The total distance of ice covered for the time period (km). This total distance includes all non-flagged data (ice).
Total O/W + Waves in Ice Dist	The total distance of waves in ice and open water covered for the time period (km). This total distance includes data flagged as open water and data flagged as waves in ice.
Total Distance	The total distance covered for the time period (km). This total distance includes ice, data flagged as open water, data flagged as waves in ice and data flagged as bad.
Sum of Keel Widths	The sum of the keel widths for the time period (km).
Sum of Keel Areas	The sum of the keel areas for the time period ($x10^3$ m^2). The area is calculated from the sum of the product of the mean draft and the width of each segment.
Number of Keels	The number of keel features in the time period.

Some statistical results from the ice keel feature database are presented as plots, including:

- the **daily** statistics of the number of keels and the total keel area for the 5, 8 and 11 m thresholds, shown in Figure 4-8 and Figure 4-9. Note that the large episodic variations in the number of ice keels and daily ice keel area are very strongly related to the episodic nature of daily ice movement distance. Site 2, located nearer the start of the Barrow Canyon and higher mean ice speeds (Table 3-12), has more keels in both total number and by total ice keel area than Site 1.
- **monthly** histograms of maximum ice drafts using the 5 m threshold are shown in Figure 4-10 and Figure 4-11.
- histograms of maximum ice drafts for the full ice **season** using the 5 m threshold are shown in Figure 4-12 and Figure 4-13.
- statistics for keels detected with the 5, 8 and 11 m thresholds are presented in Table 4-4 through Table 4-11.

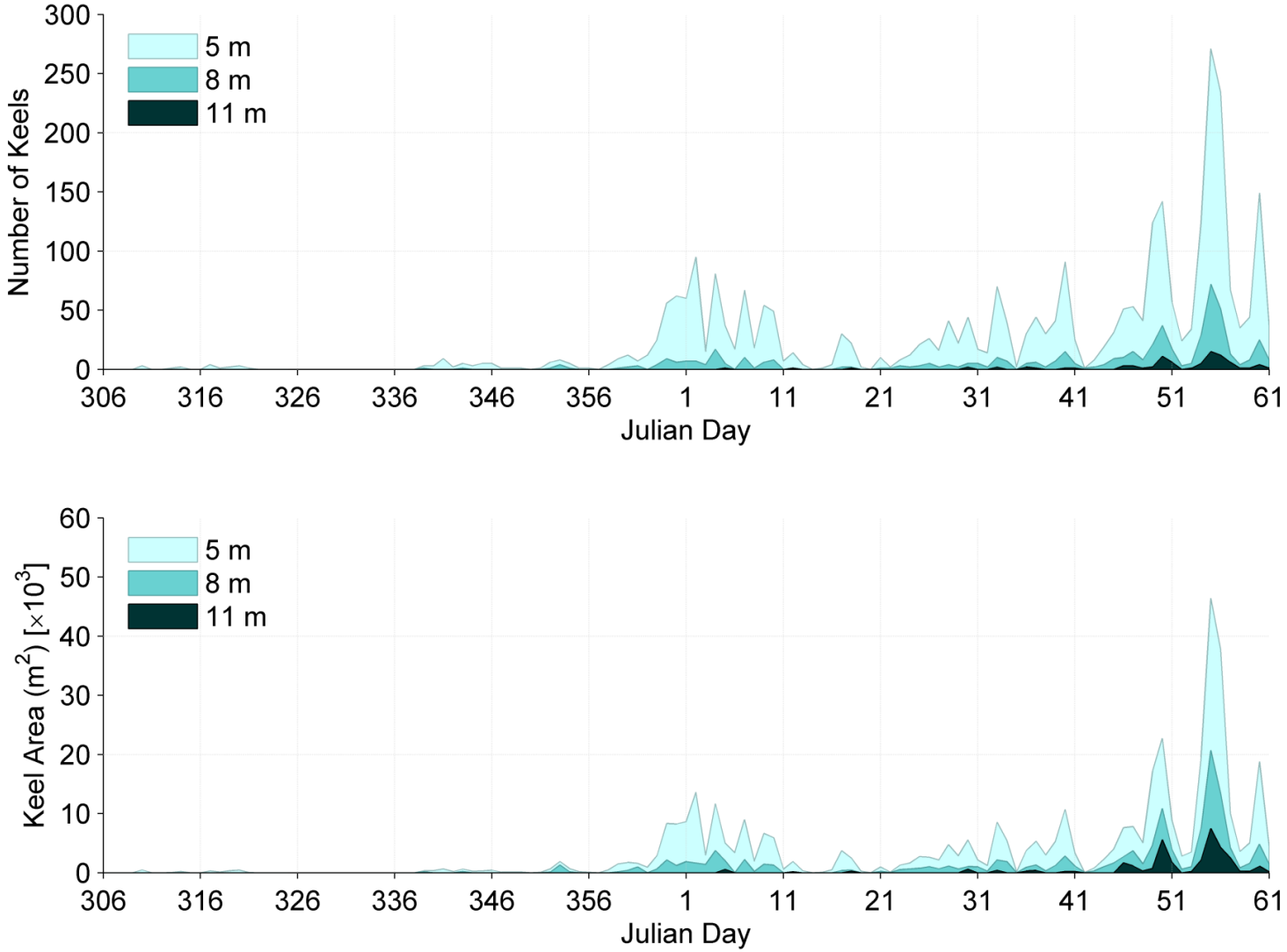

Figure 4-8. Daily numbers of keel features (top) and daily keel area (bottom) found using the 5m, 8m, and 11m thresholds at Site 1. Note that the ADCP record, and resulting spatial series record, ended on March 2, 2011.

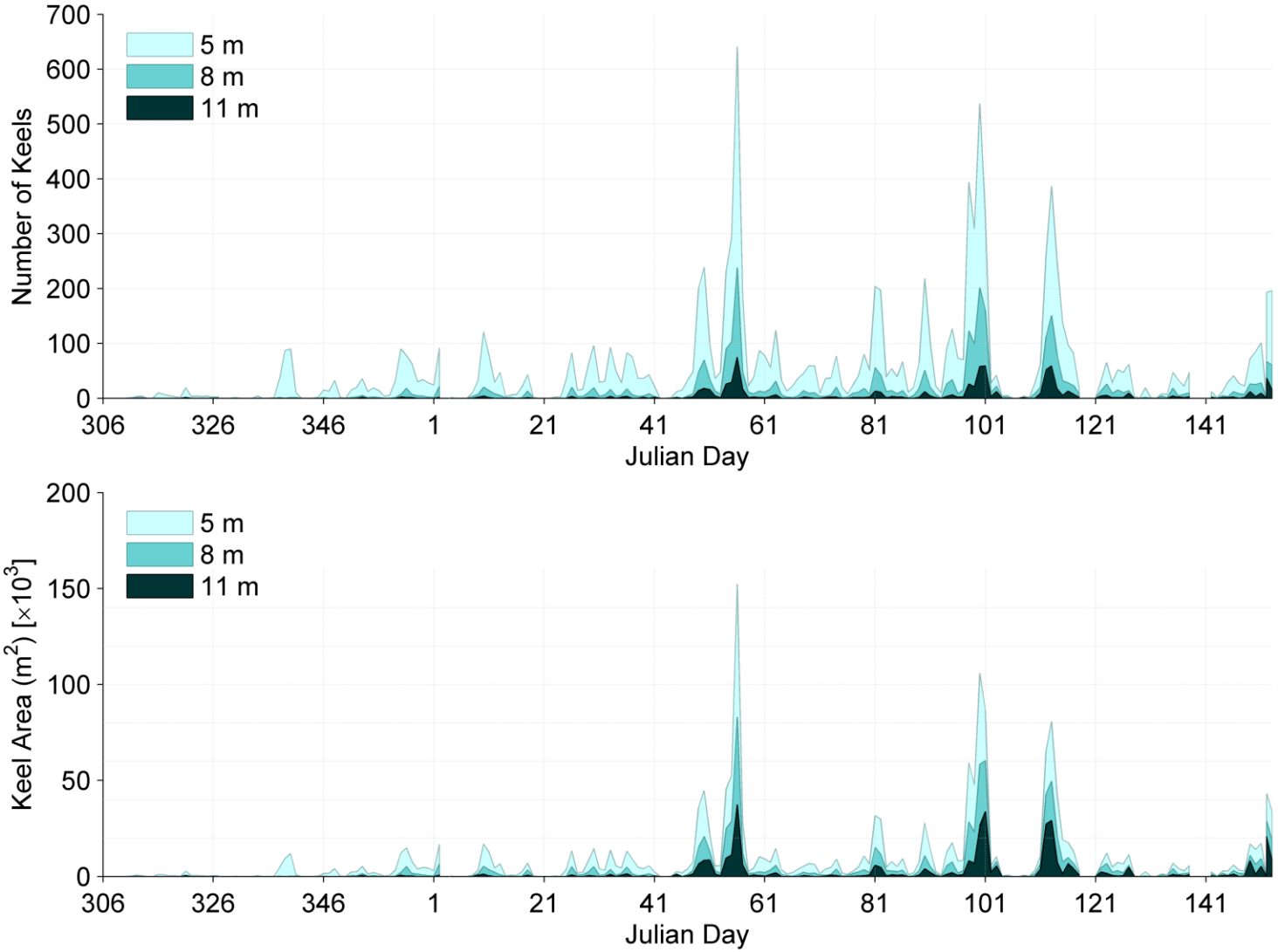

Figure 4-9. Daily numbers of keel features (top) and daily keel area (bottom) found using the 5m, 8m, and 11m thresholds at Site 2.

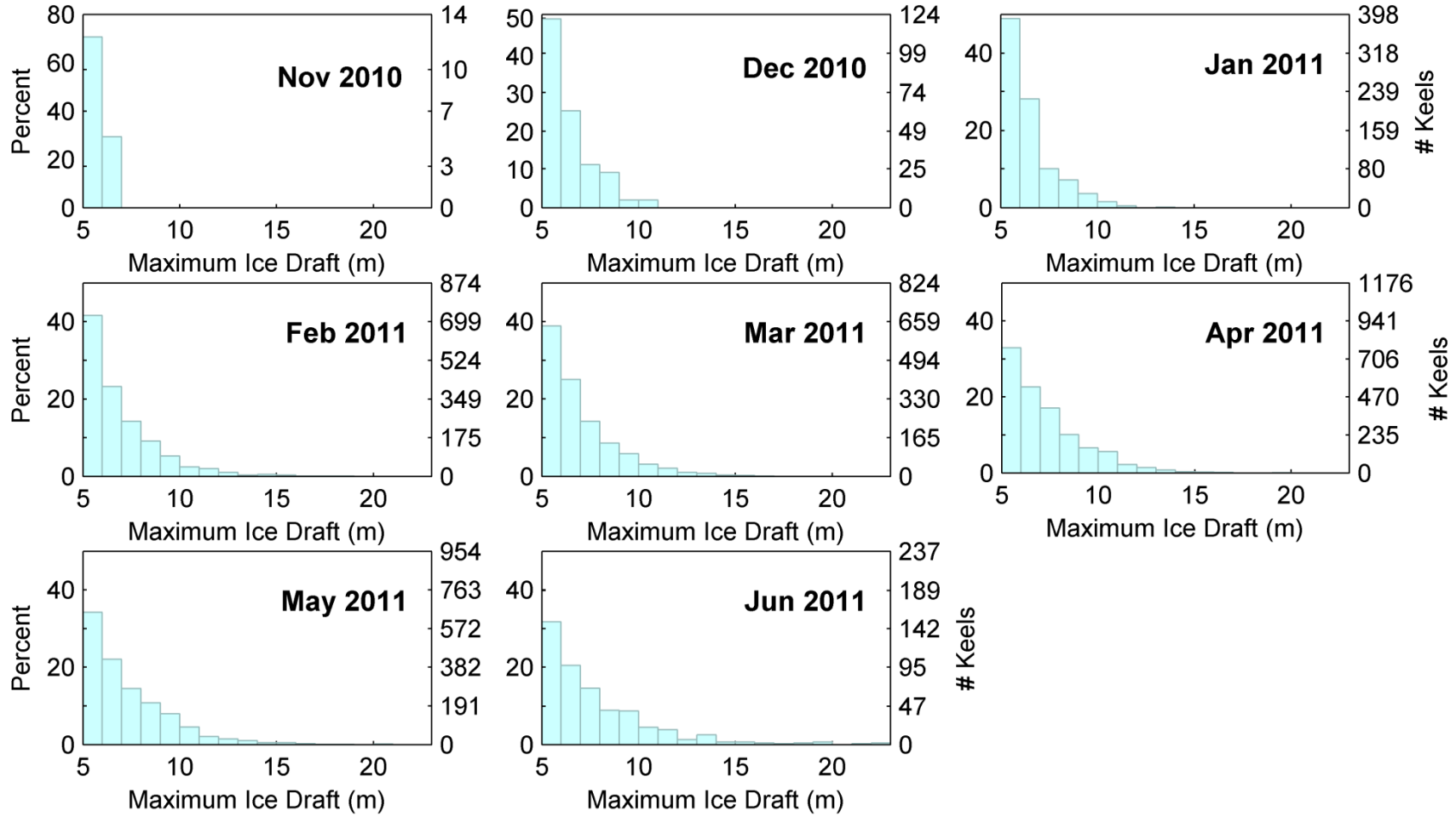

Figure 4-10. Monthly histograms of maximum ice draft for keels found using the 5 m threshold at Site 1. Note that keels after March 2, 2011 were identified from a pseudo-spatial series because the ADCP ice velocity record ended early.

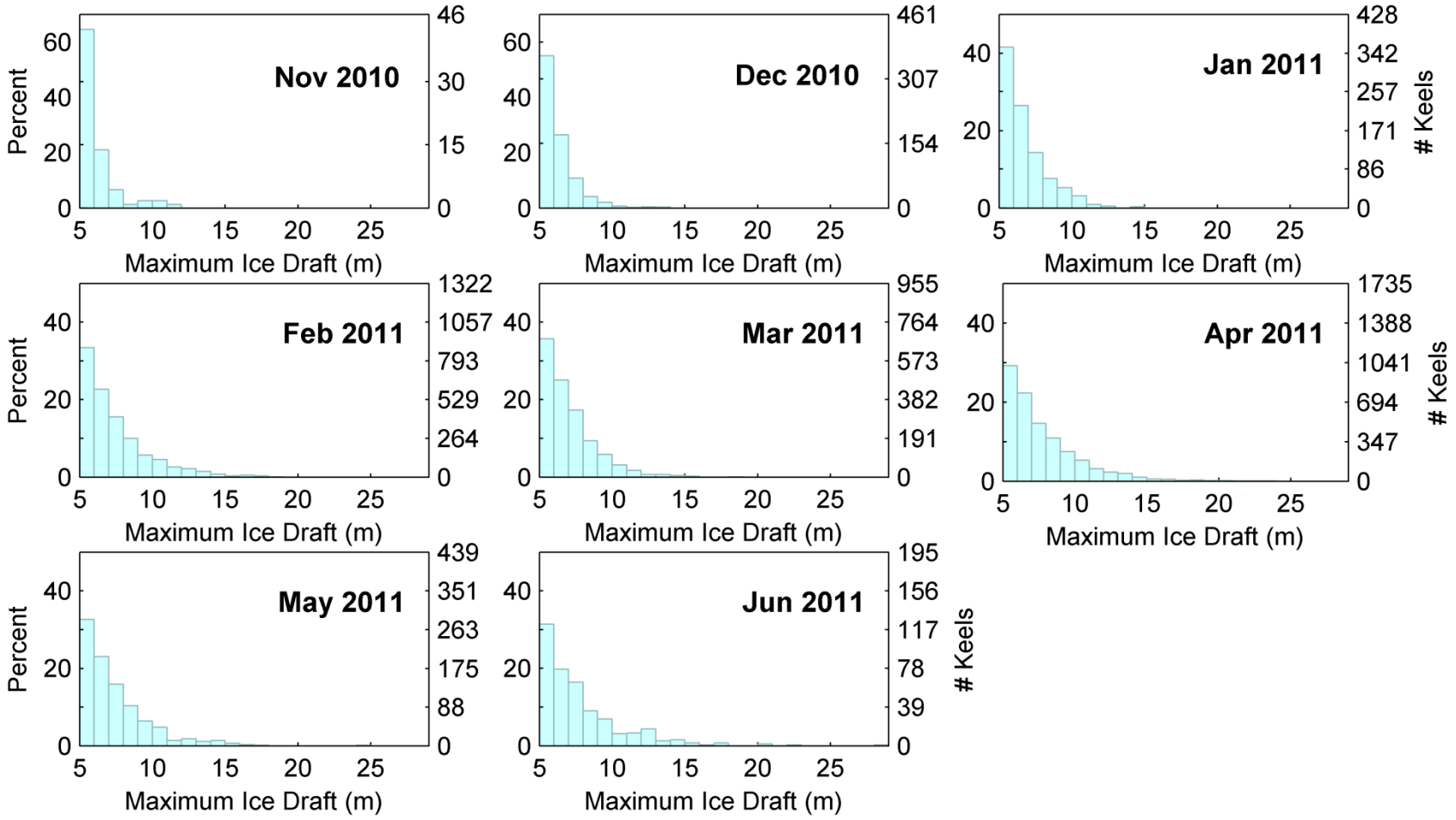

Figure 4-11. Monthly histograms of maximum ice draft for keels found using the 5 m threshold at Site 2.

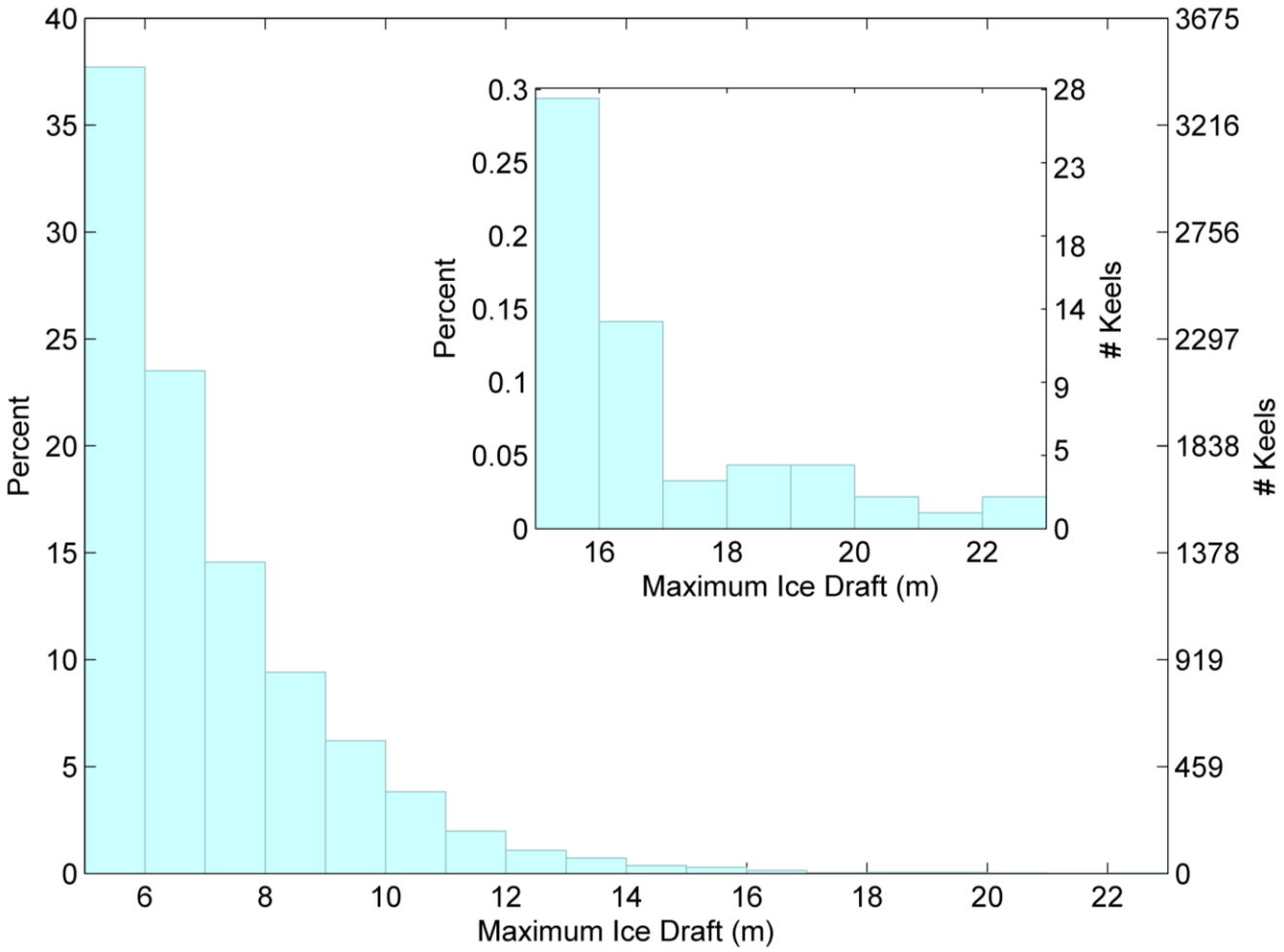

Figure 4-12. Full ice season histogram of the maximum ice draft for keels found using the 5 m threshold at Site 1. Note that keels after March 2, 2011 were identified from a pseudo-spatial series because the ADCP ice velocity record ended early.

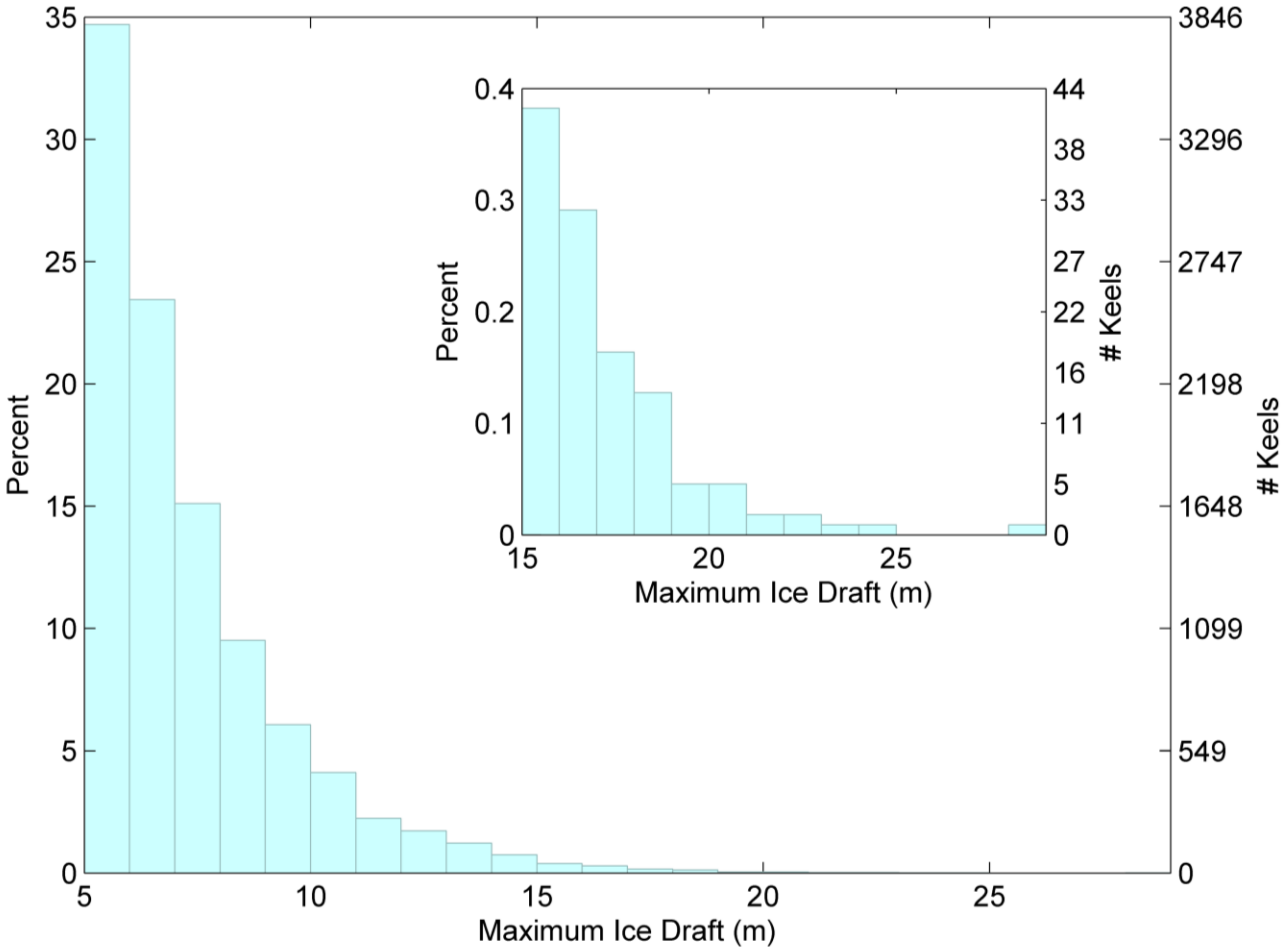

Figure 4-13. Full ice season histogram of the maximum ice draft for keels found using the 5 m threshold at Site 2.

Table 4-4. Site 1 monthly statistics of keel features for the 5 m threshold level.

Site 1, 2010-2011: 5 m Threshold *Draft statistics calculated from pseudo-spatial series after March 2, 2011																
Month	Maximum Draft				Mean Draft		Width				Distance			Keels		
	Min (m)	Mean (m)	Max (m)	StdDev (m)	Mean (m)	StdDev (m)	Min (m)	Mean (m)	Max (m)	StdDev (m)	Total Ice (km)	Total O/W + WI (km)	Total (km)	Sum of Width (km)	Sum of Area ($\times 10^3$ m^2)	Number
November	5.02	5.80	6.85	0.50	4.18	0.56	7.00	27.12	70.00	14.91	460.59	41.32	501.92	0.46	2.02	17
December	5.01	6.39	10.62	1.25	4.39	0.79	6.00	28.53	124.00	17.51	708.47	0.18	708.65	7.05	32.90	247
January	5.00	6.41	13.88	1.32	4.42	0.89	4.00	28.02	167.00	18.00	408.87	1.37	410.27	22.31	105.61	796
February	5.00	6.89	18.03	1.85	4.65	1.13	2.00	28.18	223.00	18.34	572.85	0.00	572.93	49.23	251.90	1747
March*	5.00	6.92	16.55	1.82	4.89	1.13	-	-	-	-	-	-	-	-	-	1596
April*	5.00	7.21	19.41	1.95	5.04	1.18	-	-	-	-	-	-	-	-	-	2267
May*	5.00	7.30	20.54	2.11	5.10	1.22	-	-	-	-	-	-	-	-	-	1824
June*	5.01	7.74	22.16	2.82	5.46	1.83	-	-	-	-	-	-	-	-	-	454

Table 4-5. Site 2 monthly statistics of keel features for the 5 m threshold level.

Site 2, 2010-2011: 5 m Threshold																
Month	Maximum Draft				Mean Draft		Width				Distance			Keels		
	Min (m)	Mean (m)	Max (m)	StdDev (m)	Mean (m)	StdDev (m)	Min (m)	Mean (m)	Max (m)	StdDev (m)	Total Ice (km)	Total O/W + WI (km)	Total (km)	Sum of Width (km)	Sum of Area ($\times 10^3$ m^2)	Number
November	5.03	6.16	11.27	1.31	4.37	0.99	6.00	25.86	59.00	13.80	713.05	316.81	1029.8	1.96	9.14	76
December	5.00	6.22	13.48	1.19	4.26	0.76	3.00	28.63	175.00	19.06	792.52	0.00	792.52	21.99	100.21	768
January	5.01	6.73	14.96	1.56	4.58	1.00	4.00	28.80	196.00	20.23	620.04	0.01	620.10	24.62	123.17	855
February	5.00	7.39	18.99	2.28	4.97	1.37	3.00	32.47	216.00	24.42	490.40	0.00	490.41	85.83	481.37	2643
March	5.00	7.00	18.01	1.79	4.74	1.13	2.00	24.35	216.00	16.99	200.06	0.00	200.06	46.52	242.94	1910
April	5.00	7.69	23.00	2.54	5.15	1.56	2.00	30.53	240.00	24.81	655.26	17.96	673.21	105.93	636.17	3470
May	5.00	7.38	24.05	2.29	4.98	1.43	1.00	27.79	275.00	24.24	298.90	33.61	332.51	24.37	141.02	877
June	5.00	7.85	28.73	2.98	5.30	1.87	3.00	29.69	294.00	29.45	46.19	7.36	53.55	11.55	76.58	389

Table 4-6. Site 1 monthly statistics of keel features for the 8 m threshold level.

Site 1, 2010-2011: 8 m Threshold *Draft statistics calculated from pseudo-spatial series after March 2, 2011

Month	Maximum Draft				Mean Draft		Width				Distance			Keels		
	Min (m)	Mean (m)	Max (m)	StdDev (m)	Mean (m)	StdDev (m)	Min (m)	Mean (m)	Max (m)	StdDev (m)	Total Ice (km)	Total O/W + WI (km)	Total (km)	Sum of Width (km)	Sum of Area ($\times 10^3$ m^2)	Number
November	-	-	-	-	-	-	-	-	-	-	460.59	41.32	501.92	0.00	0.00	0
December	8.09	8.88	10.62	0.82	5.88	0.84	13.00	37.42	84.00	18.70	708.47	0.18	708.65	1.23	7.56	33
January	8.00	9.16	13.88	1.02	6.39	0.78	5.00	36.70	98.00	20.53	408.87	1.37	410.27	3.78	24.75	103
February	8.00	9.78	18.03	1.76	6.57	1.29	9.00	35.83	179.00	20.98	572.85	0.00	572.93	13.19	92.59	368
March*	8.00	9.76	16.55	1.58	7.09	1.23	-	-	-	-	-	-	-	-	-	351
April*	8.01	9.88	19.41	1.65	7.10	1.22	-	-	-	-	-	-	-	-	-	603
May*	8.00	9.92	20.54	1.88	7.19	1.26	-	-	-	-	-	-	-	-	-	557
June*	8.00	10.72	22.16	2.82	7.65	1.91	-	-	-	-	-	-	-	-	-	148

Table 4-7. Site 2 monthly statistics of keel features for the 8 m threshold level.

Site 2, 2010-2011: 8 m Threshold																
Month	Maximum Draft				Mean Draft		Width				Distance			Keels		
	Min (m)	Mean (m)	Max (m)	StdDev (m)	Mean (m)	StdDev (m)	Min (m)	Mean (m)	Max (m)	StdDev (m)	Total Ice (km)	Total O/W + WI (km)	Total (km)	Sum of Width (km)	Sum of Area ($\times 10^3$ m^2)	Number
November	8.67	9.91	11.27	0.87	7.04	0.74	13.00	36.83	53.00	15.61	713.05	316.81	1029.8	0.22	1.62	6
December	8.10	9.30	13.48	1.30	6.31	0.92	6.00	38.03	127.00	22.34	792.52	0.00	792.52	2.24	14.74	59
January	8.01	9.46	14.96	1.31	6.48	1.06	5.00	36.91	154.00	22.88	620.04	0.01	620.10	5.68	38.75	154
February	8.00	10.32	18.99	2.12	7.08	1.51	5.00	39.70	203.00	25.76	490.40	0.00	490.41	30.09	227.78	758
March	8.00	9.72	18.01	1.64	6.67	1.25	6.00	30.26	142.00	18.07	200.06	0.00	200.06	12.77	90.38	422
April	8.01	10.48	23.00	2.39	7.21	1.69	4.00	37.47	219.00	27.01	655.26	17.96	673.21	44.74	355.19	1194
May	8.00	10.26	24.05	2.25	7.07	1.66	2.00	35.82	243.00	28.66	298.90	33.61	332.51	8.99	70.00	251
June	8.02	11.13	28.73	3.13	7.79	2.04	8.00	41.33	287.00	36.08	46.19	7.36	53.55	5.25	47.29	127

Table 4-8. Site 1 monthly statistics of keel features for the 11 m threshold level.

Site 1, 2010-2011: 11 m Threshold *Draft statistics calculated from pseudo-spatial series after March 2, 2011																
Month	Maximum Draft				Mean Draft		Width				Distance			Keels		
	Min (m)	Mean (m)	Max (m)	StdDev (m)	Mean (m)	StdDev (m)	Min (m)	Mean (m)	Max (m)	StdDev (m)	Total Ice (km)	Total O/W + WI (km)	Total (km)	Sum of Width (km)	Sum of Area ($\times 10^3$ m^2)	Number
November	-	-	-	-	-	-	-	-	-	-	460.59	41.32	501.92	0.00	0.00	0
December	-	-	-	-	-	-	-	-	-	-	708.47	0.18	708.65	0.00	0.00	0
January	11.09	11.94	13.88	1.14	8.53	1.63	18.00	35.40	50.00	11.52	408.87	1.37	410.27	0.18	1.57	5
February	11.00	12.68	18.03	1.60	8.51	1.57	11.00	44.82	179.00	29.16	572.85	0.00	572.93	3.32	29.94	74
March*	11.06	12.50	16.55	1.27	9.45	1.17	-	-	-	-	-	-	-	-	-	64
April*	11.01	12.62	19.41	1.52	9.24	1.24	-	-	-	-	-	-	-	-	-	112
May*	11.01	12.99	20.54	1.86	9.54	1.58	-	-	-	-	-	-	-	-	-	115
June*	11.05	13.65	22.16	2.75	9.74	1.65	-	-	-	-	-	-	-	-	-	44

Table 4-9. Site 2 monthly statistics of keel features for the 11 m threshold level.

Site 2, 2010-2011: 11 m Threshold																
Month	Maximum Draft				Mean Draft		Width				Distance			Keels		
	Min (m)	Mean (m)	Max (m)	StdDev (m)	Mean (m)	StdDev (m)	Min (m)	Mean (m)	Max (m)	StdDev (m)	Total Ice (km)	Total O/W + WI (km)	Total (km)	Sum of Width (km)	Sum of Area ($\times 10^3$ m^2)	Number
November	11.27	11.27	11.27	0.00	7.80	0.00	53.00	53.00	53.00	0.00	713.05	316.81	1029.8	0.05	0.42	1
December	11.30	12.54	13.48	0.82	8.56	0.82	23.00	31.33	43.00	8.73	792.52	0.00	792.52	0.19	1.66	6
January	11.01	12.36	14.96	1.35	8.48	1.03	13.00	40.20	85.00	23.42	620.04	0.01	620.10	0.60	5.18	15
February	11.00	13.10	18.99	1.77	9.12	1.49	9.00	46.57	203.00	26.33	490.40	0.00	490.41	10.15	96.64	218
March	11.01	12.70	18.01	1.43	8.91	1.21	10.00	38.37	130.00	21.32	200.06	0.00	200.06	2.69	24.92	70
April	11.00	13.41	23.00	2.26	9.43	1.76	8.00	47.09	219.00	31.03	655.26	17.96	673.21	17.05	170.99	362
May	11.02	13.53	24.05	2.06	9.65	1.82	4.00	47.97	209.00	33.46	298.90	33.61	332.51	2.93	29.70	61
June	11.12	13.86	28.73	3.23	9.85	2.03	7.00	50.29	277.00	44.26	46.19	7.36	53.55	2.62	29.10	52

Table 4-10. Site 1 ice season statistics of keel features for the three thresholds (5, 8 and 11 m).

Site 1, 2010-2011 *Note – these statistics computed for keels for which width information was available. This only includes keels observed until March 2, 2011.																
Threshold	**Maximum Draft**				**Mean Draft**		**Width**				**Distance**			**Keels**		
	Min (m)	**Mean (m)**	**Max (m)**	**StdDev (m)**	**Mean (m)**	**StdDev (m)**	**Min (m)**	**Mean (m)**	**Max (m)**	**StdDev (m)**	**Total Ice (km)**	**Total O/W + WI (km)**	**Total (km)**	**Sum of Width (km)**	**Sum of Area ($\times 10^3$ m^2)**	**Number**
5*	5.00	6.70	18.03	1.67	4.56	1.04	2.00	28.01	223.00	17.94	2171.77	42.87	2214.76	83.80	415.60	2992
8*	8.00	9.59		1.59	6.49	1.18	5.00	35.64	179.00	20.38				19.14	131.18	537
11*	11.00	12.58		1.55	8.48	1.53	11.00	43.42	179.00	27.80				3.65	32.77	84
Draft statistics for entire IPS record. A pseudo-spatial series was used after March 2, 2011																
5	5.00	6.83	22.16	1.70	4.77	1.09	-	-	-	-				-	-	8948
8	8.00	9.73		1.65	6.84	1.22	-	-	-	-				-	-	2163
11	11.00	12.73		1.69	9.17	1.47	-	-	-	-				-	-	414

Table 4-11. Site 2 ice season statistics of keel features for the three thresholds (5, 8 and 11 m).

Site 2, 2010-2011																
Threshold	**Maximum Draft**				**Mean Draft**		**Width**				**Distance**			**Keels**		
	Min (m)	**Mean (m)**	**Max (m)**	**StdDev (m)**	**Mean (m)**	**StdDev (m)**	**Min (m)**	**Mean (m)**	**Max (m)**	**StdDev (m)**	**Total Ice (km)**	**Total O/W + WI (km)**	**Total (km)**	**Sum of Width (km)**	**Sum of Area ($\times 10^3$ m^2)**	**Number**
5	5.00	7.29	28.73	2.25	4.92	1.39	1.00	29.37	294.00	23.06	3816.41	375.75	4192.22	322.77	1810.60	10988
8	8.00	10.26		2.22	7.06	1.59	2.00	37.02	287.00	26.08				110.00	845.74	2971
11	11.00	13.27		2.14	9.32	1.68	4.00	46.20	277.00	30.17				36.27	358.61	785

4.3 ESTIMATION OF EXTREME KEELS DRAFTS

4.3.1 EXTREME ICE KEELS

The 10 largest keels observed at Site 1 and Site 2 are listed in Table 4-12 and Table 4-13. At Site 1, the maximum depths of the listed exceptional keels ranged from 21.51 to 26.67 m. At Site 2, the maximum keel depths ranged from 21.91 to 29.96 m. Overall, 19 keels at Site 1 and 24 keels at Site 2 were observed with depths in excess of 20 m.

Table 4-12. List of keels with the ten largest drafts observed at Site 1. The draft values are provided as the maximum and mean (average) draft computed for each of the 10 largest individual ice keels.

Site 1 *Draft statistics after March 2, 2011 calculated from pseudo-spatial series		
Date/ Time	**Max Draft (m)**	**Mean Draft (m)**
02-Jun-2011 22:02:43*	22.16	14.37
02-Jun-2011 21:53:41*	21.76	12.01
30-May-2011 13:24:42*	20.54	16.21
03-May-2011 11:31:51*	20.17	14.73
10-Apr-2011 05:02:30*	19.41	16.06
02-Jun-2011 22:26:00*	19.25	11.13
22-May-2011 04:58:58*	18.33	12.48
02-Jun-2011 20:26:11*	18.26	13.13
02-Jun-2011 21:21:23*	18.10	14.36
24-Feb-2011 03:15:54	18.03	13.66

Table 4-13. List of keels with the ten largest drafts observed at Site 2. The draft values are provided as the maximum and mean (average) draft computed for each of the 10 largest individual ice keels.

Site 2		
Date/ Time	**Max Draft (m)**	**Mean Draft (m)**
01-Jun-2011 10:32:12	28.73	15.08
29-May-2011 04:15:44	24.05	18.38
11-Apr-2011 13:39:14	23.00	14.95
11-Apr-2011 06:45:52	22.88	18.47
01-Jun-2011 10:16:35	22.02	15.41
11-Apr-2011 11:34:27	21.70	16.09
10-Apr-2011 19:15:52	21.35	14.96
10-Apr-2011 12:39:37	20.98	11.48
21-Apr-2011 03:13:05	20.84	14.72
11-Apr-2011 10:54:24	20.52	14.77

4.3.2 METHODOLOGY FOR EXTREMAL ANALYSIS

Probability estimation for extreme keel depth occurrences is limited due to both the short duration of our measurement program (2008-2011 at Site 1 and 2009-2011 at Site 2) and the limitations on maximum measurable draft imposed by the depth of IPS-5 transducer. The parameter most relevant to such estimates is the 100-year return draft value, D_{100}, which is representative of the largest keel depth likely to be encountered in 100 years at a given site. Previously, 100-year return values were derived by fitting the high draft end of the empirical keel probabilities to a three-parameter Weibull probability distribution. However, as a result of the limitations noted above, the return values calculated are not deemed statistically reliable, and hence, not presented here. As data collection spans more years, these results will become more statistically robust.

4.3.3 SELECTION OF FEATURES OF EXTREME DRAFT

The selection of ice keels for inclusion in our analyses of extreme draft probabilities followed a two-step process (ASL, 2011):

1. The largest individual ice keels were selected for each site from the final version of the 1 m smoothed spatial data set, by selecting individual big keel segments having a maximum ice draft above a chosen threshold level. The threshold was set to eventually allow selection of roughly 100 or more extreme keel values as representatives of the largest ice keel drafts observed at a given site.

2. Each of the ice keel data segments, as selected (as per item 1) were plotted and manually reviewed. In a few cases, two or more individual keels were combined into

a single keel of greater horizontal extent. The final set of the largest ice keels by site are presented as individual plots of ice draft spatial series in the Project Archive which can be downloaded from ASL's FTP site.

4.3.4 STATISTICAL ANALYSIS

The distributions of maximum keel draft values in 2010-2011 for keels with maximum drafts above the 13 m threshold are presented in Table 4-14 for Site 1 and Site 2.

Table 4-14. Ice draft distributions in 2010-2011 for ice keels exceeding 13.0 m maximum draft. Draft statistics for Site 1 calculated from pseudo-spatial series after March 2, 2011.

	Number of Keels	
Draft (m)	**Site 1**	**Site 2**
13.0 - 13.5	32	63
13.5 - 14.0	32	73
14.0 - 14.5	17	46
14.5 - 15.0	15	36
15.0 - 15.5	14	30
15.5 - 16.0	7	13
16.0 - 16.5	5	18
16.5 - 17.0	5	14
17.0 - 17.5	3	10
17.5 - 18.0	0	8
18.0 - 18.5	4	7
18.5 - 19.0	0	7
19.0 - 19.5	2	1
19.5 - 20.0	0	4
20.0 - 20.5	1	2
20.5 - 21.0	1	3
21.0 - 21.5	0	1
21.5 - 22.0	1	1
22.0 - 22.5	1	1
22.5 - 23.0	-	1
23.0 - 23.5	-	1
23.5 - 24.0	-	0
24.0 – 24.5	-	1
24.5 – 25.0	-	0
25.0 – 25.5	-	0
25.5 – 26.0	-	0
26.0 – 26.5	-	0
26.5 – 27.0	-	0
27.0 – 27.5	-	0
27.5 – 28.0	-	0
28.0 – 28.5	-	0
28.5 – 29.0	-	1

To provide an appreciation of the character of the largest ice keels, plots of spatial profiles are provided in Figure 4-14 and Figure 4-15 for the widest and deepest keels encountered at each site. Arguably, the widest keels in the entire data sets could be considered to be part of rubble ice fields. Note, however, that the detected keels in the ice keel database are defined according to the quantitative criteria specified above in section 4.2.1 for large ice keels. More advanced analysis methods to distinguish between different ice deformation processes such as singular large keels and rubbled and/or hummocky ice are recommended for further investigation of these very extensive Ice Profiler data sets.

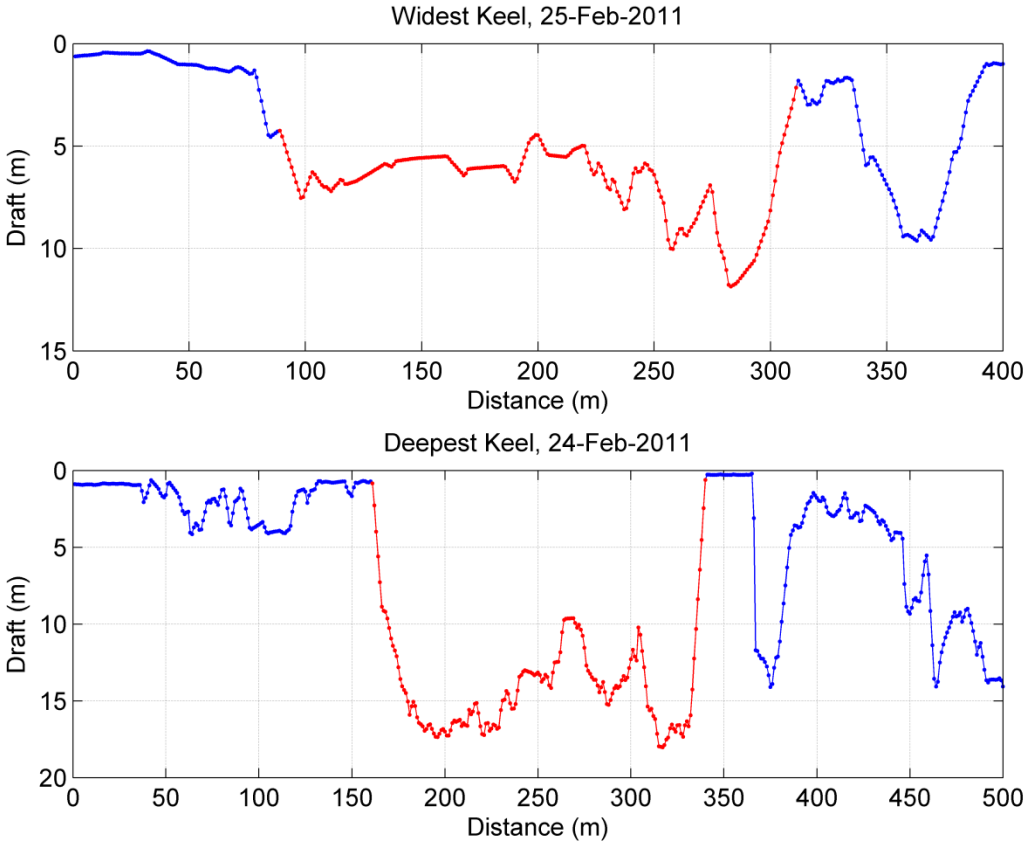

Figure 4-14. At Site 1, width information was only available until March 2, 2011, when the ADCP record ended. The widest keel (223 m, *top*) observed before March 2 at Site 1 occurred on February 25, 2011 and the deepest keel (18.03 m, *bottom*) occurred on February 24, 2011.

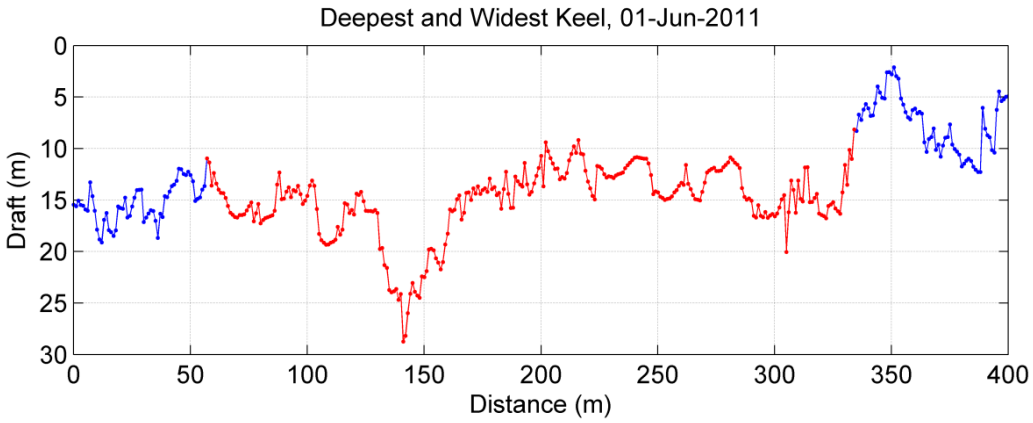

Figure 4-15. At Site 2, the widest keel observed (294 m) was also the deepest keel (28.73 m) and occurred on June 1, 2011.

4.4 ICE MOTION: EPISODES OF LARGE MOVEMENT AND SLOW MOVEMENT

The ice velocity measurements (Section 3.3) and the resulting distances of ice movement measured were subjected to further analyses to identify the episodes of alternately large and then negligible ice movements for the winter and spring of 2010-2011 at Sites 1 and 2 where ice velocity measurements were made.

Each episode of large ice movement was identified using a criterion of having an average speed exceeding 19 cm/s over a minimum duration of 12 hours. The episodes of large ice movement are presented in Table 4-15 and Table 4-16 for Site 1 and Site 2 respectively. Information on the winds (direction from and maximum wind speed) is also presented for each episode of large ice movement. The period of 2 to 8 November 2010 with a maximum wind speed of 14.4 m/s had the largest ice velocity at Site 1 and was the period with the second largest ice velocity for Site 2. The maximum ice velocity of 142 cm/s at Site 2 occurred between 29 December 2010 and 2 January, 2012 when the winds reached 16.9 m/s.

As presented earlier in Table 3-10, the percentage of slow-motion observations at Site 2 is, on average, larger than that of at Site 1, which is consistent with Site 2 being closer to the land fast ice zone. The maximum of no-motion episodes occurred in January with a value of 10.4 % at Site 2 and 7.2 % at Site 1. However, the mean (and maximum) ice speed calculated for the entire 2009-2010 measurement period were higher for Site 2 with a value of 23.8 cm/s (142.3 cm/s) than that of Site 1 with a value of 23.6 cm/s (91.2 cm/s). The higher maximum ice speed at Site 2 and the consistently higher mean ice speeds from November through January indicate that Site 2 is located in a more dynamic region. Thus, when ice concentrations are not very close to 100%, ice floes travel at higher speeds at Site 2.

By December, Site 2 started exhibiting (2.5 %) periods of slow-motion, while Site 1 which is further offshore and where high concentrations of new sea ice occur later in the year did not show slow-motion ice episodes until January 2011. Overall, the slow-motion episodes were registered at Site 2 from December 2010 to April 2011 and only January and February 2011 for Site 1.

Table 4-15. Large ice motion events at Site 1.

Start Date/Time	Stop Date/Time	Duration (days)	Distance Travelled (km)	Average Speed (cm/s)	Max Speed (cm/s)	Net Ice Dir (deg True)	Max Wind Speed (m/s)	Wind Dir from (deg)
02-Nov-2010 18:17	07-Nov-2010 03:18	4.38	223.27	59.07	91.23	256.26	14.42	E
08-Nov-2010 07:03	09-Nov-2010 02:48	0.82	16.87	23.72	29.38	211.87	6.69	E
12-Nov-2010 10:18	13-Nov-2010 22:48	1.52	32.45	24.69	33.36	245.50	7.19	E
16-Nov-2010 12:03	18-Nov-2010 19:48	2.32	99.00	49.33	78.83	62.63	20.58	W
02-Dec-2010 06:48	08-Dec-2010 07:19	6.02	241.27	46.38	85.85	249.52	13.39	E
09-Dec-2010 15:19	11-Dec-2010 02:04	1.45	30.90	24.70	30.95	149.54	8.22	W
12-Dec-2010 12:34	13-Dec-2010 09:04	0.85	18.44	24.99	33.60	101.97	9.25	W
17-Dec-2010 08:34	19-Dec-2010 10:34	2.08	50.03	27.79	42.32	358.61	11.31	E
19-Dec-2010 11:04	21-Dec-2010 10:04	1.96	55.69	32.91	47.47	94.13	9.78	W
21-Dec-2010 23:49	22-Dec-2010 13:04	0.55	14.67	30.75	41.51	116.35	8.04	W
23-Dec-2010 11:34	24-Dec-2010 16:19	1.20	25.28	24.42	29.65	265.49	10.81	E
25-Dec-2010 06:04	28-Dec-2010 08:04	3.08	89.11	33.45	47.12	235.62	7.19	E
29-Dec-2010 15:19	03-Jan-2011 20:04	5.20	171.97	38.29	85.04	246.98	16.88	E
05-Jan-2011 05:04	06-Jan-2011 02:04	0.88	22.11	29.25	36.06	203.67	8.23	E
06-Jan-2011 15:04	07-Jan-2011 21:19	1.26	34.24	31.44	44.47	81.70	9.07	W
09-Jan-2011 10:04	10-Jan-2011 23:04	1.54	49.74	37.34	73.13	64.43	9.78	W
29-Jan-2011 19:20	30-Jan-2011 09:35	0.59	13.35	26.02	31.64	58.05	6.69	E
02-Feb-2011 02:50	03-Feb-2011 22:35	1.82	51.57	32.74	45.82	77.05	9.25	W
05-Feb-2011 06:35	06-Feb-2011 12:20	1.24	49.66	46.36	66.52	82.53	14.42	W
07-Feb-2011 12:35	08-Feb-2011 05:35	0.71	14.59	23.84	29.08	315.67	12.86	E
09-Feb-2011 07:50	10-Feb-2011 07:20	0.98	19.55	23.11	26.11	174.42	9.25	W
13-Feb-2011 16:05	14-Feb-2011 06:05	0.58	12.02	23.84	27.00	133.14	13.39	W
15-Feb-2011 11:51	17-Feb-2011 10:06	1.93	38.95	23.40	30.30	21.83	10.81	E
17-Feb-2011 19:51	20-Feb-2011 07:36	2.49	111.71	51.93	80.35	64.50	17.50	W
23-Feb-2011 02:21	26-Feb-2011 13:36	3.47	164.09	54.75	85.84	61.71	21.08	W
	Total of Events	48.93	1650.52					

Table 4-16. Large ice motion events at Site 2.

Start Date/Time	Stop Date/Time	Duration (days)	Distance Travelled (km)	Average Speed (cm/s)	Max Speed (cm/s)	Net Ice Dir (deg True)	Max Wind Speed (m/s)	Wind Dir from (deg)
02-Nov-2010	08-Nov-2010	5.55	404.31	84.28	133.71	248.91	14.42	E
09-Nov-2010	10-Nov-2010	1.31	24.77	21.84	25.91	167.31	6.69	W
12-Nov-2010	14-Nov-2010	1.95	62.02	36.85	56.05	243.00	7.19	E
14-Nov-2010	14-Nov-2010	0.76	17.16	26.12	37.02	225.22	4.64	E
15-Nov-2010	19-Nov-2010	3.72	184.73	57.49	106.75	81.65	20.58	W
19-Nov-2010	22-Nov-2010	2.59	82.58	36.85	67.31	77.85	7.72	E
22-Nov-2010	23-Nov-2010	1.04	55.85	62.06	82.80	83.86	10.28	W
26-Nov-2010	29-Nov-2010	2.47	61.58	28.87	41.82	107.86	6.69	W
29-Nov-2010	29-Nov-2010	0.71	17.61	28.78	39.77	84.88	5.14	E
30-Nov-2010	02-Dec-2010	2.01	91.19	52.50	78.37	104.10	8.22	W
02-Dec-2010	07-Dec-2010	4.88	211.04	50.10	78.43	258.53	13.39	E
17-Dec-2010	18-Dec-2010	0.99	22.40	26.20	34.30	329.75	9.25	E
18-Dec-2010	19-Dec-2010	0.69	16.46	27.70	33.11	9.01	11.31	E
19-Dec-2010	21-Dec-2010	1.99	60.61	35.26	52.70	95.44	9.78	W
21-Dec-2010	22-Dec-2010	0.71	15.59	25.48	34.55	107.91	8.04	W
25-Dec-2010	29-Dec-2010	4.07	169.48	48.16	71.60	254.84	7.19	E
29-Dec-2010	02-Jan-2011 15:32	3.96	232.14	67.88	142.28	252.35	16.88	E
04-Jan-2011	08-Jan-2011 06:02	4.22	155.32	42.61	70.84	132.87	9.07	E
08-Jan-2011	11-Jan-2011 13:17	3.07	124.62	46.94	105.36	91.06	9.78	E
25-Jan-2011	27-Jan-2011 08:32	2.15	58.62	31.62	39.39	248.27	7.19	E
29-Jan-2011	31-Jan-2011 06:17	1.59	40.94	29.73	41.85	81.84	9.78	E
02-Feb-2011	03-Feb-2011	1.74	54.86	36.50	49.85	78.11	9.25	W
05-Feb-2011	06-Feb-2011	1.03	40.44	45.39	67.21	78.59	14.42	W
17-Feb-2011	20-Feb-2011	2.46	107.99	50.84	86.04	74.45	17.50	W
23-Feb-2011	26-Feb-2011	3.29	158.75	55.82	106.10	75.10	21.08	W
22-Mar-2011	23-Mar-2011	1.47	34.46	27.16	37.25	84.17	8.75	W
31-Mar-2011	01-Apr-2011 07:48	0.96	24.65	29.77	37.05	71.62	11.31	W
04-Apr-2011	05-Apr-2011 08:48	0.82	20.17	28.37	37.51	241.15	7.19	E
07-Apr-2011	12-Apr-2011 08:03	4.41	176.36	46.32	66.53	254.67	9.78	E
13-Apr-2011	15-Apr-2011 09:18	2.28	92.93	47.15	65.04	268.98	9.25	E
16-Apr-2011	18-Apr-2011 03:33	1.17	27.00	26.79	35.20	108.47	6.17	W
18-Apr-2011	19-Apr-2011 12:48	1.01	28.20	32.30	52.21	123.06	9.25	W
22-Apr-2011	27-Apr-2011 10:49	5.45	204.08	43.36	75.79	262.54	10.81	E
29-Apr-2011	30-Apr-2011 06:49	0.55	15.93	33.39	48.87	258.94	7.19	E
04-May-2011	05-May-2011	0.74	14.62	22.88	27.72	86.27	4.11	E
12-May-2011	13-May-2011	1.09	29.35	31.05	40.01	77.78	6.69	E
16-May-2011	18-May-2011	1.60	44.20	31.89	41.45	246.76	11.31	E
30-May-2011	31-May-2011	1.30	28.32	25.17	30.57	111.15	4.11	W
01-Jun-2011	02-Jun-2011 15:34	1.23	48.55	45.72	63.82	263.26	12.33	E
	Total of Events	83.03	3259.89					

4.5 OCEAN WAVE RESULTS

The time series of significant wave height (H_s) and peak period (T_p) for Sites 1 and 2 are presented in Figure 4-16 and Figure 4-17, respectively.

There were no storms with H_s exceeding 5 m at either site. Four events at Site 1 had H_s values greater than 4 m (September 25, October 21, 27 and 31) and seven events had H_s greater than 3 m. At Site 2, Hs exceeded 4 m on September 25. Four events exceeded the 3 m level (August 2, September 25, October 28 and 31). Except for a few hours where Hs fell to about 1.5 m, the significant wave height was consistently in excess of 2 m between October 18 and November 1. At Site 1, H_s reached 4.3 m and T_p went up to 9 s. At Site 2, the significant wave height only reached 3.4 m, and peak periods reached 8 s. At this time, wind speeds at Wainwright and Point Lay were from the east and northeast at 15-30 knots. There was a reduction in the storm intensity (H_s, T_p, and H_{max}) between October 25 and October 27 12:00 that corresponds to decreased wind speeds (5-10 knots) at Wainwright and Point Lay. This event is shown in detail in Figure 4-18. In 2009/2010, the largest storm produced waves of 5.5 m with peak periods exceeding 10 seconds. On September 25, a storm produced maximum wave heights of 7.6 m at Site 1 and 8.6 m at Site 2.

Statistics and joint frequency tables of significant wave height (H_s) and peak period (T_p) for Sites 1 and 2 are presented in Table 4-17 to Table 4-20. Site 2 required more flagging due to high concentrations of ice in early November. Most of the peak period data corresponding to wave heights below 0.1 m was flagged due to low signal levels and the corresponding uncertainty in identifying the correct peak period. The joint frequency tables show that most of the waves have a period in the 4-8 second range and were 0.5-1.5 m. Phase 4 was sampled every 2 seconds (0.5 Hz) and the smallest resolvable period was 4 seconds (0.25 Hz). For this phase, the lower data sampling rate may sometimes results in a minor underestimate of the H_s values due to not including contributions for waves with periods of 2 to 4 seconds. The presence of ice in the region, however, compensates in that it damped out most of the high frequency energy. Anticipating a late start to ice formation again this year, the ice profiling mode was started later in the season when preparing the deployment files for the 2011-12 season.

The percent exceedances of H_s are presented in Table 4-21 and Figure 4-19 for both sites. For both data sets, more than 50% of the data had H_s greater than 0.75 m. Site 1 had 22.4 % of the data above 2 m and Site 2 had 11.5 %. Site 1 had 7.0 % of the data above 3 m and Site 2 had 0.9 %.

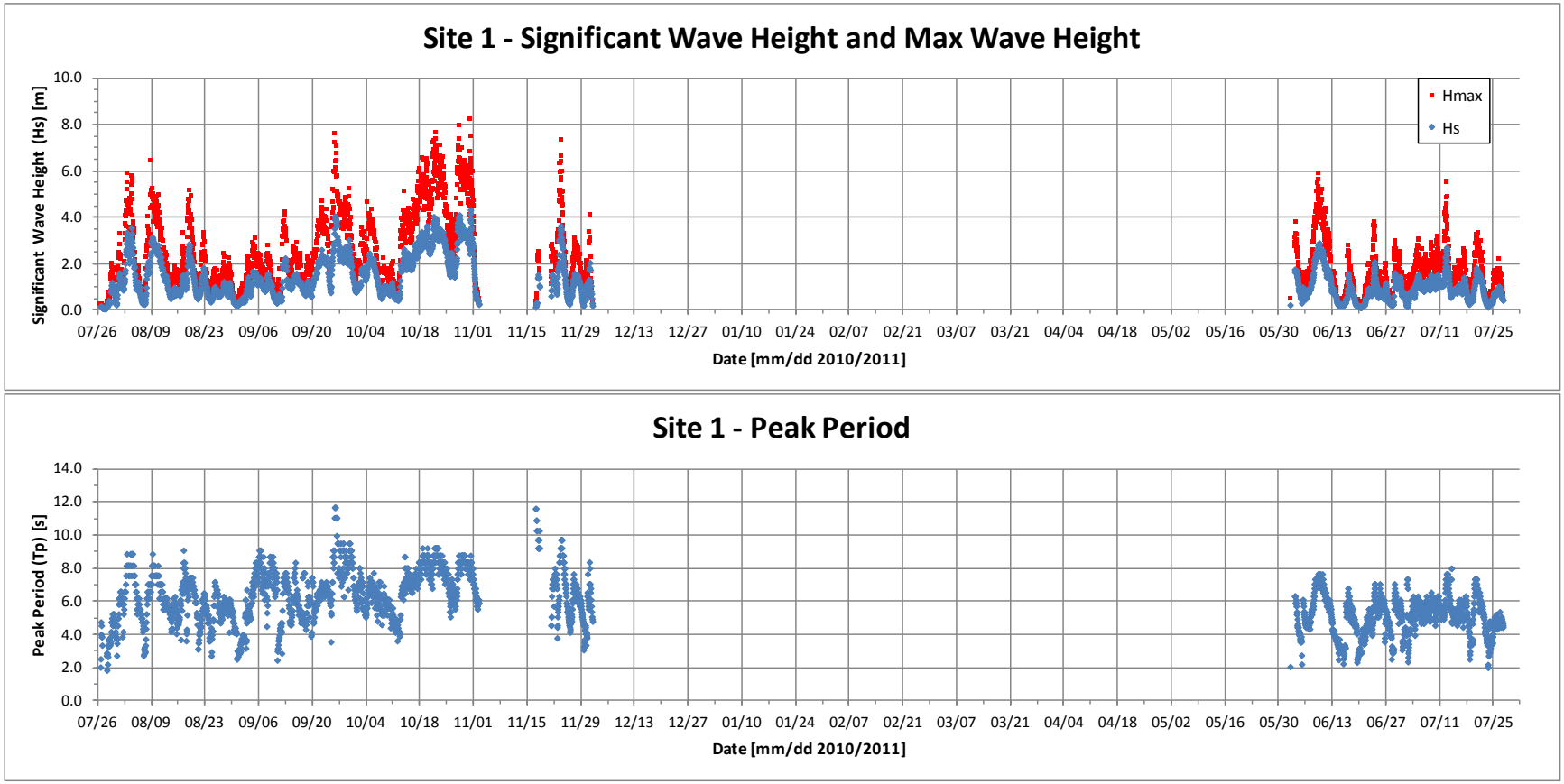

Figure 4-16. Significant wave height (Hs) (upper panel, blue marker), maximum wave height (Hmax) (upper panel, red marker) and peak period (Tp) at Site 1 for 2010/2011.

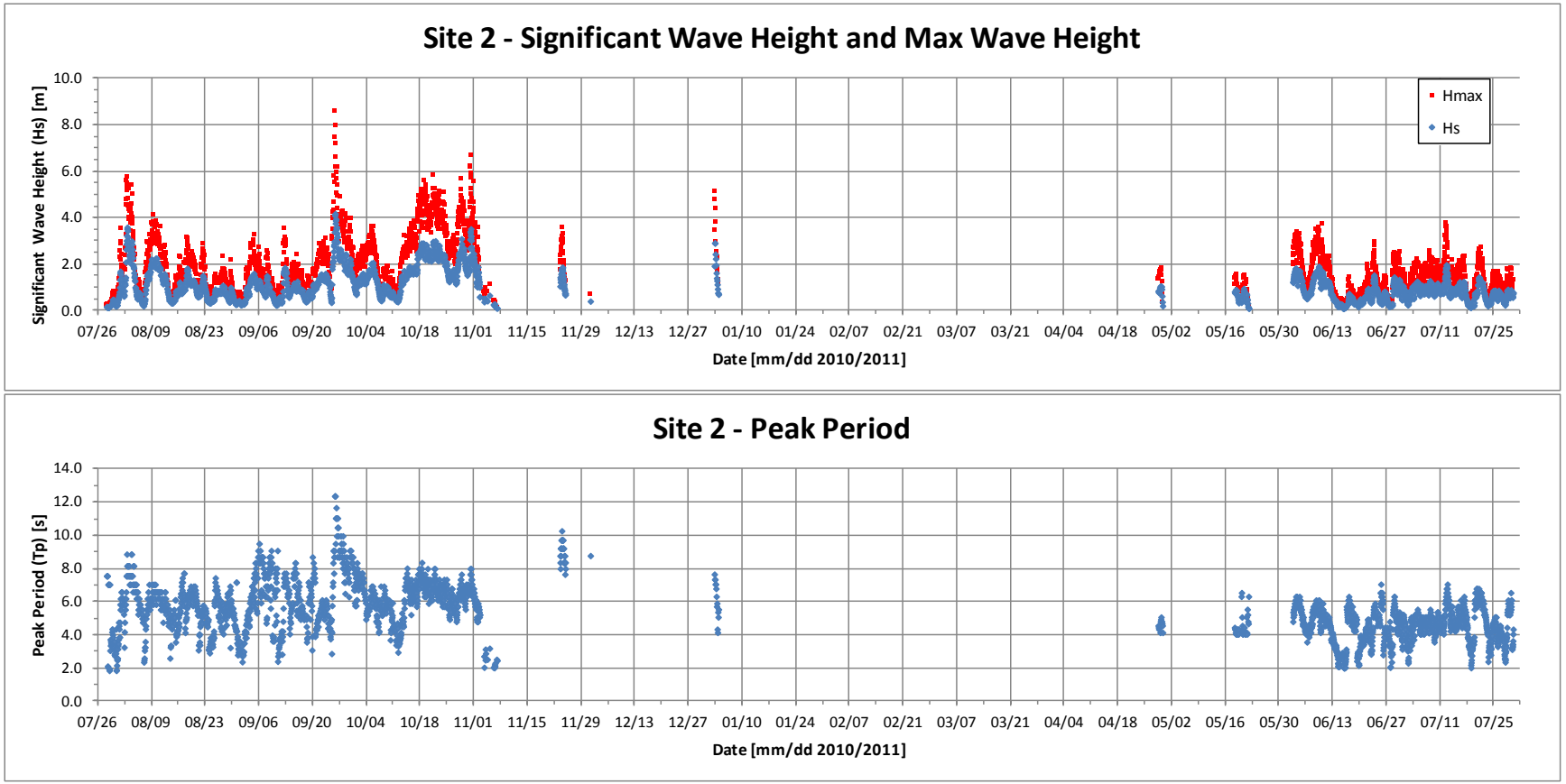

Figure 4-17. Significant wave height (Hs) (upper panel, blue marker), maximum wave height (Hmax) (upper panel, red marker) and peak period (Tp) at Site 2 for 2010/2011.

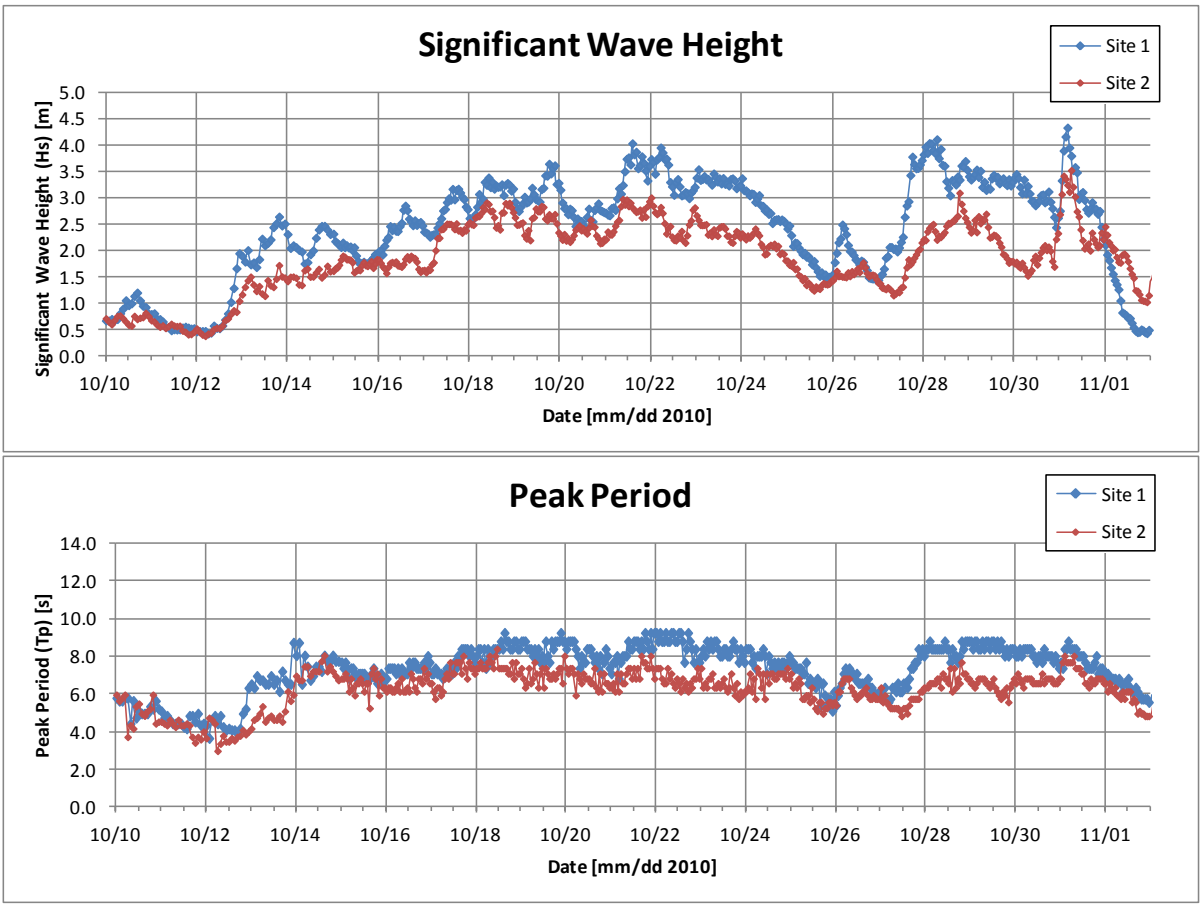

Figure 4-18. Significant wave height (Hs) and peak period (Tp) for both sites from October 10 – November 2, 2010.

Table 4-17. Monthly statistics of significant wave height (H_s) and peak period (T_p) at Site 1.

Site 1: Date		25%	50%	mean	75%	95%	99%	max	# valid	total #
26-Jul-2010 to 31-Jul-2010	Hs (m) :	0.15	0.36	0.55	0.96	1.46	1.57	1.60	86	86
	Tp (s) :	3.5	4.2	4.3	5.0	6.6	6.6	6.6	69	86
August 2010	Hs (m) :	0.67	0.98	1.26	1.75	2.86	3.22	3.55	496	496
	Tp (s) :	5.1	5.8	5.9	6.9	8.2	8.9	9.1	496	496
September 2010	Hs (m) :	0.94	1.24	1.45	2.04	2.69	3.88	4.06	480	480
	Tp (s) :	5.5	6.7	6.7	7.7	9.1	11.0	11.7	480	480
October 2010	Hs (m) :	1.57	2.42	2.30	3.13	3.66	3.96	4.33	632	632
	Tp (s) :	6.3	7.3	7.2	8.4	8.8	9.2	9.2	632	632
November 2010	Hs (m) :	0.61	1.10	1.18	1.44	2.97	3.50	3.64	287	719
	Tp (s) :	5.4	6.3	6.5	7.3	9.7	10.9	11.6	287	719
December 2010	Hs (m) :	0.50	1.27	1.18	1.75	1.84	2.05	2.05	13	372
	Tp (s) :	5.1	6.1	6.3	7.1	8.0	8.4	8.4	13	372
January 2011	Hs (m) :								0	372
	Tp (s) :								0	372
February 2011	Hs (m) :								0	336
	Tp (s) :								0	336
March 2011	Hs (m) :								0	372
	Tp (s) :								0	372
April 2011	Hs (m) :								0	360
	Tp (s) :								0	360
May 2011	Hs (m) :								0	371
	Tp (s) :								0	371
June 2011	Hs (m) :	0.45	0.80	0.95	1.34	2.40	2.72	2.89	664	720
	Tp (s) :	4.0	5.1	5.0	5.9	7.3	7.7	7.7	664	720
01-Jul-2011 to 27-Jul-2011	Hs (m) :	0.65	0.89	0.93	1.18	1.59	2.42	2.71	637	637
	Tp (s) :	4.7	5.2	5.2	5.9	7.1	7.7	8.0	637	637

Table 4-18. Joint Frequency Table of H_s vs. T_p at Site 1.

Location: DVH10-S1
Instrument: IPS5-1088
For period: 2010/07/26 15:30:01 to 2011/07/27 12:31:56

		Hs (m)										
		0.00 to 0.50	0.50 to 1.00	1.00 to 1.50	1.50 to 2.00	2.00 to 2.50	2.50 to 3.00	3.00 to 3.50	3.50 to 4.00	4.00 to 4.50	4.50 to 5.00	Row Total (%)
Tp (s)												
0.00	1.00											0.00
1.00	2.00	0.03										0.03
2.00	3.00	2.47	0.03									2.50
3.00	4.00	5.92	2.62	0.12								8.66
4.00	5.00	4.61	10.07	1.80								16.47
5.00	6.00	1.25	12.29	10.25	2.47							26.27
6.00	7.00	0.40	3.17	6.77	5.06	3.05	0.34					18.79
7.00	8.00	0.34	0.88	2.47	1.92	4.39	4.27	1.34	0.15			15.77
8.00	9.00	0.03	0.31	1.13	0.37	1.07	1.74	3.02	1.16	0.18		9.00
9.00	10.00			0.40	0.06	0.34	0.34	0.49	0.34			1.95
10.00	11.00	0.15		0.03								0.18
11.00	12.00	0.06							0.24	0.06		0.37
12.00	13.00											0.00
13.00	14.00											0.00
Column Total (%)		15.25	29.38	22.97	9.88	8.85	6.68	4.85	1.89	0.24	0.00	

Filename: Site1_201007_HsTp.dat
Max Hs: 4.33 m
Mean Hs: 1.34 m
non-flagged Hs records: 3295
non-flagged Tp records: 3278

Table 4-19. Monthly statistics of significant wave height (H_s) and peak period (T_p) at Site 2.

Site 2: Date		25%	50%	mean	75%	95%	99%	max	# valid	total #
28-Jul-2010 to 31-Jul-2010	Hs (m) :	0.19	0.26	0.41	0.46	1.54	1.62	1.69	60	60
	Tp (s) :	3.1	3.7	4.1	4.8	7.6	7.6	7.6	60	60
August 2010	Hs (m) :	0.59	0.87	1.05	1.35	2.28	3.02	3.59	496	496
	Tp (s) :	4.9	5.8	5.6	6.5	7.6	8.2	8.9	496	496
September 2010	Hs (m) :	0.69	1.02	1.17	1.45	2.43	3.75	4.17	480	480
	Tp (s) :	5.1	6.3	6.4	8.0	9.1	11.0	12.4	480	480
October 2010	Hs (m) :	1.33	1.75	1.78	2.34	2.79	3.09	3.52	632	632
	Tp (s) :	5.8	6.5	6.3	6.9	7.7	8.0	8.4	632	632
November 2010	Hs (m) :	0.75	1.27	1.24	1.74	2.02	2.29	2.45	89	719
	Tp (s) :	4.9	6.1	6.4	8.8	9.7	9.7	10.3	89	719
December 2010	Hs (m) :	0.40	0.40	0.40	0.40	0.40	0.40	0.40	1	372
	Tp (s) :	8.8	8.8	8.8	8.8	8.8	8.8	8.8	1	372
January 2011	Hs (m) :	0.93	1.51	1.64	2.23	2.90	2.91	2.91	14	372
	Tp (s) :	5.4	6.1	6.1	7.1	7.3	7.7	7.7	14	372
February 2011	Hs (m) :								0	336
	Tp (s) :								0	336
March 2011	Hs (m) :								0	372
	Tp (s) :								0	372
April 2011	Hs (m) :	0.77	0.90	0.82	0.99	1.05	1.05	1.05	15	360
	Tp (s) :	4.4	4.6	4.6	4.8	4.9	5.1	5.1	15	360
May 2011	Hs (m) :	0.39	0.62	0.59	0.81	0.89	0.95	0.95	38	371
	Tp (s) :	4.0	4.2	4.5	4.6	6.3	6.5	6.5	37	371
June 2011	Hs (m) :	0.34	0.67	0.78	1.17	1.64	1.77	1.90	681	720
	Tp (s) :	3.8	4.6	4.5	5.4	6.1	6.3	7.1	677	720
01-Jul-2011 to 30-Jul-2011	Hs (m) :	0.57	0.76	0.77	0.97	1.24	1.81	1.96	699	699
	Tp (s) :	4.0	4.7	4.6	5.2	6.3	6.8	7.1	699	699

Table 4-20. Joint Frequency Table of H_s vs. T_p at Site 2.

Location: DVH10-S2
Instrument: IPS5-1060
For period: 2010/07/28 06:30:00 to 2011/07/30 02:30:20

		Hs (m)										
		0.00 to 0.50	0.50 to 1.00	1.00 to 1.50	1.50 to 2.00	2.00 to 2.50	2.50 to 3.00	3.00 to 3.50	3.50 to 4.00	4.00 to 4.50	4.50 to 5.00	Row Total (%)
Tp (s)												
0.00	1.00											0.00
1.00	2.00	0.13										0.13
2.00	3.00	5.03	0.06									5.09
3.00	4.00	7.44	4.16	0.03								11.63
4.00	5.00	4.22	15.53	4.81	0.03							24.59
5.00	6.00	2.16	9.22	9.75	4.13	0.31						25.56
6.00	7.00	0.75	3.44	4.16	5.69	3.78	1.13					18.94
7.00	8.00	0.53	1.13	1.31	1.50	1.91	2.00	0.34	0.03			8.75
8.00	9.00	0.09	0.84	1.03	0.59	0.53	0.19	0.06	0.06			3.41
9.00	10.00	0.03	0.03	0.25	0.44	0.53	0.13	0.03	0.06			1.50
10.00	11.00				0.03		0.06	0.03				0.13
11.00	12.00						0.03	0.03	0.13			0.19
12.00	13.00									0.09		0.09
13.00	14.00											0.00
Column Total (%)		20.38	34.41	21.34	12.41	7.06	3.53	0.50	0.28	0.09	0.00	

Filename: Site2_201007_HsTp.dat
Max Hs: 4.17 m
Mean Hs: 1.08 m
non-flagged Hs records: 3205
non-flagged Tp records: 3200

Table 4-21. Percent exceedance tables of significant wave height (H_s) for Sites 1 and 2.

Site 1			Site 2		
Instrument: IPS5-1088			Instrument: IPS5-1060		
2010/07/26 15:30:01 to 2011/07/27 12:31:57			2010/07/28 06:30:00 to 2011/07/30 02:30:21		
# non-flagged Hs records: 3295			# non-flagged Hs records: 3205		
# non-flagged Tp records: 3278			# non-flagged Tp records: 3200		
Hs (m)	**# Exceeding**	**% Exceedance**	**Hs (m)**	**# Exceeding**	**% Exceedance**
0.00	3295	100.00	0.00	3205	100.00
0.25	3128	94.93	0.25	3040	94.85
0.50	2777	84.28	0.50	2546	79.44
0.75	2332	70.77	0.75	1995	62.25
1.00	1814	55.05	1.00	1447	45.15
1.25	1380	41.88	1.25	1045	32.61
1.50	1061	32.20	1.50	763	23.81
1.75	867	26.31	1.75	514	16.04
2.00	737	22.37	2.00	367	11.45
2.25	576	17.48	2.25	268	8.36
2.50	448	13.60	2.50	141	4.40
2.75	335	10.17	2.75	69	2.15
3.00	229	6.95	3.00	28	0.87
3.25	143	4.34	3.25	17	0.53
3.50	70	2.12	3.50	12	0.37
3.75	31	0.94	3.75	6	0.19
4.00	8	0.24	4.00	3	0.09
4.25	1	0.03	4.25	0	0.00
4.50	0	0.00	4.50	0	0.00
4.75	0	0.00	4.75	0	0.00
5.00	0	0.00	5.00	0	0.00

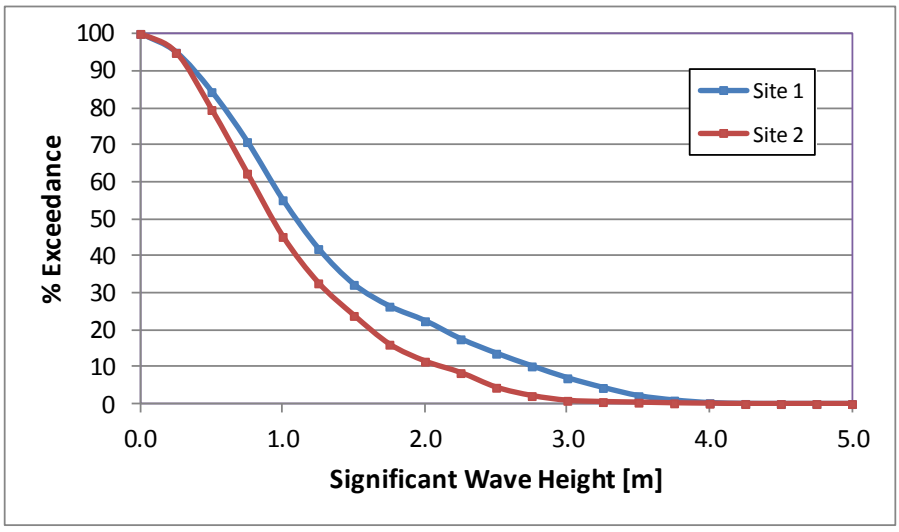

Figure 4-19. Percent exceedance plot of significant wave height (H_s) for both sites.

5 SUMMARY AND CONCLUSIONS

A program of ice keel depth and ice velocity measurements was carried out off northwestern Alaska in support of oil and gas exploration by ConocoPhillips Alaska Inc. (CPAI) in the Chukchi Sea from July 2010 to July 2011. The data collection program involved the deployment and operation of two underwater, internally recording instruments at two sites (Site 1 and Site 2) in 39-47 m depth for just over a year.

At each measurement site, an Ice Profiling Sonar (IPS-5) instrument was operated to provide ice draft measurements at one or two second intervals. The IPS-5 also provided non-directional wave measurements at 2 Hz sampling rates. Ice velocity measurements, at 5 minute sampling intervals, were obtained from Acoustic Doppler Current Profilers (ADCP), which also provided ocean current profile data.

5.1 OVERVIEW OF THE 2009-2010 ICE SEASON

Ice conditions in the region continued their recent trend of reduced ice extent from historical conditions (1979-2000) with the September 2009, 2010, 2011 ice edge well north of its median position. The region has a very dynamic ice regime with ice movement for the 2010-2011 records occurring 97% to 95% of the time at Site 1 (November to February) and Site 2 (November to June). Ice features having large vertical drafts, of up to 57% and 61% the total water depth, were observed from December until May at Site 1 and Site 2, respectively. Thousands of Ice keels with horizontal dimensions of typically 25-50 m, up to a few hundred meters, were observed. The great majority of these ice keels are individual ice keel features. A few of the very widest keels represent massively deformed features. As was seen in the previous data sets, the ice proved to be quite mobile, with only the months of January and February having more 5% slow movements for Site 2. The greatest percentage of slow-motion events in the 2010-2011 measurement period was observed in January, with 7% at Site 1 and 10% at Site 2.

The results from this measurement period were obtained during the two years with the historically second (2011) and fourth (2010) greatest summer ice retreats. Extensive open water conditions existed in the study area until late November 2010 and ice clearing began in late May, with the eastern part of the Chukchi clearing 3-5 weeks earlier in 2011 than 2010.

5.2 DEEPEST ICE KEELS

Very deep ice keels were observed at both Site 1 and Site 2 with 4 keels at Site 1 and 12 keels at Site 2 measuring over 20 m ice draft. The deepest keels at Site 1 and Site 2 were 22.2 m and 28.7 m respectively.

Keels exceeding 11 m ice draft were measured in all months from December to June at both sites. From the distance of ice passage (derived for ice velocity measurements from

November to March for Site 1 and November to June for Site 2) the total distances of sea ice passing by Site 1 and 2 were 2172 and 3816 km. This is greater than the previous year when total distances measured at both sites from November to July were 2150 and 2861 km.

Ice keels having threshold drafts of 5, 8 and 11 m were individually identified and statistics on these were compiled. The total number of ice keels greater than 5, 8 and 11 m were 8948, 2163 and 414 for Site 1 (pseudo spatial series) and 10998, 2971 and 785 for Site 2. By comparison to the previous year of measurements, there was a notable increase for the total number of keels for the 5 m threshold. The number of keels greater than 8 m was similar in the two years at Site 1 with 2010 keels and reduced at Site 2 with 2318 in 2009-2010.

5.3 WIDEST ICE KEELS

There were occurrences of ice keels with very large horizontal dimensions of up to a few hundred meters and large maximum keel depths. Detection of keels and their beginning and ending positions are determined by objective criteria as outlined in Section 4.2.1. The widest keels, using a threshold of 5 m, were 223 m for Site 1 and 294 m for Site 2. Arguably, the widest keels in the entire data sets could be considered to be part of rubble ice fields, in particular the widest keel at Site 2. More advanced analysis methods to distinguish between different ice deformation processes such as singular large keels and rubbled and/or hummocky ice are recommended for further investigation of these very extensive Ice Profiler data sets.

5.4 ICE VELOCITY

Over 20 occurrences of large ice velocities at Site 1 (even with a reduced data record) and over 30 at Site 2 were measured throughout the year. The peak ice velocities of 91 cm/s at Site 1 and 142 cm/s at Site 2 are considerably greater than the values of 76 and 115 cm/s observed in 2009-2010 and are in better agreement with the 2008-2009 values of 112 cm/s at Site 1 and 124 cm/s at Site 2. The episodes of large ice velocities were associated with strong wind events having peak speeds of up to 21.1 m/s. The median ice drift was highest in June with a value of 39.8 cm/s for Site 2. The second and third largest ice drifts occurred in November and December at Site 2 with a values of 32.3 and 24.9 cm/s, which coincided with the largest median ice speeds observed at Site 1 of 23.3 and 25.2 cm/s. Site 2 saw its lowest median ice drift in March at 5.8 cm/s while the Site 1 ADCP which stopped recording in early March observed its lowest median ice drift of 11 cm/s in January. Periods of slow motion were fewer in 2010-2011 (718 point for Site 2) in comparison with 2009-2010 at (1607 points for Site 2); however the median ice drift at Site 2 was only 2 cm/s greater than the 14 cm/s observed in 2009-2010.

5.5 OCEAN CURRENTS

The ocean currents at Site 1 were weaker than those observed at Site 2 with median speeds 25 to 45% lower. The maximum current speed near the surface was 99.0 cm/s at Site 2 and 67.2 cm/s at Site 1. From July to September currents are weak, while in late September to early January, current speeds were typically large and associated with strong wind events that were at times greater than 8 m/s as measured at Wainwright. In the period of January through to the start of May the currents are typically weak with a few episodes of strong flows when winds at times were over 10 m/s. The May to July 2011 period was relatively quiescent. As observed with the ice velocities, the currents were generally larger in 2010-2011 than the previous year with mean currents at Site 2 about 25% greater than the 16-17 cm/s observed in 2010-2011.

The currents at Site 1 were predominantly directed to the ENE, whereas the current direction at Site 2 aligned more closely to the E axis. The directionality at Site 1 was more variable than observed at Site 2. The basic directionality is similar to what was observed in previous years; however the 2010-2011 observations show less directional variability than what was observed in 2009-2010. These current directions are likely influenced by the local topography, the inflows from the Pacific Ocean and by offshore winds. The current directions at Site 1 and Site 2 are similar to the mean flows observed by Weingartner et al. (2009) where the main water flow coming in from the Pacific bifurcates and flows around the west and southern parts of Hanna Shoal. Site 2 is located in a deep and narrow channel between the Hanna Shoal and the coast, where the ocean currents are larger due to local topography.

Inertial oscillations are present in the ocean current data during the times of reduced or zero ice concentrations. These twice-daily ocean current variations produced a peak to trough current variation of up to 30 cm/s, and they appeared to be more prevalent at Site 1 than at Site 2.

5.6 OCEAN WAVES

The acoustic range data from the ASL Ice Profiler was used to derive information on ocean waves when sea ice was not present. From late September to late October, there were four storms with the significant wave heights exceeding 4 m. The largest wave heights occurred on September 25, 2010 when H_{max} was measured at 8.6 m for Site 2 with a corresponding peak period of over 12 s. Site 1 had a H_{max} of 7.6 m for the same storm. The meteorological stations at Point Lay and Wainwright recorded relatively weak winds for this period of about 10 m/s, suggesting the short lived storm was offshore. This 2010 storm had a smaller H_{max} than the >10 m maximum wave height observed in 2009. A long period of enhanced wave activity occurred during the last half of October, when significant wave heights exceeded 4 m on three occasions at Site 1 and were rarely less than 2 m. During this event, wind speeds at Wainwright and Point Lay were from the east and northeast at 15-30 knots.

5.7 RECOMMENDATONS

Further analyses of this one year data set may be useful to extract further information on the properties of the sea ice regime in the Eastern Alaskan Beaufort Sea lease areas. Possibilities for further analysis are provided below:

(1) **Additional wave analysis using a combined analysis of winds.** Using NCEP-2 Reanalysis gridded offshore winds along with the Point Lay and Wainwright weather stations and the measured non-directional wave parameters and wave spectra, wave directions can be estimated and the fetch and duration scales examined as applicable to the generation of the measured waves.

(2) **Compute the frequency and properties of Rubbled and Hummocky Ice from the ice distance series.** Rubbled and hummocky ice can pose operational threats that are comparable to those presented by large ice ridges and keels. The statistics of rubbled and hummocky ice will be derived using existing software developed for this purpose.

(3) **Prepare Joint-Bivariate Distributions of ice keel drafts (e.g. > 5m, > 8 m, > 11 m) and ice speeds, for each site.**
An important factor is statistics on ice drift direction persistence and the rates of change in ice drift direction (i.e.: the radius of curvature), for example, for tanker loading and supply vessel offloading considerations. This can be readily done for the full record, and by individual months using software that already available. It is also proposed to investigate whether the occurrence of deep-draft features is statistically independent of drift speed. From a statistical test of the null hypothesis that deep-draft features are not dependent on ice drift speed, using the data compiled for this task, the hypothesis will be tested.

(4) **Compute the radius of curvature of ice drift from the x- and y-displacement values derived from the vector velocity time series.**
From these x- and y-displacement values, the radius of curvature can be computed as a function of time. Occurrences of events for the radius of curvature values, ranging from being comparable to the vessel length to an order of magnitude greater than the hull length, will be identified and statistics on the frequency of occurrence and persistence of such events will be prepared by radius categories. An analysis of joint-bivariate distributions of radius of curvature and drift speed will also be prepared; it will be useful to examine if they have a negative correlation, and make the offloading operations manageable**.**

6 LITERATURE CITED

ASL Environmental Sciences Inc., 2011. IPS Processing Toolbox User's Guide. 2011. Report by ASL Environmental Sciences Inc., Victoria BC Canada, 21 p front material + 123 p. Available upon request from ASL Environmental Sciences Inc.

ASL Environmental Sciences Inc. 2011a. Ice Profiler™ Operators Manual for Model IPS5, Rev. GU-100-71A00A03-R14. Sidney, BC, Canada. Available upon request from ASL Environmental Sciences Inc.

ASL Environmental Sciences Inc., 2011b. Ips5LinkE User's Guide, v. 2.0.9. Sidney, BC, Canada. Available upon request from ASL Environmental Sciences Inc.

Barrett, S.A., and W.J. Stringer. 1978. Growth Mechanisms of "Katie's Floeberg". *Arctic and Alpine Research*, 10(4): 775-783.

Belliveau, D.J., G.L. Bugden, B.M. Eid and C.J. Calnan, 1990. Sea ice velocity measurements by upward-looking Doppler current profilers. *J. Atmos. Oceanic Technol.*, 7(4): 596-602.

Borg, K., J. Lawrence, T. Mudge, and D. Fissel. 2010. Recovery and Redeployment of IPS and ADCP Moorings in the Chukchi Sea July 2010. Cruise Report prepared for Shell International Exploration and Production. 24 p.

Borg, K., P. Johnston, T. Mudge, and D. Fissel. 2011. Recovery and Redeployment of Shell IPS and ADCP Moorings in the Chukchi Sea July 2011. Cruise Report prepared for Shell International Exploration and Production. 25 p.

Fissel, D.B., J.R. Marko and H. Melling, 2008. Advances in Upward Looking Sonar Technology for Studying the Processes of Change in Arctic Ocean Ice Climate. Paper to be published in the Journal of Operational Oceanography and presented at the Oceanology International Conference, London UK, 12 March 2008.

Garrison G.R., R.E. Francois and T. Wen. 1991. Acoustic reflections from Arctic ice at 15-300 kHz. *J. Acoust. Soc. Amer.* 90(2): 973-984.

Huntington, H.P., Brower, H., Jr., and Norton, D.W. 2001. The Barrow Symposium on Sea Ice, 2000: Evaluation of one means of exchanging information between subsistence whalers and scientists. Arctic 54(2):201–204.

Kovacs, A., and M. Mellor. 1974. Sea ice morphology and ice as geological agent in the southern Beaufort Sea. In: *The Coast and Shelf of the Beaufort Sea,* 113-161. Proceedings of a Symposium on Beaufort Sea and Shelf *Research*. J.C. Reed and J.A. Sater, Ed. The Arctic Institute of North America: Virginia.

Mahoney, A., H. Eicken, L. Shapiro, and T. C. Grenfell 2004. Ice motion and driving forces during a spring ice shove on the Alaskan Chukchi coast, Journal of Glaciology, 50(169), 195-207.

Melling, H., P.H. Johnston and D.A. Riedel, 1995. Measurements of the underside topography of sea ice by moored subsea sonar. *J. Atmospheric and Oceanic Technology,* 13(3): 589-602.

Norton, D.W. and G.A. Gaylord, 2004. Drift Velocities of Ice Floes in Alaska's Northern Chukchi Sea Flaw Zone: Determinants of Success by Spring Subsistence Whalers in 2000 and 2001. *Arctic,* 57 (4), 347-362.

Urick, R.J., 1983. *Principles of Underwater Sound,* Third Edition. New York: McGraw-Hill, Inc. 423 p.

Vaudrey, K., 1987. 1985-86 Ice Motion measurements in Camden Bay, AOGA Project 328, Vaudrey & Associates, Inc. San Luis Obispo, CA.

Weingartner, T., K. Aagaard, D. Cavalieri, S. Danielson, M. Kulakov, V. Pavlov, A. Roach, Y. Sasaki, K. Shimada, T. Whitledge, and R. Woodgate, 2009. Chukchi Sea Circulation. *http://www.ims.uaf.edu/chukchi/*